Durham E-Theses

The Electrical breakdown of gases at ultrahigh frequencies

Clark, J. L.

THE ELECTRICAL BREAKDOWN OF GASES AT ULTRAHIGH FREQUENCIES

by

J. L. CLARK, B.Sc.

Being an account of work carried out at the
University of Durham during the three
years ending in August 1956.

— — — — — — — — — —

Thesis submitted to the University of Durham for
Ph.D. degree examination.

— — — — — — — — — —

ACKNOWLEDGEMENTS

C O N T E N T S

CHAPTER 4   Breakdown in Nitrogen

CHAPTER 5   Breakdown in Neon

CHAPTER 6   Breakdown in Air

——————————————

Appendix 1

——————————————

List of references

——————————————

LIST OF PRINCIPAL SYMBOLS USED

V = Peak value of breakdown potential, volts.

Vr = R.M.S. breakdown potential, volts.

E = Peak value of breakdown stress, volts cm^{-1}

Er = R.M.S. breakdown stress, volts cm^{-1}

d = Electrode separation, mms.

do = Critical electrode separation, mms.

de = Amplitude of electron oscillation, mms.

p = Gas pressure, mms. Hg.

λ = Wave-length of applied field, cms.

f = Frequency of applied field cycles sec^{-1}

n = Electron density, c.c.$^{-1}$

Vi = Frequency of ionisation, ionisations, sec^{-1}

Va = Frequency of electron attachment, attachments, sec^{-1}

α = Townsends first ionisation coefficient, ionisations per electron, per cm. travel

β = Number of attachments per electron per cm. travel

D = Diffusion coefficient for electrons, diffusions through 1 cm^V sec^{-1}

μ = Electron mobility, velocity in unit field

Λ = Characteristic diffusion length of electrons, cms.

CHAPTER 1. INTRODUCTION

1.1. General considerations

Knowledge of high-frequency breakdown has increased considerably in recent years, and though studies are being increasingly pursued from a purely practical standpoint; much research has been devoted towards a better understanding of the fundamental mechanisms both preceding and following, the passage of a luminous conducting channel in a gas. In this chapter a brief summary is given of high-frequency, breakdown, as related to the work reported in the thesis.

An electrical discharge in a gas results from the movements of large numbers of ions and electrons, and breakdown theory must postulate a mechanism whereby ions are multiplied within the gas under the influence of an external field. The principles of electrical conduction in gases may be studied by expressing the electrical and optical properties of the discharge in terms of atomic data such as charge, mass, mean free path, gas pressure etc.

1.2. d.c. discharges.

Conditions are favourable for breakdown when the gain in electron population due to ionisation processes becomes equal to the loss of electrons from the system.
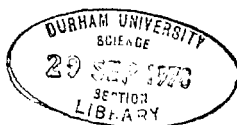
The primary factor governing the production of electrons
is generally collision ionisation between electrons
and gas molecules.   In a d.c. discharge, the production
rate/cm. travel (Townsend's α), in a lifetime limited by
mobility drift to the positive electrode is insufficient
to account for the abrupt increase in electron density
immediately preceding breakdown, and a secondary source
of electrons is necessary to initiate a discharge.
It was considered by Townsend (1947) that secondary
ionisation resulted from a number of mechanisms, notably
electron emission from the cathode due to photon and
excited-atom bombardment; ionisation due, either directly
or indirectly, to positive ions, and cathode emission
due to positive ion bombardment.   Experiments in the
1930's designed to measure the magnitude of these
secondary effects were not successful, and led some
workers to reject the interpretation put forward by Townsend,
and to the introduction of 'streamer' theories.
Secondary electrons were considered to be generated by
photo-ionisation due to photons produced in the electron
avalanche (Loeb & Meek (1940), Zeleney (1941));   such
new electrons could initiate new avalanches at points
remote from the source of the photons, producing such a
rapid propagation of the avalanche across the gap as to

exclude the possibility of secondary ionisation due to
the relatively slow-moving positive ions.   In 1952 however
a series of precision measurements by Llewellyn Jones and
his co-workers at Swansea (1952 a, b & c) showed that the
development of a discharge could, in fact, be explained
satisfactorily by a mechanism of the Townsend type.   They
concluded that no single secondary process can be said to
dominate, their relative importance being governed by such
factors as cathode surface and geometry.   Quantitative
predictions of breakdown using unidirectional fields are
therefore somewhat complex, since they require numerical
data on the efficiency of ionisation due to a number of
processes.   Breakdown resulting from the application of
a high-frequency field, however, is somewhat simpler in
character.

1.3.   Breakdown with alternating fields

The breakdown criterion in a gas stressed by
an alternating field may be described by a failure of
the equilibrium between the formation of electrons within
the test gap, and their effective removal from the intense
field region.   A slightly higher field than that necessary
to balance the opposing processes will cause breakdown to
occur.

At a given field frequency the physical nature
of electron generation, and hence the breakdown stress,

is a function of pressure and nature of gas, and the
separation of the electrodes. The importance of such
additional terms as electrode shape and size, and the
nature of the enclosing discharge chamber, has not been
fully realised until a comparatively recent date, and tends
to cloud some of the early observations.

h.f. breakdown may be broadly classified into
three main frequency bands, though the precise frequencies
at which these transitions occur, and the efficiency of
electronic processes leading to breakdown within the ranges
bounded by these transitions are functions of the
parameters mentioned above. Starting with a gas at
given pressure contained between fixed electrodes (i.e.
constant pd), breakdown at low frequencies less than about
10^5 c/s is substantially the same as for d.c. discharges.
Considering for example a 1 cm. air gap at atmospheric
pressure (Morgan 1953), the transit times of electrons
$\simeq 10^{-7}$ secs, and even the slower-moving positive ions,
$\simeq 10^{-5}$ secs, are short compared with the half-period
of the applied field, and breakdown occurs at the peak
of the voltage wave, at a potential similar to that under
corresponding d.c. conditions. This region is defined
as the low frequency, or l.f. region. (Recent observations
by Fucks (1956) suggest that breakdown at the high-
frequency end of this region is characterised by a rise

of sparking potential above the d.c. value).

As the applied field frequency is increased, the quasi-static condition is followed by a progressive reduction of onset voltage to a fairly constant value. This lowering of V is explained by the incomplete removal of positive ions during a half cycle of the field. A positive space-charge will therefore be built up sufficient to distort the electric field within the test gap, producing enhanced values of α (Reukema, 1928), and correspondingly lowering the breakdown potential. Within the frequency range describing these conditions high frequency (h.f.) breakdown, is said to occur.

When a frequency of the order of 10^7 c/s is reached, a further lowering of V, relatively much greater than before, is encountered, due to the non-removal of electrons during each half-cycle of the field. Their accumulation within the gap increases the ionising efficiency of the gas and consequently a lower field is necessary to initiate a discharge. At far higher frequencies, $> 10^9$ c/s, a further transition is reached when the frequency of collision between electrons and gas molecules approaches the same order of magnitude as the field frequency. Here the electrons make many oscillations/collision and their inability to ionize is characterised by a sudden increase in V.

In the region where the amplitude of electron
oscillation is confined to the inter-electrode
space, ultrahigh frequency, or u.h.f. breakdown, is
said to exist.

1.4. High-frequency breakdown

The region in which positive ion space-
charge affects the sparking potential has been
investigated quite thoroughly in air and hydrogen.
Some of the early work was inconclusive because of the
relatively low frequency range then available, and in
some cases unreliable, owing to non-uniformities in field
distribution (caused by undesirable electrode shapes),
and contamination of the gas by mercury vapour.   The
latter would tend to give spurious values of breakdown
potential due to the Penning (1927) effect.   Recent
observations by a number of workers, however, notably
Seward (1939), Ekstrand (1940), Pim (1949) and Bright
(1950), confirm a gradual lowering of onset voltage up
to 15% below the corresponding 50 c/s value.
Quantitative interpretation of results in this region
are complicated by the inherent field distortion within
the gap, though the breakdown criterion has been derived
approximately by both Pim and Bright.

1.5. Ultrahigh-frequency breakdown

Under u.h.f. conditions, with electrons

oscillating within the gap, the secondary sources of
electrons necessary for the initiation of a d.c.
discharge, are no longer a prerequisite of breakdown.
Except at very low pressure the production of electrons
is controlled almost entirely by ionisation caused
by collisions between electrons and gas molecules.
The breakdown condition at u.h.f. is thus less
complicated than at lower frequencies or d.c., and may
be defined in terms of the generation of electrons by
primary ionisation and their loss by one or more of a
number of removal processes.

The true nature of the u.h.f. transition was
first established by Gill and Donaldson (1931), who
used a long cylinderical discharge tube arranged
either parallel, or at right-angles to the external
electrodes. Breakdown observations using both
configurations showed a minimum in the V- curves;
the transverse arrangement also resulted in a second
minimum, caused by electrons oscillating within the
confines of the gap.

Since 1946 a considerable body of experimental
evidence has accumulated of breakdown in the microwave
region, using both pulsed and sustained oscillations at
frequencies up to 10,000 Mc/s. A quantitative picture
of breakdown under specialised condition at these

rlin and Brown (1948)

in the United States; discussion of results in this
field is reserved until later.

1.6. Low-pressure breakdown

At low gas pressures, the mean free
path of electrons becomes large compared with the
dimensions of the containing vessel, and collision
ionisation becomes highly unlikely.   Using external
electrodes, breakdown under these conditions has been
studied by Gill and van Engel (1948).   Discharges
are initiated by electrons generated by direct
electron bombardment of the walls.   Because of this
the breakdown potential is shown to be independent
of the nature of the gas, but is a function of the
nature of the walls of the confining vessel.

1.7. The experimental problem – u.h.f. breakdown mechanism

Conditions are generally favourable
for an electrical discharge in a gas when the rate of
increase of electron population due to collision
ionisation becomes equal to the loss of electrons
from the system.   In a d.c. discharge, this loss is
due primarily to the mobility motion due to the steady
field.   Under u.h.f. conditions, however, electron
removal must be accounted for by such factors as
diffusion, recombination and attachment.

In the diffusion theory, developed by
Herlin and Brown (1948), diffusion is considered
to be the loss mechanism controlling the discharge,
and it is possible to calculate the breakdown field
by equating the gain in electron density due to
collision ionisation to removal by diffusion.
The theory has beensatisfactorily tested in a
variety of gases at microwave frequencies.   Subject
to certain limits, discussed by McDonald & Brown
(1949), the factors involved in a diffusion-controlled
system should be independent of frequency, and a
wide application of the theory over a considerable
frequency range might be expected.   An analysis
of the results of several workers, in particular
those of Githens (1940) and Thomson (1937), at
frequencies up to 100 Mc/s shows satisfactory
agreement with the diffusion theory when treated with
respect to the proper variables.   On the other hand, Pim
(1949), has obtained data at 200 Mc/s which suggest
that breakdown stress is independent of electrode
separation in the u.h.f. region.   This is at variance
with the diffusion theory, which demands a dependence
of breakdown stress on gap width.   Pim confined his
measurements to air, and the discrepancy may partly
be explained by considering electron attachment to the
oxygen atoms present.   However, the possibility of

u.h.f. breakdown stress being a characteristic of
the gas independent of gap width has been supported
by the results of Fucks, Graf & Muller (1956), and
Prowse and Lane (1955).   In the latter case, results
of an exploratory nature suggested constancy of
breakdown stress in both attaching and non-attaching
gases at frequencies up to 10 Mc/s.

The situation has been further obscured
by breakdown measurements involving short-duation
u.h.f. pulses.   Under breakdown conditions governed
by diffusion an electron may be considered to have a
mean life-time during which it achieves a Brownian
drift to the electrodes or laterally out of the
strongfield region.   A discharge will occur if during
its lifetime an electron creates at least one new ion
pair by collision ionisation;   thus it would be
expected that the time taken for an appreciable growth
of electron density to be considerably greater than
the mean life an electron.   Oscillographic measurements
of breakdown in a number of polyatomic gases by Prowse
& Jasinski (1951), however, have established that a
discharge can occur in time intervals the order of
10^{-8} sec. after the application of the field, too
short for electrons to have diffused from the gap.
Again pulsed measurements by Labrum (1947) suggest a
mechanism whereby the onset of a discharge is governed

by the build up of electron population to a
certain critical value, without any removal taking
place.

In view of the anomalies in breakdown
behaviour presented above, it was decided to make
a systematic investigation of u.h.f. breakdown in
a number of gases, both monatomic and diatomic,
attaching and non-attaching, using properly
profiled parallel plate electrodes, and a frequency
range admitting of direct measurement of applied
voltage.

The work reported in this thesis describes
u.h.f. breakdown in hydrogen, nitrogen, neon and
air, and is concerned principally with the interpretation
of the breakdown measurements in terms of the mechanisms
preceding the onset of a discharge.

Fig. 1.   Schematic Diagram of Apparatus.
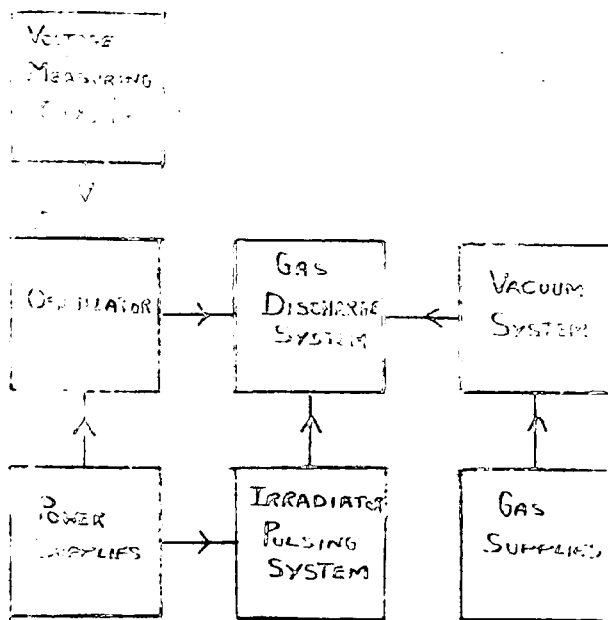
Fig. 2. General View of Apparatus.

(a)
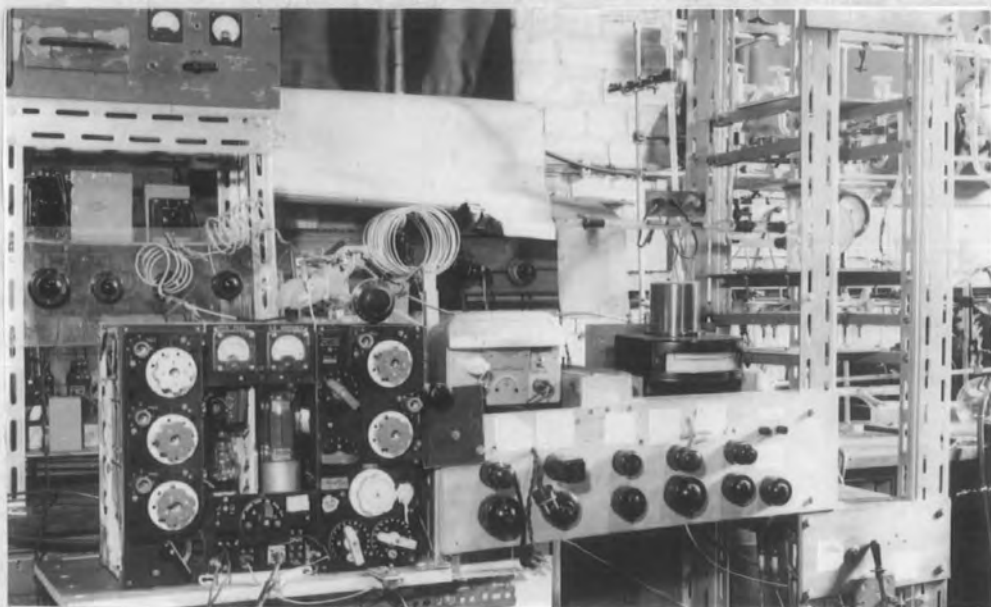
(b)
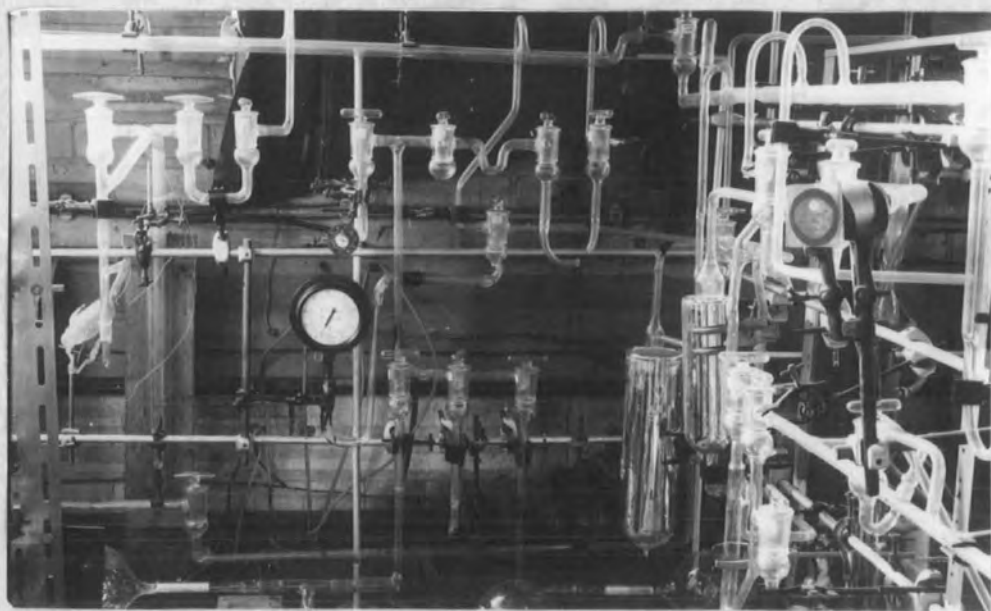
CHAPTER 2. APPARATUS

The essential parts of the final apparatus
developed are shown schematically in Fig.1.   Care
was taken in design to allow variation, over as wide
a range as possible, of all the important parameters,
namely:

> Pressure and nature of the gas.
> Electrode separation and size.
> Field frequency.

A prerequisite of breakdown is that a
triggering, or casual, electron be present within the
gap.   A suitable means of irradiation was therefore
employed capable of satisfying this condition.
The general lay-out of the apparatus is shown in
Figs. 2 (a) and (b).

2.1.   The discharge chamber and accessories

A glass pipeline formed the basis of the
discharge chamber, the complete apparatus being shown
in Fig.3.   The electrodes were centrally situated
in the chamber, their spacing being varied by the use
of specially-constructed bellows, and measured by
micrometer heads referred to steel balls sunk into
the top of threaded shafts integral with the bellows.

Fig. 3. Discharge Chamber, Electrodes, and Accessories.

Micrometer

Handle

Bellows

u.h.f.

Discharge Chamber.

Steel Base Plate

Irradiator Pulse.

Earth

Window

Irradiator Spark Gap.

Gas Inlet

Electrode.

Gas Outlet

Collimator

Insulating Bush

u.h.f

Threaded Spindle.

Earthed Structure
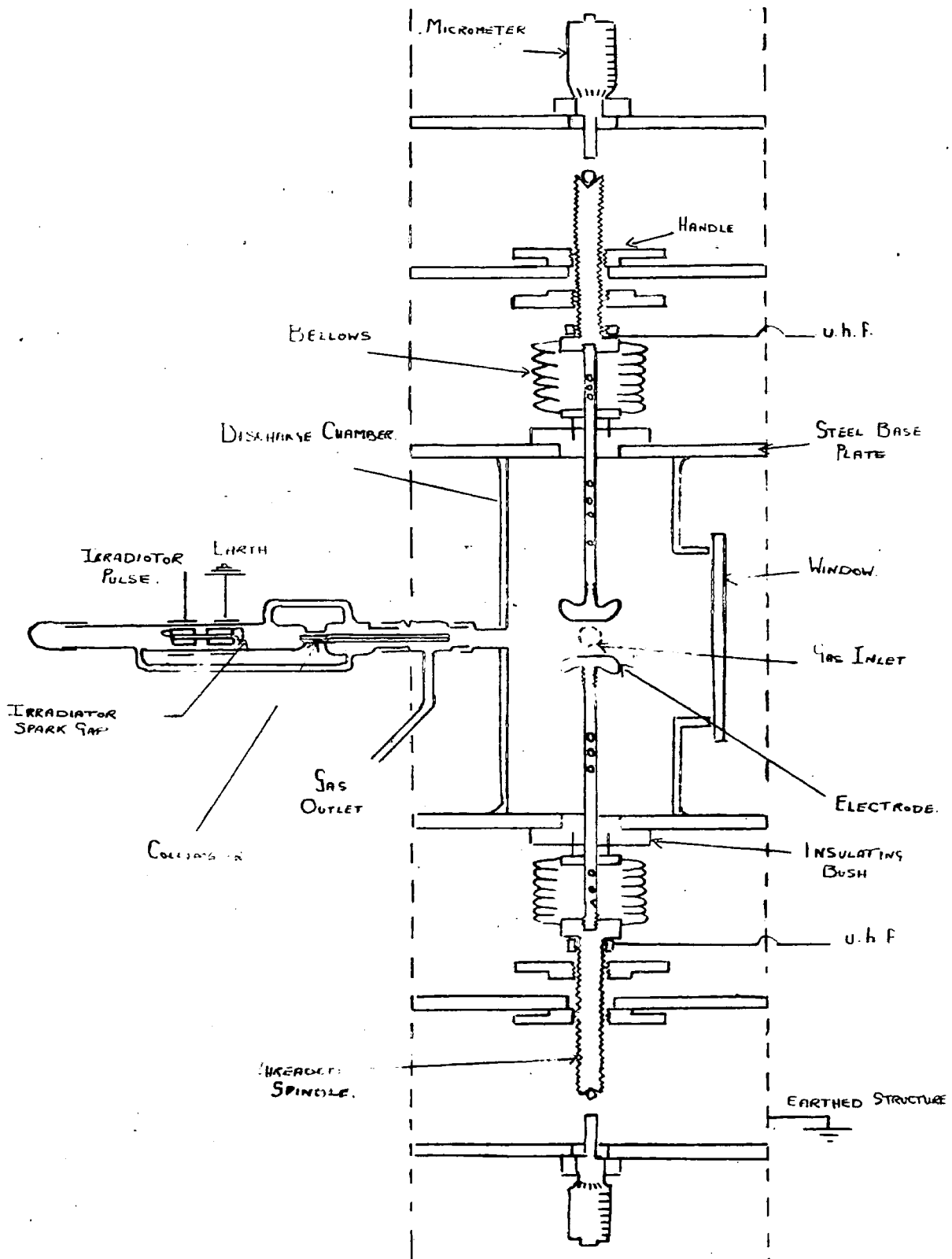
2.1.1. The discharge chamber

The chamber, Fig. 4, consisted of a thick-walled Pyrex pipeline, 6" long and 3" diameter, specially made at the Wear Glass Works, Sunderland. The horizontal open ends, fine-ground and parallel to one another, were vacuum-sealed to mild steel base plates using the epoxy resin Araldite 103 (Johnson 1954). These metal glass unions remained leak-free for a period of two years.

Continuous circulation of gas in the system was ensured by providing two outlet vents in the discharge chamber. One of these openings, centrally situated, also provided a path for the irradiating pulses, whose generation is described in Section 2.6.2. Access to the interior of the chamber was made possible by a 3" diameter glass window, normally sealed by a ground glass cover plate.

2.1.2. Variation of electrode separation

An essential feature of discharge chamber construction was that electrode spacing be varied without disturbing vacuum conditions. For this reason the silver-steel shafts carrying the electrodes were attached to a pair of bellows, Fig. 5, whose end connections were designed to the requirements of the system to allow vertical traverse of the shafts.

Fig. 4. The Discharge Chamber.
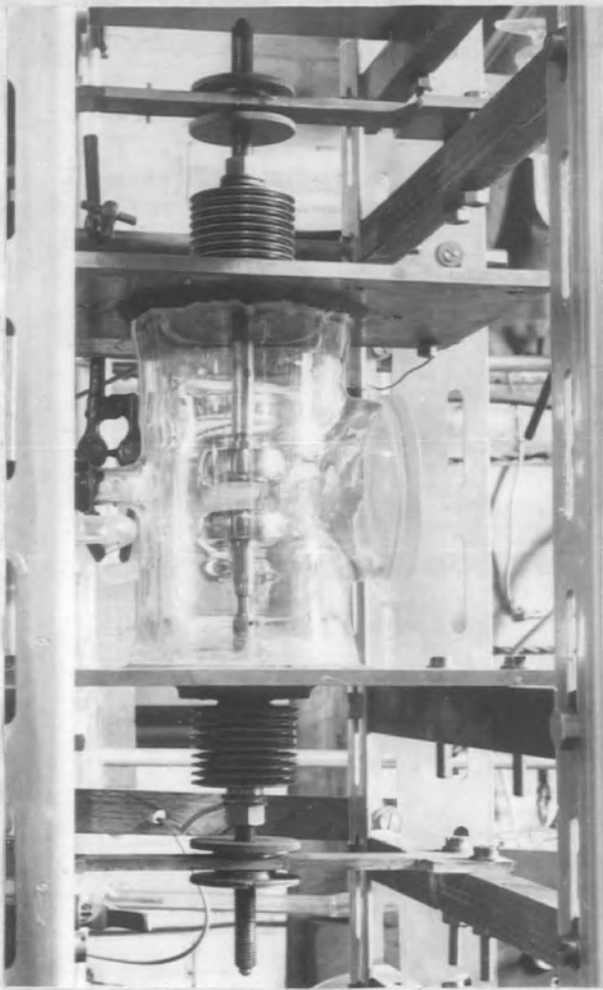
Fig. 5. Electrodes and Supporting Arrangement.
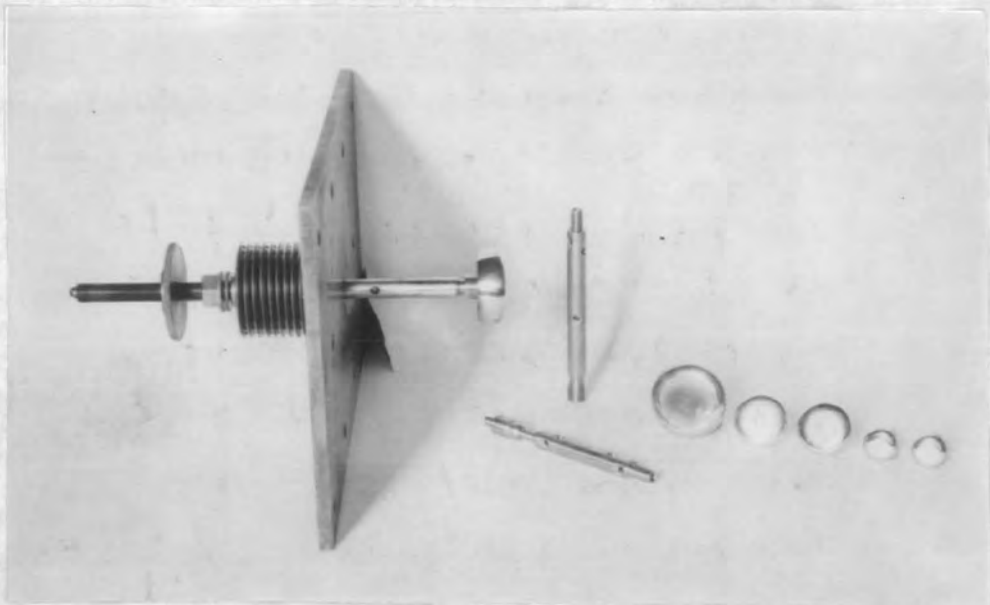
The bellows were made by Negretti & Zambra Ltd., and incorporated the following features.

Each pair consisted of a stack of 9 Cu/Be diaphragm capsules. The normal working deflection/capsule, .05", gave a total movement (and hence maximum electrode separation) of .9" at 22.5 mms.

The ends of each stack were not of the normal type. At one end was:

(i)   A ring of metal, height 3/16", thickness
       .015", and internal diameter .8", used to
       seal the open end of the bellows to the
       insulating bush centrally situated in each
       base plate.

(ii)   A central bush, 3/8" diameter, to support
       the electrode shaft.

At the other end:

(i)   An internal thread 1/4" B.S.F., and .3"
       deep, into which the shaft was screwed.

(ii)   A steel spindle, externally threaded 3/8"
       B.S.F. and of length 2¾", which passed
       through a clearance hole in a rigid steel
       plate and carried two special nuts,
       bevelled circumferentially and situated
       one on either side of the support.
       This provided a suitable means of compressing

or contracting the bellows, and
hence varying the electrode
separation.

2.1.3.   Measurement of electrode separation

Micrometer heads with a vertical
traverse were used to measure the electrode
separation, and referred to the steel balls,
cemented into 90° counter-sinkings, at the
top of each spindle.   The micrometers were
suitably adjusted at zero gap width, this
position being determined electrically using a
d.c. voltage source and milliameter.

2.1.4.   Vacuum and other considerations

In all the breakdown experiments,
measurements were taken with the discharge chamber
partially evacuated.   Since the steel shafts passed
through the bellows to the chamber, a small gas leak
from the bellows to the chamber was inevitable.
To overcome this, it was decided to ensure that the
gas pressure within the bellows be at all times the
same as that in the discharge chamber, and a device
similar to that used by Thomson (1937) was adopted.
The shafts were hollowed-out along their axes, and
radial slots then drilled at suitable points,

providing an adequate gas vent between the chamber and bellows.

The chamber and fittings were mounted on a rigid earthed steel structure. High-frequency field connections were made to the bellows and transmitted in this way to the electrodes. All other metal parts of the system were earthed to the supporting structure.

2.2. Rogowski profiled electrodes.

2.2.1. Importance of correct profiling

In breakdown measurements employing simple plane-parallel disc electrodes, an undesirable non-uniformity of electric field distribution arises from 'edge' effects at the periphery of the electrodes. Profiles of special shape, however, have been derived by Rogowski (1923) to simulate a pair of infinite plane conducting sheets, and so greatly reduce this source of error. Such profiles were used in all the breakdown measurements and are mushroom-shaped surfaces with plane tops joined to the stem by transition surfaces of gradually increasing curvature.

2.2.2. Construction of profiles

Solid brass cylinders were used as the electrode material, profiled to the correct shape in a lathe by optically projecting the image of the electrode

Fig. 6(a)   Apparatus for construction of Rogowski Profiles
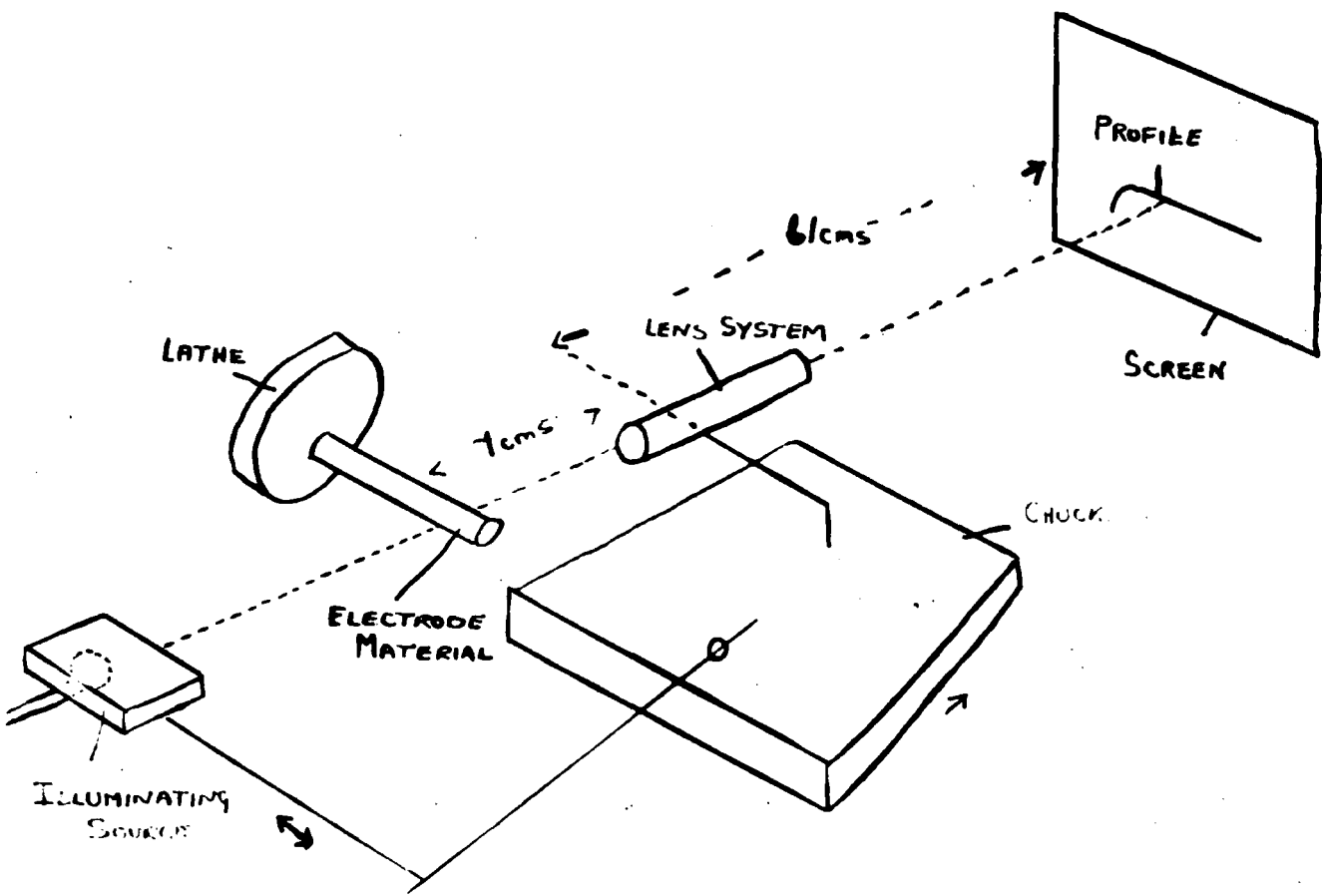
Figs. 6 (b) and (c)   Typical Profiled Electrodes
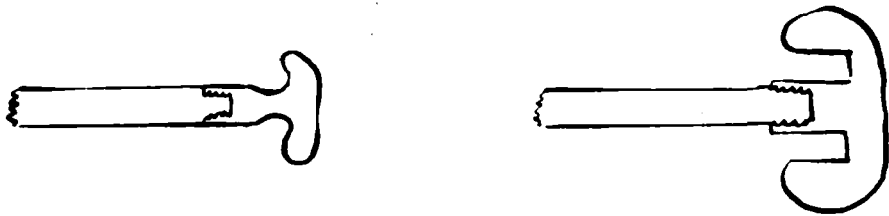
surface on to a distant screen upon which were drawn
Rogowski profiles of different sizes, corresponding
to the diameter of each set of electrodes required.
A diagram of the apparatus is shown in Fig. 6 (a).
Such factors as lens magnification, distance between
lens and screen, optimum illumination, etc., were
determined by a set of preliminary experiments.

The profile envelopes drawn on the screen
were constructed from a Master Profile contained in
a report by Jones (1953); scaled to give surfaces
of the required size.

After carefully aligning the various components
the electrode material was filed in the lathe until
the image of the profile almost coincided with its
corresponding surface drawn on the screen.
Coincidence was then approached using succeedingly
finer grades of emery paper, and finally by metal
polish. Given pairs of electrodes were then ground
with alumina, in conjunction with a reference flat,
until plane top surfaces were obtained.

An internal screw thread was sunk into the
back of each electrode for attachment to the steel
shafts; to reduce overall weight the electrodes were
hollowed out as far as possible. Typical electrodes
are illustrated in Figs. 6 (b) and 6 (c). Four pairs
of electrodes were used; their dimensions are given in
Table 3.

Fig. 7. Vacuum System. Pressure Measurement and Pump Side
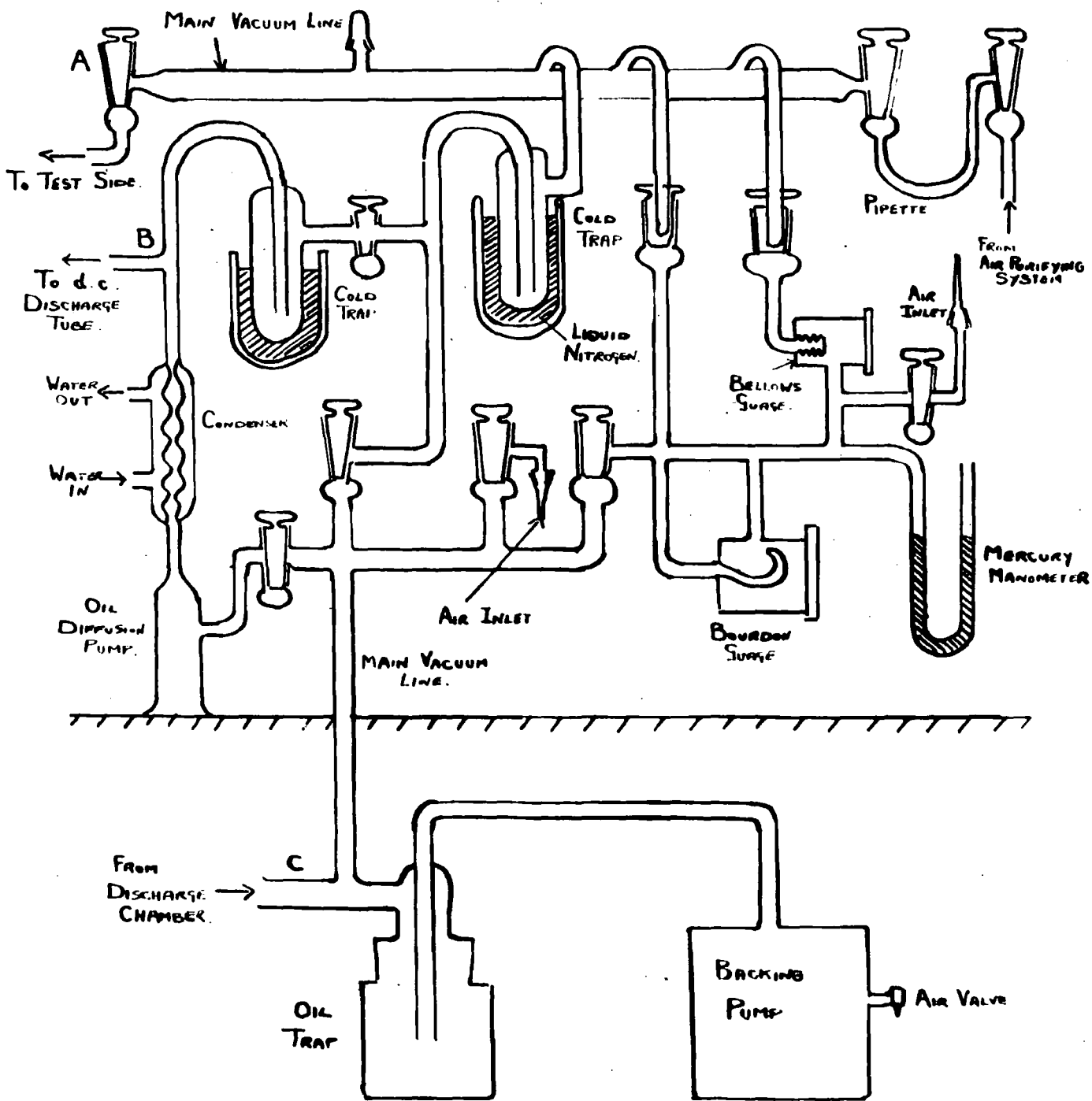
2.3. The vacuum system and pressure measurement.

2.3.1. Main vacuum system

The vacuum system, Figs. 7 & 8, was designed to fulfil the following requirements:

(i) Be suitable for use with different gases.

(ii) Have provision for pipetting small volumes of gas into the system.

(iii) Have an accurate means of measuring pressure.

(iv) Be free from mercury contamination.

Wide-bore Pyrex glass was used throughout the system to ensure a high pumping speed; stopcocks were vacuum-tested with 10 mms. plug bores and sealed hollow plugs. Standard pumping procedure was adopted, the backing pressure being derived from a 'Speedivac' rotary oil pump, and the fore-vacuum from a single-stage 'Metrovac' oil diffusion pump, giving an ultimate vacuum of 10^{-5} mms.Hg., with a pumping speed of 7 litres sec^{-1}. Permanent ground joints were sealed with black Apiezon wax; the stopcocks were treated with Dow Corning high vacuum grease. Two gas outlets in the discharge chamber ensured continuous circulation of gas through the apparatus.

A d.c. discharge tube was used

Fig. 8.   Vacuum System.   Test and Gas Supply Side
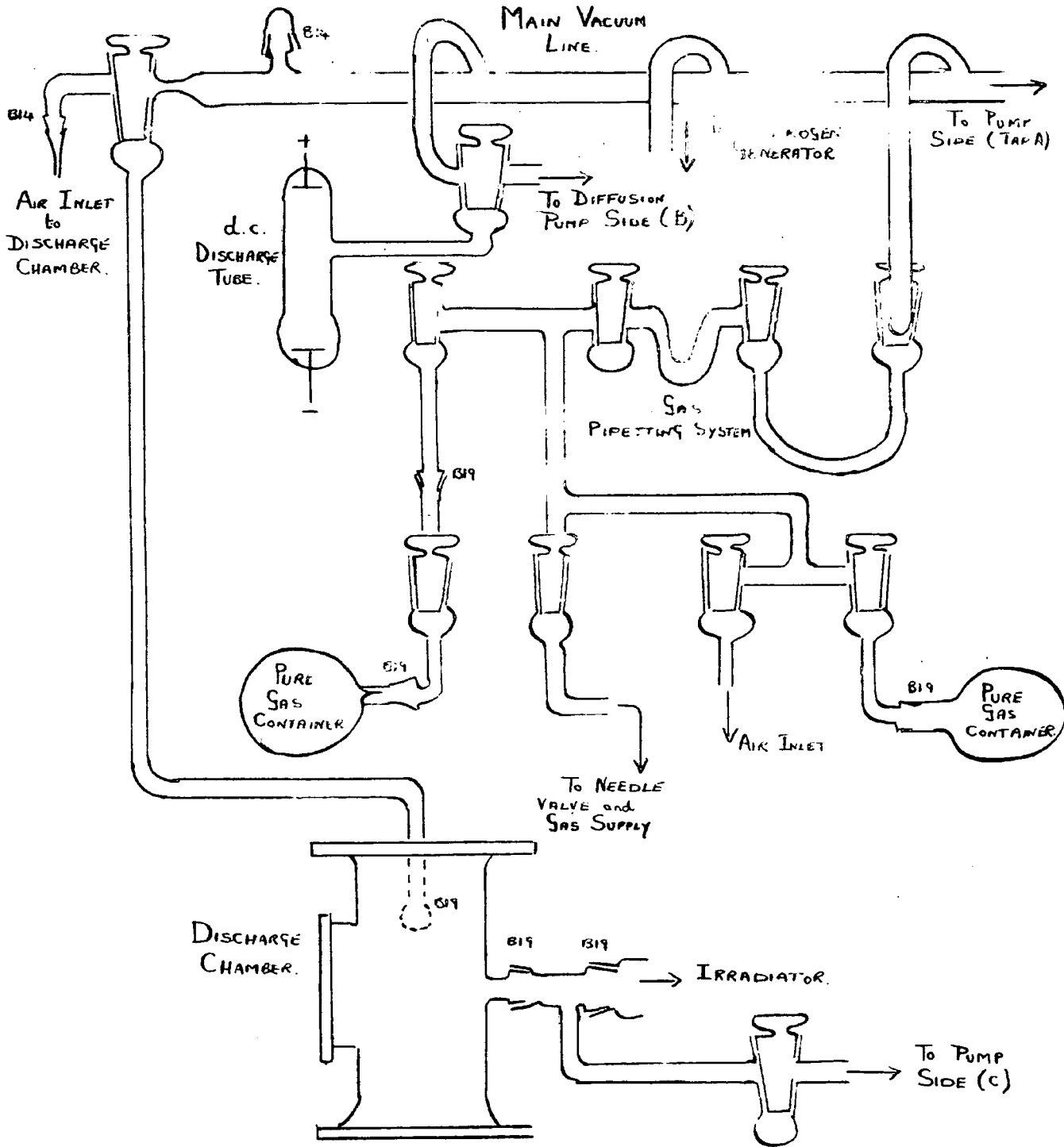
to give a rough indication of vacuum conditions in
either the test or diffusion pump sides of the system,
the glow discharge 'blacking out' below a pressure
of about 10^{-2} mms. Hg. The tube was stressed by a
7 Kv. d.c. supply, with large series resistors
to limit the current.

Gas occlusion on the walls was reduced as
far as possible by passing a Tesla coil along the
system, and the electrodes cleaned by maintaining
a low pressure glow discharge between them. Liquid
nitrogen traps were also incorporated.

After sustained pumping for 2-3 hours, a
'black' discharge could be maintained, with the pumps
shut off, for a period of time far exceeding the
duration of an experimental run.

2.3.2. <u>Gas supplies</u>

Provision was made for the inlet of
different gases into the apparatus via the pipetting
system shown in Fig. 8. Spectrally pure supplies of
the gases used were provided by the British Oxygen
Company in 1 litre glass containers. The air used was
dried by bubbling through concentrated sulphuric acid
contained in Dreschel bottles, and finally through a
glass wool trap to collect any spray before being
pipetted into the system, as shown in Fig. 7.

Fig. 9(a)   Modified Bourdon Gauge

SMALL MIRROR

"O" RING

FINE SPRING

TEST SIDE

CLAMP

REFERENCE SIDE

Fig. 9(b)   Moving Bellows Gauge

REFERENCE SIDE.

TEST SIDE

BELLOWS

"O" RING SEAL.
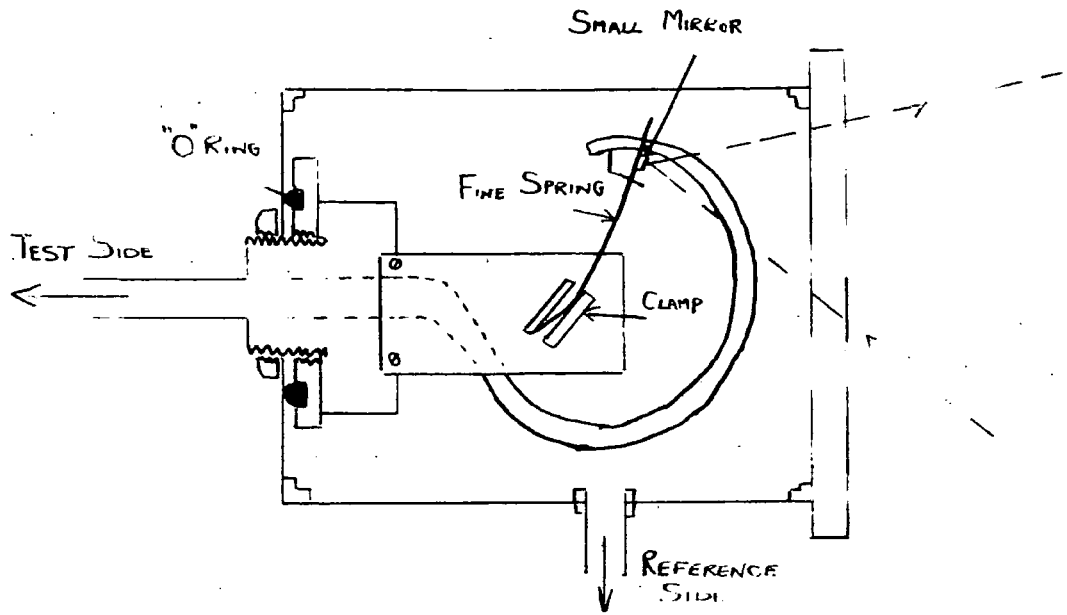
GLASS COVER PLATE
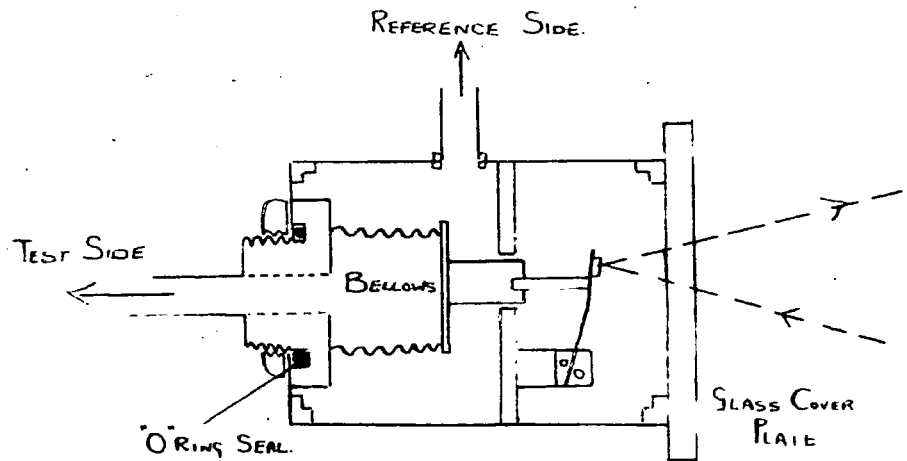
Hydrogen could also be generated by the electrolysis of barium hydroxide in a similar manner to that used by Thomson (1937); in practice, however, this method was seldom adopted.

2.3.3.   <u>Pressure measurement</u>

In order to avoid mercury contamination of the gas resulting in the undesirable (Penning 1927) effect, differential gauges were used for pressure measurement.   Fig 9 (a), shows the modified Bourdon gauge, most frequently used in the experiments. The gauge was calibrated against a mercury manometer situated in the reference side of the vacuum system, using the following procedure.

(i)   The inner portion of the gauge was evacuated by the test side of the vacuum system.

(ii)   The outer casing of the gauge, sealed to the reference side of the apparatus, was also evacuated.   Since no pressure difference existed between the inner and outer compartments the gauge then read zero; the mercury manometer registered atmospheric pressure.

(iii) A small quantity of air was admitted into the reference side via a fine jet, and readings taken of both the Bourdon gauge

Fig. 10. Bourdon Gauge. Calibration Curve
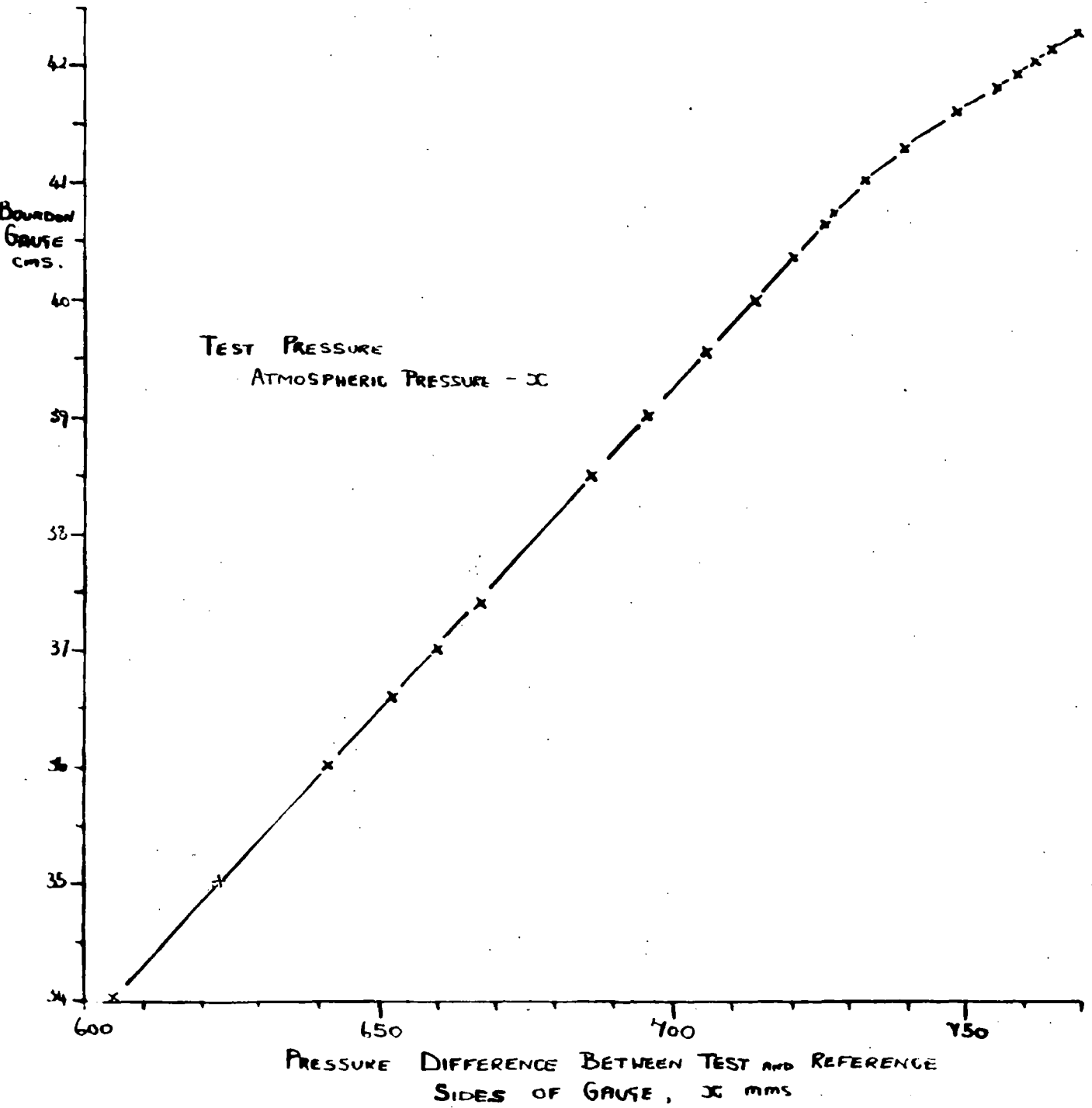
and mercury manometer. Further readings were then taken until air in the reference side reached atmospheric pressure.

(iv) The calibration curve so obtained is given in Fig.10. The curve is seen to be linear from 400 mms.Hg. down to 15 mms.Hg. below which the gauge became less sensitive. For this reason low pressure measurements were taken using the Dial Gauge described below.

A small moving bellows gauge, Fig. 9 (b), was also used, though on account of its limited range it was utilised mainly to indicate equality of pressure between the test and reference sides of the system in the above calibration.

Low pressures were recorded on a direct-reading Edwards Model C.G.1 Dial Gauge.

2.4. The Oscillator

Preliminary measurements were taken in hydrogen using a simple tuned-anode tuned-grid oscillator, but for the majority of gases the peak voltage available, 1000 v. was insufficient to break down the test gap in the u.h.f. region.

A second oscillator was therefore used,

Fig. 11.   Oscillator Output Circuit
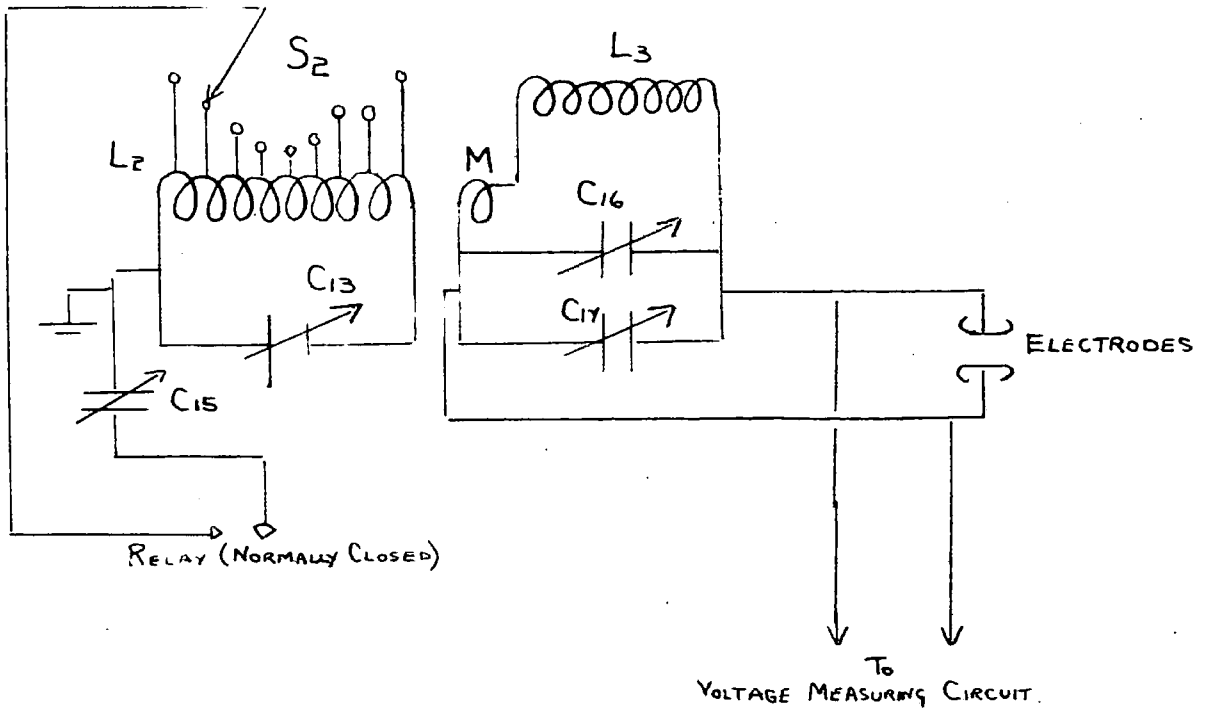
based on an ex-R.A.F. Transmitter T.1154A, and
suitably modified.   Details of the oscillator are
given in Appendix 1.

Maximum voltage across the test gap can best
be developed by using a tuned circuit critically
coupled to the driving oscillator.   This is shown in
Fig.11. L_2 C_{13} formed the output elements of the
oscillator. C_{13} was variable, and L_2 could be set in
one of nine positions using S2.   The oscillations
developed across L_2 C_{13} were transferred to the tuned-
element L_3 C_{16} C_{17} using the magnetic coupling loop
M.   A single loop of 13 gauge wire was employed, and
formed part of the inductive element of the circuit.
The setting-up procedure was as follows.

The master oscillator was tuned to the
required frequency (normally 9.5 Mc /s), L_2 and C_{13}
then being adjusted to give the approximate condition
for resonance, the accurate setting then being
effected by the trimming condenser C_{15}.   The position
of M was then adjusted for critical coupling and the
coupling element L_3 C_{16} C_{17} tuned to the frequency
of the master oscillator.   Final tuning for maximum
output voltage was then performed using the trimmer
C_{17}.   Under experimental conditions, C_3 and C_{16}
were pre-set in the positions described above, the

Fig. 12. Voltage Measuring Circuit
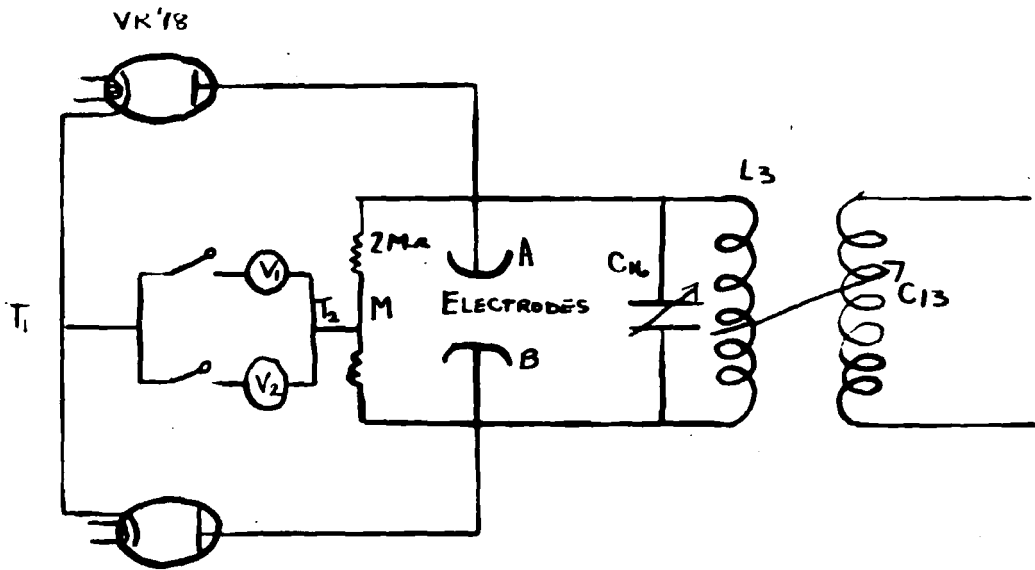
voltage required being coarsely and finely
adjusted by C13 and C15 respectively.   Working
under these conditions, the power input associated
with a given pre-breakdown voltage across the
electrodes was as small as possible.

A maximum voltage of 2,200 volts peak was
obtainable, the amplitude remaining constant at
any required value.

2.5.   The Voltage Measuring Circuit

The output voltage was measured by employing
a diode voltmeter circuit similar to that used by
Gill & Von Engel (1948), being based on two VR.78
diodes and an electrostatic voltmeter, the reading
of the latter being half the peak voltage applied.
This method has disadvantages at both low voltages
(cramped scale) and high frequencies (Williams 1952),
but was found to work quite satisfactorily.

The electrodes AB, Fig.12, formed part of
the oscillatory circuit L_3 C_{16}, tuned by C_{16}
to the frequency of the oscillator as previously
described, Sect. 2.4.   To ensure that the diodes
had a very small inter-electrode capacitance,
indirectly-heated valves of the acorn type (VR.78)
were used.   The anodes were connected to A & B and

both cathodes joined to the mid-points of two
2 M resistances. These resistances were
sufficiently large not to disturb the oscillatory
circuit but passed ample current to work the voltmeter.

The mid-point M being a potential node,
when a voltage $E \sin \omega t$ is applied across AB the
potentials between T_2 and A or B is $\pm \frac{1}{2} E \sin \omega t$
with peak values $\pm \frac{1}{2} E$. The valves pass current until
at the peak there is no voltage across the valve,
which results in the voltmeter reading $\frac{1}{2} E$.

Screened leads were used, arranged so that no
E.M.F. was induced in them from the generator.

Since the scale of an electrostatic voltmeter
is cramped at its lower end, three voltmeters of
different ranges were used in the breakdown
experiments. Calibration curves for the meters are given
in Chapter 7.

(i) <u>Ayrton-Mather electrostatic voltmeter (low range)</u>

This instrument covered a voltage range
0-130 volts., and was sensitive above 40 volts.
Measurements in neon and low pressure hydrogen were
recorded using this meter.

(ii) <u>Ayrton-Mather electrostatic voltmeter (medium range)</u>

This voltmeter was most commonly used in the
breakdown experiments, being sensitive in the range 100-
600 volts.

Fig. 13. Modified Voltage Measuring Circuit
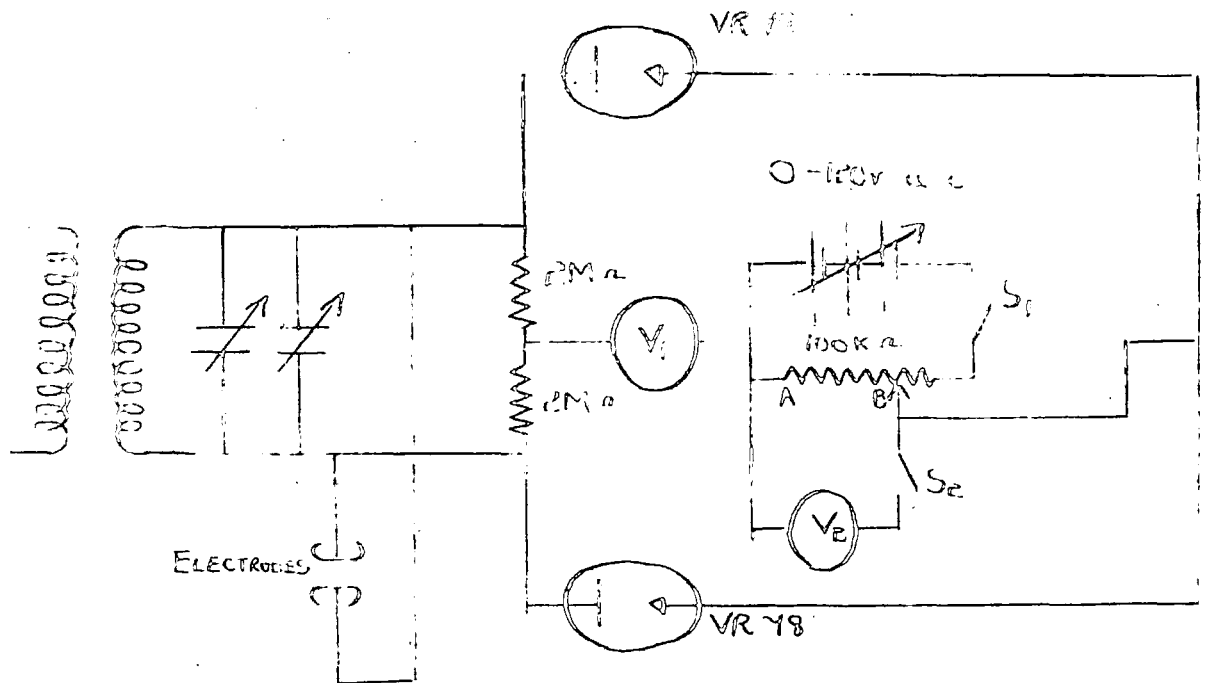
(iii)   Pye Scalalamp electrostatic voltmeter (high range)

Having a sensitive range from 500-2,000 volts, this instrument was used for recording high-voltage breakdown.   The scale was calibrated in 100 volt intervals only (compared with 5 volt intervals in (ii) and 1 volt intervals in (1) above,) and to enable intermediate voltages to be read with accuracy the measuring circuit was modified to the form shown in Fig.13.   The voltage developed across the potentiometer by the 120 volts. H.T. battery was used to bias the electrostatic voltmeter and so return it to nearest 100 volt interval, the bias voltage being measured on the test meter V_2.   Since the electrostatic meter passed no current, flow was confined to the closed circuit consisting of the potentiometer and H.T. source, and never exceeded 1 m Λ .   The test meter recording the bias had a resistance of 20,000 Ω volt^{-1} and passed very little current.   The divided fraction of the voltage across A B could therefore be added or subtracted to the rectified voltage by closing S_1.

This provided a precise method of sub-dividing the electrostatic voltmeter scale, and enabled small variations in breakdown voltage to be identified.

Fig. 14.   The Irradiator Spark Gap

DISCHARGE CHAMBER

IRRADIATOR PULSE. +   EARTH. −

B19

B19

GAS OUTLET   COLLIMATOR

ELECTRODE

CYLINDERICAL COPPER SLEEVE

B14

SPARK GAP

COPPER LEAD.

SILVER STEEL CYLINDER

GLASS TUBE
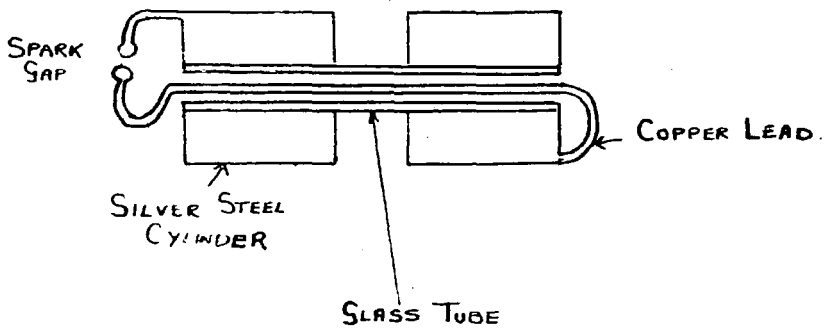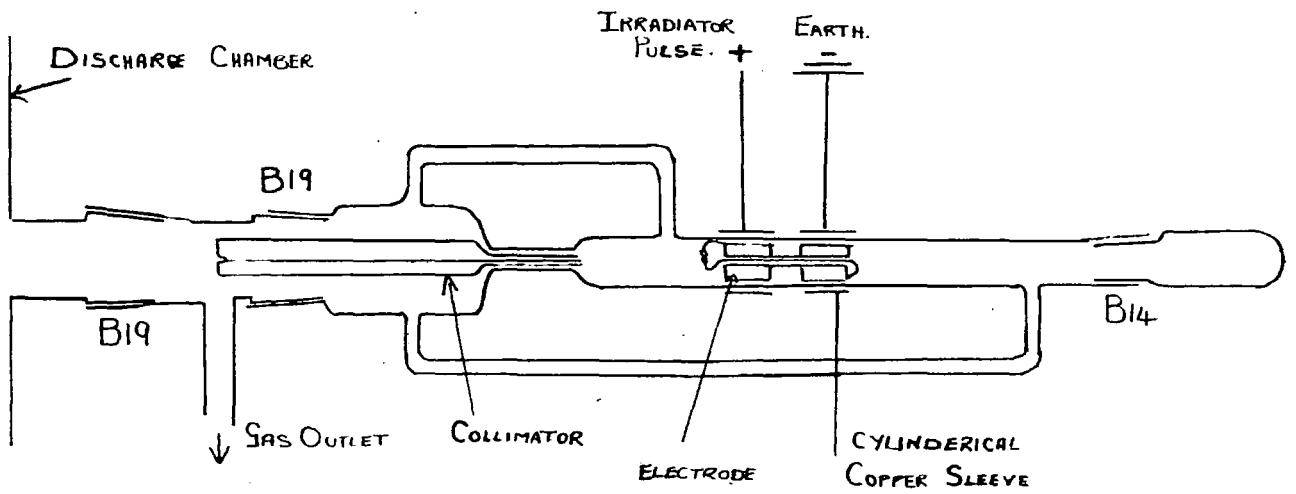
2.6. Irradiation

2.6.1 The irradiating spark gap

A necessary prerequisite of breakdown
is that a triggering, or casual, electron be present
within the test gap. Statistical time lags
associated with a discharge are usually determined by
the arrival of this electron. The condition may
be achieved by photo-irradiation of the gap.
Irradiation by small radio-active capsules placed
behind an electrode is favoured by many workers,
but the possibility of secondary electrode effects
cannot be overlooked in this case. Mid-gap
irradiation by means of a small subsidiary spark
in a side-arm of the discharge chamber was therefore
used; it has already been shown by Prowse & Lane
(1955) that if such a spark is generated at a
suitable distance from the gap, onset values of
breakdown stress are unaffected and statistical
lags considerably reduced.

The irradiator spark-gap, shown in
Fig. 14, had cylinderical steel electrodes which
enabled its position to be moved magnetically in the
side-arm without disturbing the enclosing vacuum.
Leads of thick copper wire connected the
electrodes to the spark gap; the glass tube

Fig. 15.   Neon, 9.5 Mc/s.   Breakdown Potential as a

Function of Irradiator Position
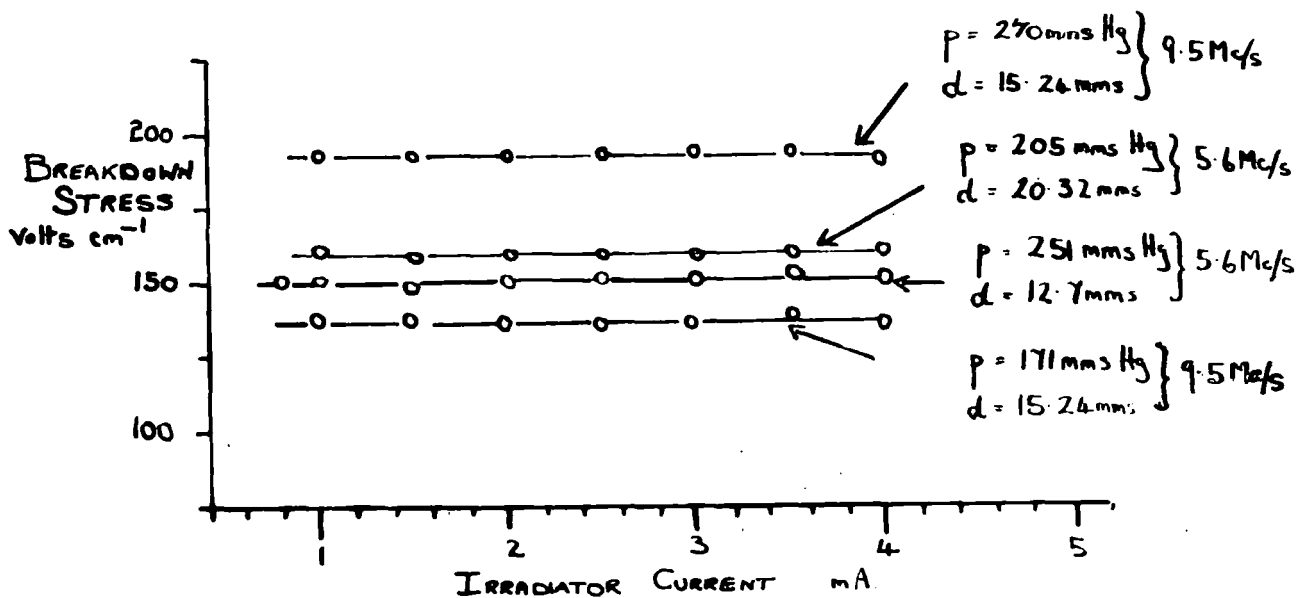
joining the two electrodes served as insulation
and prevented auxiliary sparking. High-voltage
recurring pulses, sufficient to break down the
gap, were applied to a pair of external copper
sleeves, concentric with the electrodes, and
the pulses transferred to the electrodes by
capacitative coupling through the dividing glass
wall of the side-arm. Subsidiary glass arms
fitted to the irradiator tube by-passed the
electrodes and facilitated evacuation of the
apparatus.

Breakdown observations in a number of
gases confirmed that onset potentials were
unaffected by irradiator position in the
neighbourhood of that commonly used (28 cms.
from mid-gap). Typical results for neon are
given in Fig.15.

2.6.2. Irradiator pulsing circuit

The circuit, designed to supply
high voltage pulses of known frequency to the
irradiator spark gap, is given in Fig.16.
A train of negative pulses from the multivibrator,
whose pulse recurrence frequency as governed by the
C.R. time of the grid circuit, was normally 1,000
pps. passed to the control grid of the power pentode

Fig. 16.   Irradiator Pulsing Circuit

+450v H.T

$\sim$ 0-30mA.

50KΩ

L (20H)

5MΩ

6.8KΩ

IRRADIATOR SWITCH

1μF

10KΩ

7KΩ

.001μF

ML4

PT15.

O/P

1MΩ

4μF.

0v
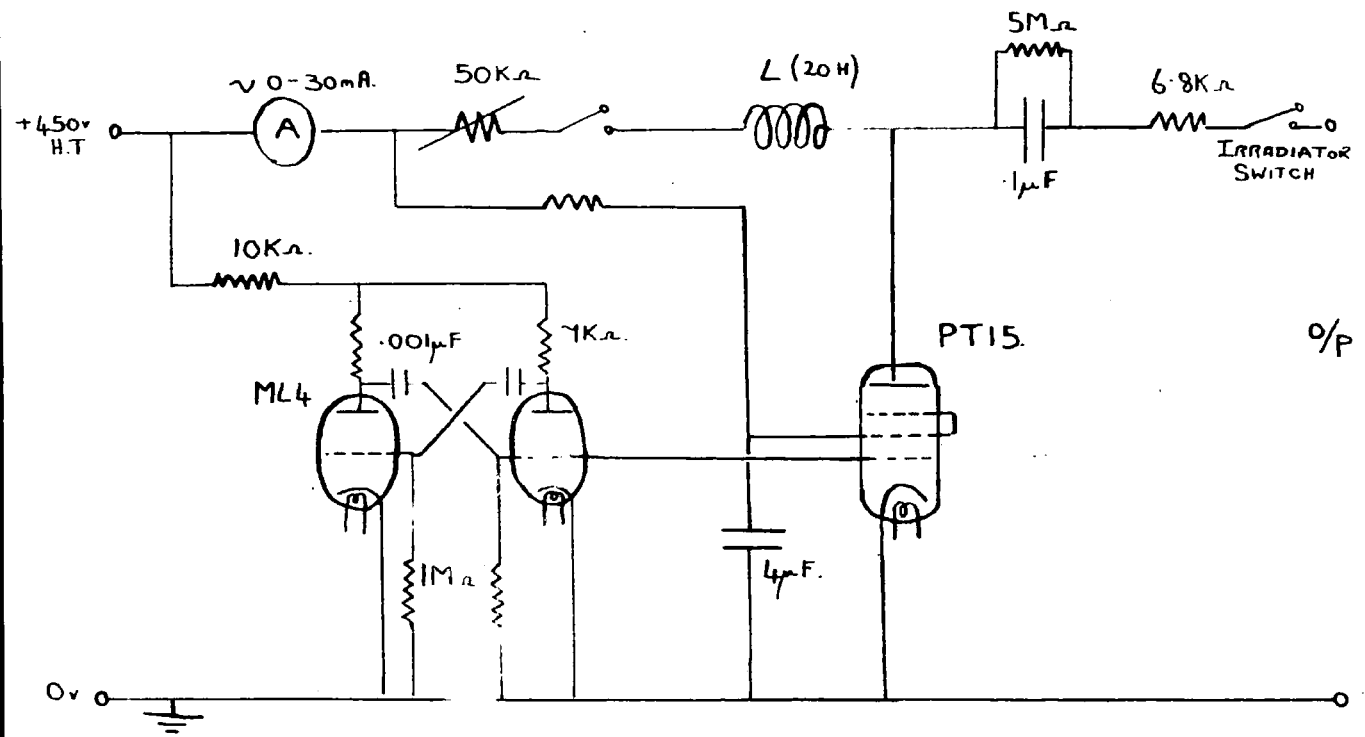
PT.15.   Assuming the pentode to be originally
in a conducting state, the arrival of the leading
edge of a pulse at the grid was sufficient to cause
cut-off.   The anode of the pentode being
inductively loaded with a heavy duty (4 Kv.) choke,
L., the change in current caused by cut-off induced
an E.M.F. $L\frac{di}{dt}$ across it.   At the end of the pulse

from the multivibrator, the valve reverted once
again to its conducting state.   High-voltage pulses
were therefore developed in the anode circuit of the
pentode at a frequency determined by the pulse
recurrence frequency of the multivibrator.   An
earthed coaxial feed carried the pulses, via the
irradiator switch to the external sleeves of the
irradiator spark gap.

CHAPTER 3.

BREAKDOWN IN HYDROGEN

The breakdown measurements in hydrogen fall
into three main groups:

(a) the variation of breakdown stress
with electrode separation and gas
pressure

(b) the variation of breakdown stress
with gas pressure for different
electrode geometries, using fixed
gaps

(c) low pressure breakdown measurements.

3.1. Experimental procedure

The procedure adopted was fairly
standard for each of the gases used. After pumping
down the test side of the vacuum system for two
to three hours, using the diffusion pump, backing pump,
and liquid nitrogen traps, samples of hydrogen were
successively pipetted into the system, and allowed to
circulate before being flushed out by the pumps.
Finally a pure sample of the gas, at the required
pressure was introduced. After the ultra-violet

Fig. 17. Hydrogen, 9.5 Mc/s.
Variation of Breakdown Stress with Electrode Separation. "A" Electrodes.
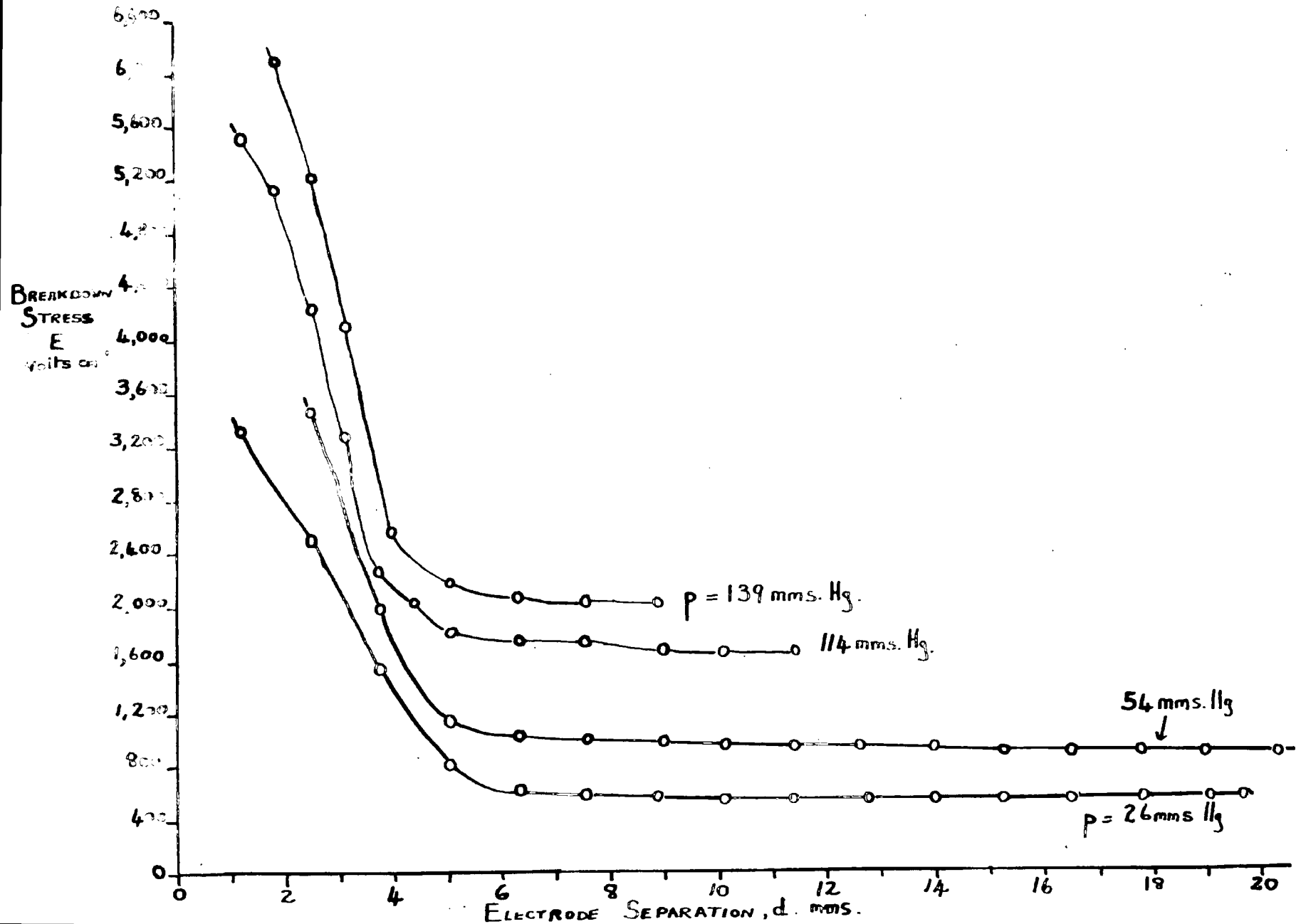
irradiating source had been switched on a small
field was applied to the gap. This stress was
increased in small regular steps until breakdown
occurred.

The threshold voltage for breakdown was
determined by re-applying the field at a slightly
smaller amplitude than that at which breakdown had
occurred, this process being repeated until the
minimum value was found. It was found necessary
to wait a minute or two between successive readings
to allow the gas to 'recover'. Statistical
lags were encountered, usually of the order of
seconds. These times were relatively shorter in
hydrogen than in the other gases investigated,
agreeing qualitatively with measurements by Prowse
& Jasinski (1952).

3.2. Variation of breakdown stress with electrode
separation and gas pressure.

A typical family of curves relating
peak breakdown stress and electrode separation at a
frequency of 9.5 Mc/s is shown in Fig.17. In each
case an increase in the electrode spacing causes a
rapid fall-off in stress up to a certain critical
value of the gap d_c. different for each pressure,
beyond which the onset stress decreases slowly with

increasing gap width. Measurements in gaps
greater than the critical value, d_c, refer to
true u.h.f. breakdown, the electrons oscillating
within the gap each half-cycle of the applied field.
The separation d_c. corresponds to the point at
which electrons just reach an electrode as the
electric field reverses its sign.

The increase in stress at shorter gaps is due
to the fall-off in ionising efficiency resulting
from the removal of electrons to the electrodes.
Nevertheless ionisation in this region is still
more effective than in the corresponding d.c. case,
because the slower-moving positive ions are notremoved.
The space-charge so built up is sufficient to distort
the field and so produce 'enhanced' values of $\propto$
(Reukema 1928).

3.2.1. Numerical calculations of electron ambits.

Referring once more to conditions in the
u.h.f. region, the total amplitude of electron
oscillation (electron ambit) may be calculated at
any point on a particular curve from the breakdown
data and a knowledge of the electron drift velocity.
The electric field may be written as E_t = Epsinwt,
and if it is assumed that the electron drift velocity

is in place with the field variation, then:

$$V_t = V \sin \omega t$$

The electron ambit, d.e., defined as the distance travelled in one half-cycle of the field, is given by:

$$d_e = \int_{t_1}^{t_2} V_t \, dt = \int_{t_1}^{t_2} V \sin \omega t \, dt$$

$$= 2 \int_0^t V \sin \omega t \, dt \qquad \left[\begin{array}{l} t = 0, \ \omega t = 0 \\ t = t, \ \omega t = 2 \cdot \frac{\pi}{2} \end{array} \right]$$

$$\therefore d_e = \frac{2v}{\omega} = \frac{v}{\pi f}$$

The quantity V must now be replaced by data available from the breakdown curves, namely E and p. Gill and Van Engel (1949) point out that the value of V at the peak of E/p is the decisive factor. Accurate values of drift velocity in hydrogen are not available for the entire range of E/p measured; however a sufficiently accurate relationship can be deduced by extrapolating the results of Bradbury and Nielson (1936), and may be presented as:

$$v = 3.5 \times 10^5 \ E/p$$

$$\text{Hence } d_e = 3.5 \times 10^5 \cdot \frac{E}{p} \cdot \frac{1}{\pi f} = 1.15 \times 10^{-2} \frac{E}{p} \text{ cms.}$$
$$(\text{at } 9.5 \text{ Mc/s})$$

The transition from h.f. to u.h.f. conditions must inevitably occur at a finite range of gap width rather than at an ideal critical value, due to a

diffusion spread of electrons crossing the gap.
A 'step' in the E-d curves would therefore be
expected, at the bottom end of which electron
removal would be complete. The top of the 'step'
is not clearly indicated in the hydrogen results,
and calculations of electron ambits, Table 1, are
based on breakdown data at points where the curves
begin to smooth out.

TABLE 1. CALCULATIONS OF ELECTRON AMBITS

E Volts Cm^{-1}	P mm Hg	E/P	d_e (calc.) mms	d (obs) mms
820	26	31.4	3.7	5
1400	54	38.6	4.45	4.5
2280	114	2.0	2.3	3.8
2560	139	1.9	2.2	4.0

It is seen from the table that the calculated values
of d.c. are in each case numerically less than the
electrode separation. Hence electron removal of
these points is complete and at these and larger gaps
breakdown is under u.h.f. conditions.

Fig. 18. Hydrogen, 9.5 Mc/s. Variation of Breakdown Stress with Gas Pressure. "A" Electrodes
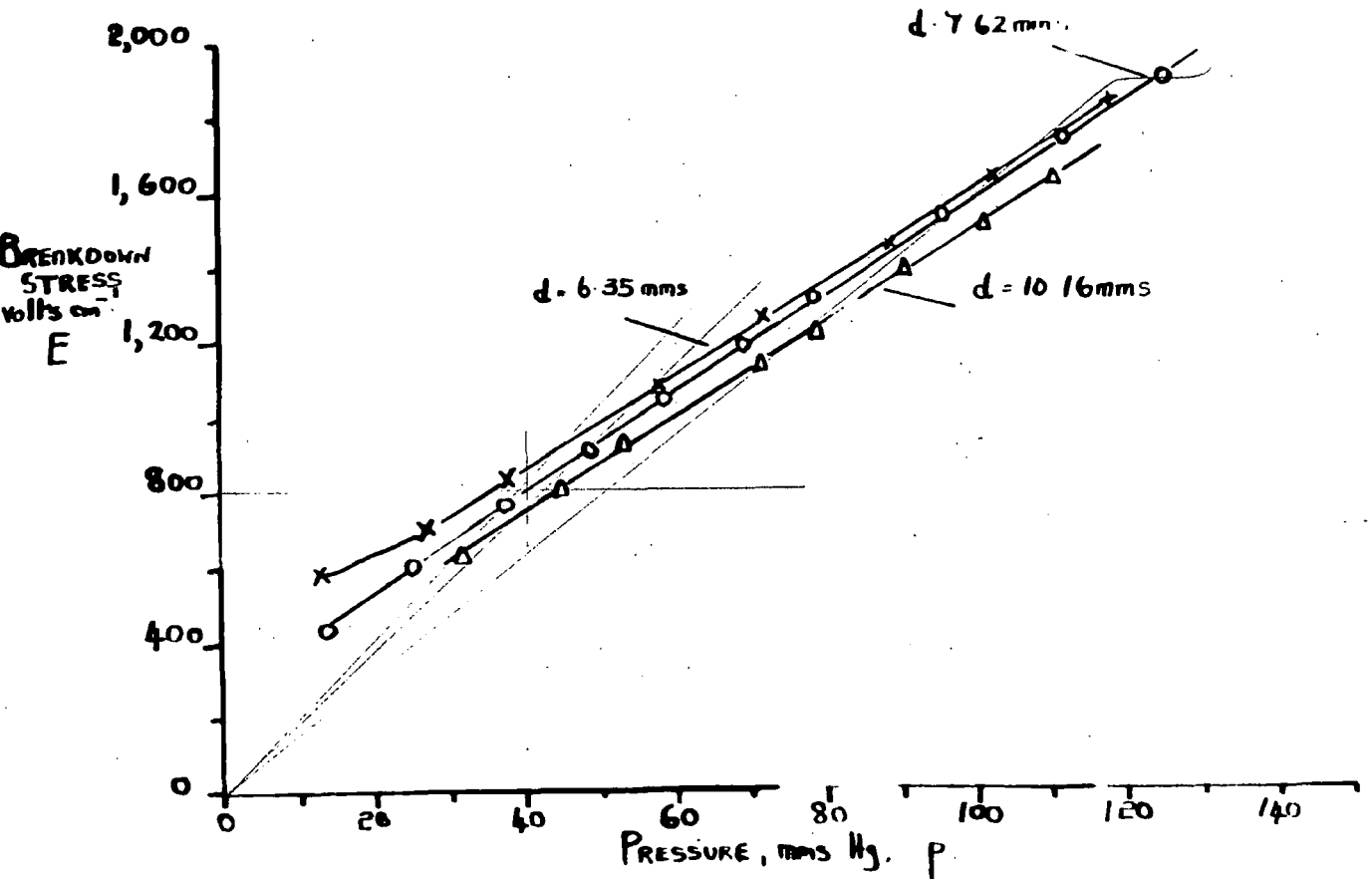
3.2.2. Qualitative interpretation of hydrogen results.

Before discussing the results in
a quantitative manner, it is possible from the
geometry of the curves to obtain some information
regarding the breakdown mechanism. A direct
comparison with the results of Prowse & Lane (1955)
and Fuchs (1956) immediately shows a significant
difference in the form of the curves, for whereas
the results of Fig.17 show a small but steady
decrease in E with increasing d, Prowse and Lane
found breakdown stress to be independent of plate
separation in the u.h.f. region. As stated in
the introduction, their observations were of a
preliminary nature, and the anomalous results
may possibly be attributed to field distortion at
the edges of the electrodes. Moreover, if in
fact u.h.f. breakdown stress was a characteristic of
the gas independent of gap width, it would be
necessary for the E-P curve to exhibit a single
straight line for all gaps in the u.h.f. region.
Measurements were taken employing the variables,
and are given in Fig.18. It is evident from these
results that the breakdown stress, though a linear
function of pressure for any given gap, nevertheless
decreases with increasing d, supporting the results
of Fig.17.

Since a gas breaks down when the gain in electron density caused by ionisation just exceeds their loss, a discharge is controlled by the relative magnitudes of the removal processes. In a d.c. discharge, this loss results primarily from the capture by the electrodes caused by the unidirectional field. Under u.h.f. conditions where electrons remain within the gap, their loss must be accounted for by such factors as diffusion, recombination and attachment. Hydrogen is a non-attaching gas. Recombination, discussed later (3.4), should only become important at pressures of atmospheric order and above, far greater than those employed. The diffusion of electrons in the direction of the negative concentration gradient towards the electrodes or away from the intense field region, must now be considered.

An analysis of the results in the light of the Diffusion Theory proposed by Herlin & Brown (1948) is treated in Section 3.5.1, but it is at once evident that the form of the curves do not contradict the conception of a loss mechanism controlled by diffusion. In particular, reference may be made to the lowering of the breakdown field at larger separations, clearly shown in Figs. 17 & 18.

This lowering would be expected in a diffusion-controlled system, since electron losses are necessarily lower at larger separations. Such a reduction is a fact demanded by the Diffusion Theory.

3.3. General considerations at ultra-high frequencies.

Under u.h.f. conditions, with an electron able to move only a fraction of the distance between the electrodes during a half-cycle of the applied field, the physical mechanisms governing both production and removal of electrons differ from the corresponding d.c. case. Electrons accelerated by a unidirectional field retain most of their kinetic energy during their scatter following collisions with gas molecules, since the mass of the molecule is large compared with that of the electron. The randomly-directed velocities immediately after collision contribute nothing to the flow of electrons in the field direction. Only the small component of velocity in the direction of field contributes to an electron current.

The motion of electrons in a u.h.f. field must be considered in terms of two components,

the oscillatory drift motion and the
random motion due to scatter at collisions.

It is inherent that at high frequencies
and/or low pressures, electrons will tend
to oscillate out of phase with the field,
and the transfer of energy from field to
electrons will be incomplete.

The efficiency of energy
transfer, a function of applied frequency
and collision frequency, was first studied
by Gill and Donaldson (1931), and more
recently by Margeneau (1946) who derives
an 'effective field' E_e, related to the
applied field by the equation:

$$E^2 = E_e^2 \left(1 + \frac{f^2}{f_c^2} \right)$$

f_c = collision frequency
of electrons.

The fractional loss in energy is thus governed by
the magnitude of $\frac{F}{Fc}$. Fc varies with pressure, and
to some extent with the gas used.

In hydrogen, for example, $fc = 1.02 \times 10^9$ p sec^{-1}
(see section 3.5.2.). At microwave frequencies the
fraction $\frac{F}{Fc}$ is thus quite large, but at the
frequency, 9.5 Mc/s, and pressures (always 1 mm.Hg),
used in the experiments, its maximum value given by:

$$\frac{f}{f_c} = \frac{9.5 \times 10^6}{1.02 \times 10^9} \simeq 10^{-3}$$

is small enough to be neglected.

Breakdown under the conditions described above
occurs when the net gain in electron population
due to collision ionisation just exceeds the net loss.
Under the experimental conditions, the factors most
likely to contribute to electron removal are
recombination and diffusion.

3.4. <u>Recombination under experimental conditions.</u>

The extent to which volume recombination
between electrons and positive ions influences the
growth of primary ionisation has been studied by a
number of workers, notably Brown (1948), under
conditions similar to those used, who conclude that
the density of the electron cloud at breakdown is
low enough for recombination effects within the volume

of the gas (the rate of which is proportional to
the square of the ion concentration) to be
neglected.   The problem has been treated
theoretically by Hartman (1948).   An infinite
medium was considered (in which diffusion losses
are, by necessity, zero) and breakdown computed
with volume recombination as the controlling
mechanism.   Such a system would require extremely
high gas pressures and very large, widely-spaced
plates - conditions well removed from the
experimental range considered.

Three-body recombination at the walls of the
discharge chamber and the electrode faces would be
expected to occur more readily, but since an
electron would need to be transported there by a
diffusive process such effects need not be considered
here.

Removal by diffusion will now be considered and
it will be shown in the following sections that the
results obtained in hydrogen may be interpreted by
applying the Diffusion Theory to breakdown at u.h.f.
frequencies.

3.5.   Breakdown in hydrogen in terms of a diffusion-controlled mechanism

(Theoretical considerations in this section
are based on that contained in the paper by Herlin
and Brown (1948)).

3.5.1. Diffusion Theory

If electron losses before
breakdown are assumed to be due to diffusion
processes alone, the breakdown criterion at
ultra-high frequencies lends itself to mathematical
treatment in a relatively simple manner.   Such
a theory has been proposed by Herlin & Brown (1948)
to explain breakdown at microwave frequencies.
Considering the flow of electrons from a volume of
high concentration, the total flow of particles
may be written as:

$$ J = -\nabla(Dn) = -D\nabla n - n\nabla D \quad\dots\dots\; 3.1 $$

where: J = electron current density, electrons
$\text{sec}^{-1} \; \text{cm}^{-2}$

D = diffusion co-efficient of electrons

n = electron density

The second term in Eqn. 3.1. is
inserted to include the possibility of non-
uniformity in the field resulting in a kinetic-
energy gradient (C.H. Kennard 1938).   The build-
up of ionisation leading to breakdown may be
studied by considering the continuity equation
for electrons.   Under the experimental conditions
employed, this may be written as:

$$ \frac{\partial n}{\partial t} = \nu n - \nabla J \quad\dots\dots\; 3.2 $$

(ν is the ionisation rate per electron, i.e. the number of new ion pairs formed within the gap in unit time by one electron).

The original electrons in the inter-electrode space (provided by a flash of u.v. from the irradiator) may be included as an additional term in the above equation, but since they are no longer necessary once collision ionisation has set in, will not be included here.

Substituting the value of given in Equation 3.1., and letting $\psi = Dn$ (the current density potential):

$$\frac{1}{D} \cdot \frac{\partial \psi}{\partial t} = \nabla^2 \psi + \frac{\nu}{D} \cdot \psi \qquad \ldots \; 3.3$$

As the electric field is raised a point is reached where the ionisation just replaces diffusion losses. Any increase in the field will then cause a failure in the equilibrium, and the breakdown criterion may thus be defined by the condition:

$$\nabla^2 \psi + \left(\frac{\nu}{D} \right) \psi = 0 \qquad \ldots \; 3.4.$$

In explaining the results at 9.5 Mc/s by a diffusion-controlled mechanism, it is first necessary to establish that certain assumptions, basic to the Diffusion Theory, are justified under the experimental

—

conditions used. These limits to the theory,
(Brown & McDonald 1949,) are conveniently analysed by
referring the breakdown data to a set of proper
variables.

The breakdown field at high frequencies is a
function of gas pressure (p), wavelength (λ), and
a parameter Λ describing the electrode configuration.
A very useful set of variables involving the
fundamental units, volts and centimetres is:

$$ E\Lambda \quad , \quad p\Lambda \quad , \text{ and } \quad p\lambda $$

The analogy between these variables and those
familiar to d.c. is readily seen, $E\Lambda \equiv V$,
$p\Lambda \equiv pd$; $p\lambda$ has no meaning in d.c. The length
parameter Λ is called the characteristic diffusion
length, and is a measure of the life-time of an
electron in the gap as limited by diffusion either
to the electrodes or laterally away from the intense
field region.

3.5.2. Examination of diffusion theory limits
(i) Uniform field limit

The solution of Eqn. 3.4. for the case
of a uniform field may be given as:

$$ \psi = A \sin\left(\frac{x}{\Lambda}\right) \qquad \dots 3.5. $$

Where A = Constant, x = Distance, from one electrode to some point in the gap. A limit exists to this uniform field condition in that the size of the discharge vessel must be able to sustain a single loop of a standing wave of the field.

This may be written as:

$$\frac{\lambda}{2} \geqslant \pi \Lambda$$

or $\lambda \geqslant 2\pi\Lambda$ the limit being described by equality.

The largest value of $2\pi\Lambda$, calculated from Section 3.5.3., is 1.3 cms. When this is compared with the wavelength of oscillations at the highest frequency used, $\lambda = 3,150$ cms. it is seen that the uniform field limit is readily complied with.

(ii) <u>Mean free path limit</u>

The diffusion theory is not applicable where the electron free path becomes comparable with the dimensions of the discharge tube.

That is, in all cases:

$$\Lambda \geqslant \ell$$

The mean free path may be obtained from the relation $P_c = \frac{1}{p\ell}$, where P_c = collision probability.

Hence: $p\Lambda \geqslant \frac{1}{P_c}$

Using the value of Pc measured by Brode (1933),
the condition becomes:

$$p \Lambda \geqslant \frac{1}{49}$$

It can be seen from Table 2 that at the extreme
pressure and plate separations used, the m.f.p.
is always very small compared with the diffusion
length.

TABLE 2   MEAN FREE PATH LIMIT

Condition for mean-free path limit	$p \Lambda >$	$\frac{1}{49} \; (= \cdot 0202)$
P, mm Hg	Λ cms	$p \Lambda$
26	0.215	5.6
54	0.194	10.4
114	0.155	17.6
139	0.155	21.5

(iii) Collision frequency transition

A further departure from diffusion-
governed breakdown occurs when the collision
frequency, $V_c = 2\pi f_c$, between electrons and gas
molecules equals the field frequency.

The pressure at which this occurs
(corresponding to the change from many collisions per
oscillation to many oscillations per collision) can

Fig. 19. **Hydrogen, 9.5 Mc/s.** **Variation of Breakdown Potential with pd**
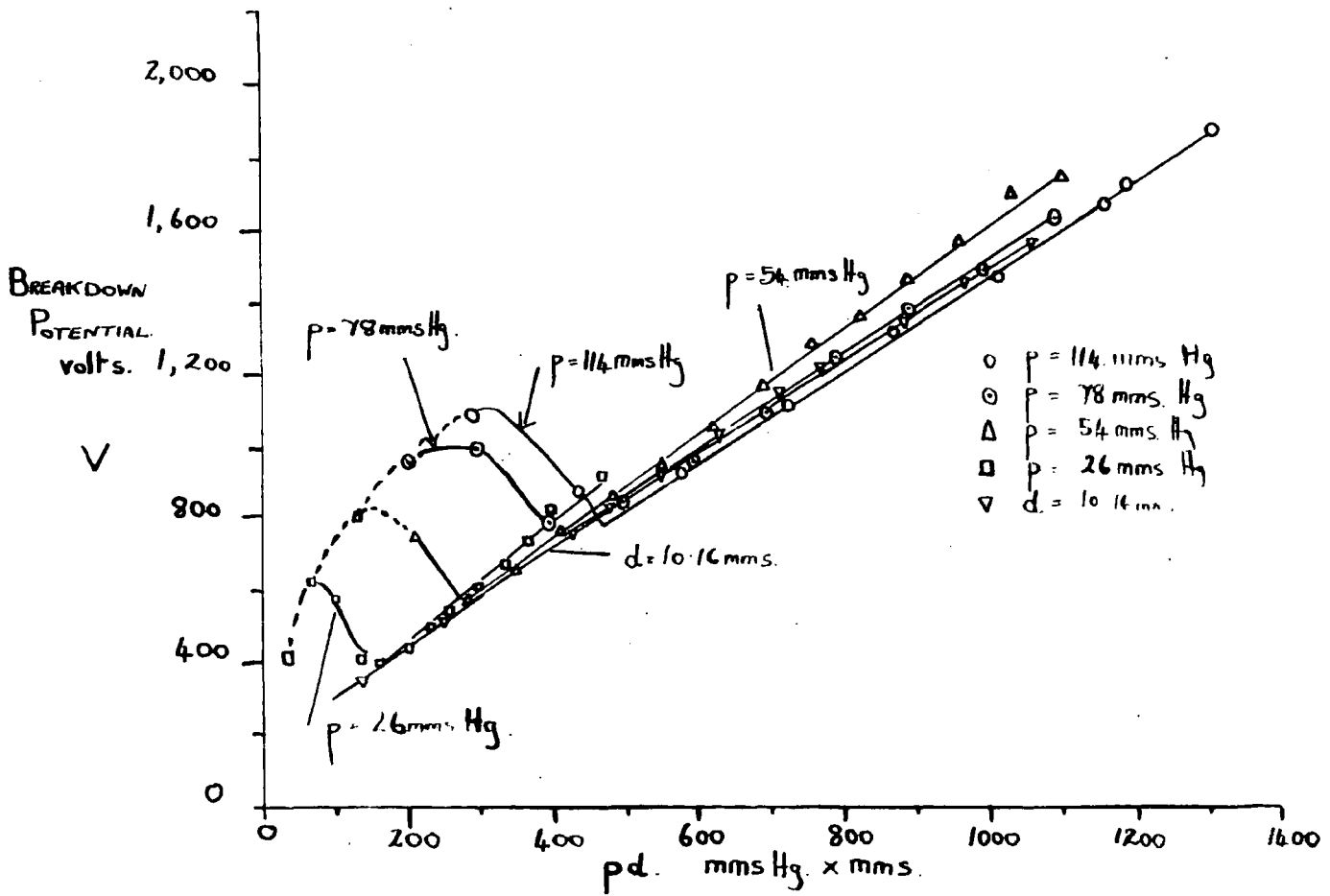
be approximately predicted from the formula

$$f_c = \tfrac{1}{4}\bar{V}P_c$$

where $\bar{V}$ is the random velocity corresponding

to the average electron energy.

Using Townsend's (1947) value for $\bar{V}$, given as 5×10^7

cm. sec.$^{-1}$, and the value of P_c given in (11) above.

$$f_c = 1.02 \times 10^9 p$$

This is the limiting case and for the theory to apply:

$$f_c < 1.02 \times 10^9 \, p$$

$$p > \frac{f_c}{1.02 \times 10^9} \text{mms.Hg}$$

Inserting the maximum frequency used, 9.5 Mc/s.

$$p > 1.02 \times 10^{-3} \text{ mms.Hg.}$$

Since the minimum pressure used was above 1 mms.Hg,

in no case was the imposed limit approached.

3.5.3. Applicability of the diffusion theory

In a d.c. discharge breakdown curves as

a function of pressure (at constant gap width) or

electrode separation (at constant pressure) are often

drawn as Pashen Curves, in which breakdown voltage,

$V = Ed$, is plotted against pd. It is found that all

such curves have the same shape, i.e. the breakdown

voltage at a given value of pd. is independent of

either p or d. The same quantities can be related

to high-frequencies, and Fig.19 shows V plotted against

pd for a variety of pressures and electrode
separations at 9.5 Mc/s. A minimum indicates a
point on a particular curve where the electron
ambit just fills the tube. It is seen that
in the v.h.f. region the breakdown curves be
approximately parallel to one another but do not
coincide. The amplitude of V at a fixed value of
pd is thus dependent upon the relative magnitudes
of p & d. This is consistent with the demands of
the diffusion theory, in which breakdown voltage is
a function of electrode separation.

It is more informative at u.h.f., however,
to express breakdown in terms of the proper variables
derived by McDonald & Brown (1949), and in this way
a direct test of the Diffusion Theory may be made.
In a diffusion-controlled discharge the distinguishing
feature is that the life-time of an electron in the
gap is limited by its removal by diffusion to the
boundaries, namely, the electrode faces or laterally
out of the intense field region. This life-time
may be expressed direct in terms of the parameter Λ ,
which for a parallel plate electrode system is a
function of electrode diameter and gap width.
If breakdown in a particular system is diffusion
controlled, plots of effective breakdown voltage $(E\Lambda)$

against $p \wedge$ give a unique curve, the magnitude
of $E \wedge$ at any point being independent of the
relative values of $\wedge$ or p. This provides a
quantitative test of the applicability of the
diffusion theory. If diffusion is the removal
mechanism of electrons, then plots of $E \wedge$
against $p \wedge$ for various pressures and electrode
configurations should give a smooth continuous
curve, values of $\wedge$ having been computed on the
assumption that the mean life of an electron created
in the gap is limited by diffusive processes alone.

Calculation of Diffusion Lengths

The characteristic diffusion length of an
electron may be calculated exactly for the parallel
plate spark-gap used in the experiments.

At short gaps, electron removal to the
electrodes dominates, whereas for larger separations
lateral diffusion away from the intense field region
is the important factor.

Incorporating both these terms, the diffusion
length $\wedge$ may be written, (Brown & McDonald 1949) as:

$$\left(\frac{1}{\wedge} \right)^2 = \left(\frac{\pi}{d} \right)^2 + \left(\frac{2.405}{a} \right)^2 \quad \ldots \ldots 3.6$$

where 'a' is the radius of the electrodes.

Fig. 20. Diffusion Length as a Function of Electrode Separation. "A" Electrodes.
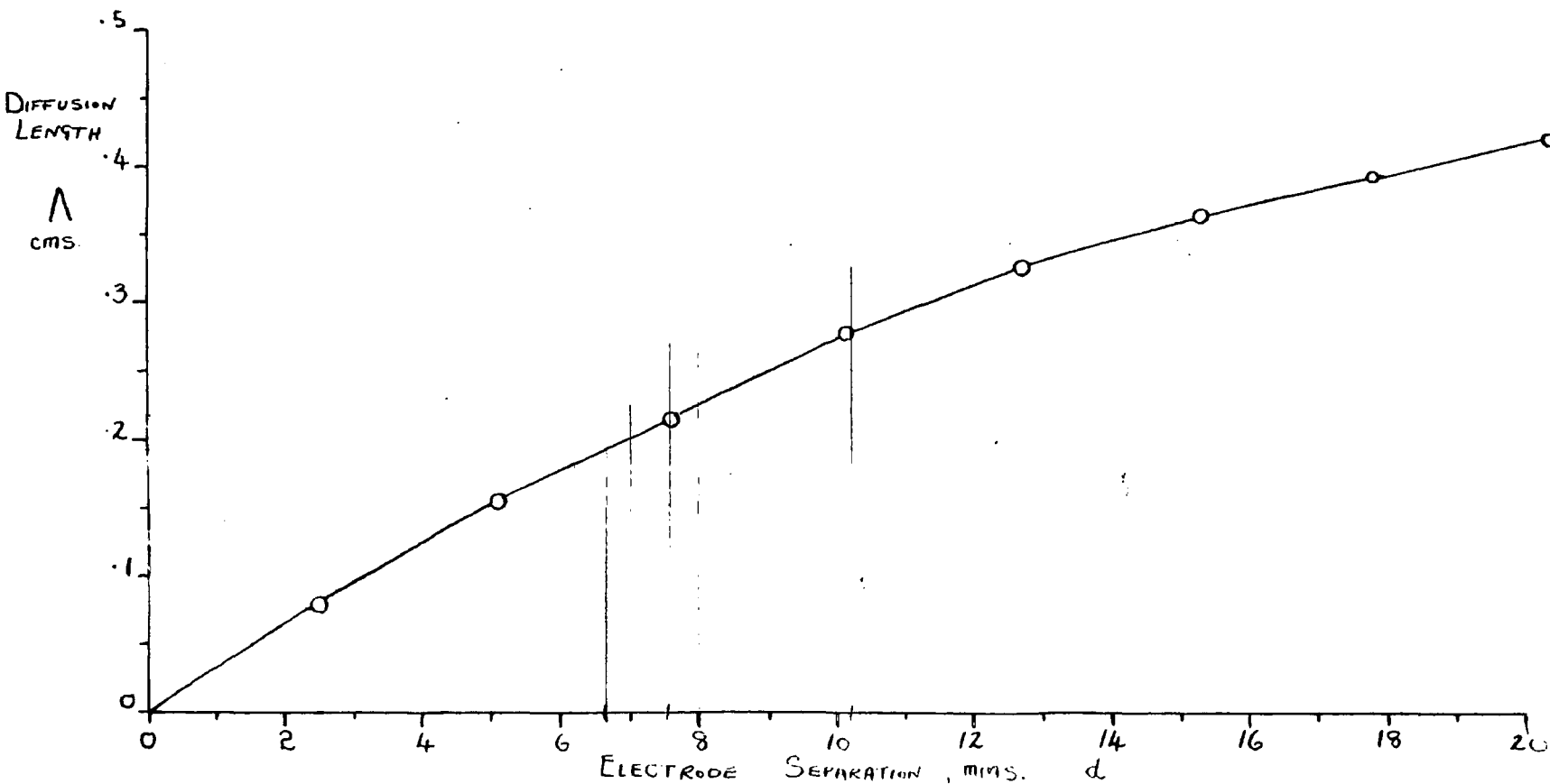
For a given pair of electrodes the diffusion length is consequently a function of electrode separation. The 'A'-type Rogowski-profiled electrodes used in the above experiments were of maximum diameter 3.69 cms. and uniform field diameter 2.67 cms. Lateral losses were considered to be effective after the electrons had diffused from the uniform field boundary.

Inserting the appropriate value of 'a' in equation 3.6. , a curve was constructed, Fig. 20, with diffusion length plotted as a function of electrode separation.

Variation of $E \Lambda$ with $p \Lambda$

By computing the breakdown data in terms of $E \Lambda$ and $p \Lambda$, the series of curves displayed in Fig. 21., was constructed. It can be seen that points in the u.h.f. region lie on a common curve, approximately straight, which can be drawn so that no experimental point varies from it by more than 4%. Each discontinuity appearing describes the condition that, as the electrode separation is decreased at a given pressure, a point is reached where the electron ambit fills the tube.

The results agree with the diffusion theory in that points in the u.h.f. region lie on a smooth continuous curve, and it is evident that breakdown in

Fig. 21.   Hydrogen, 9.5 Mc/s.

Variation of $E_r \Lambda$ with $p \Lambda$.

$E_r \Lambda$
volts

$\triangle$ p = 114 mms. Hg
$\circ$ p = 78 mms Hg.
$\times$ p = 54 mms Hg
$\triangledown$ p = 26 mms Hg
$\square$ d = 10.16 mms.

$+$ 5.5 Mc/s.

$p \Lambda$ mms Hg × cms
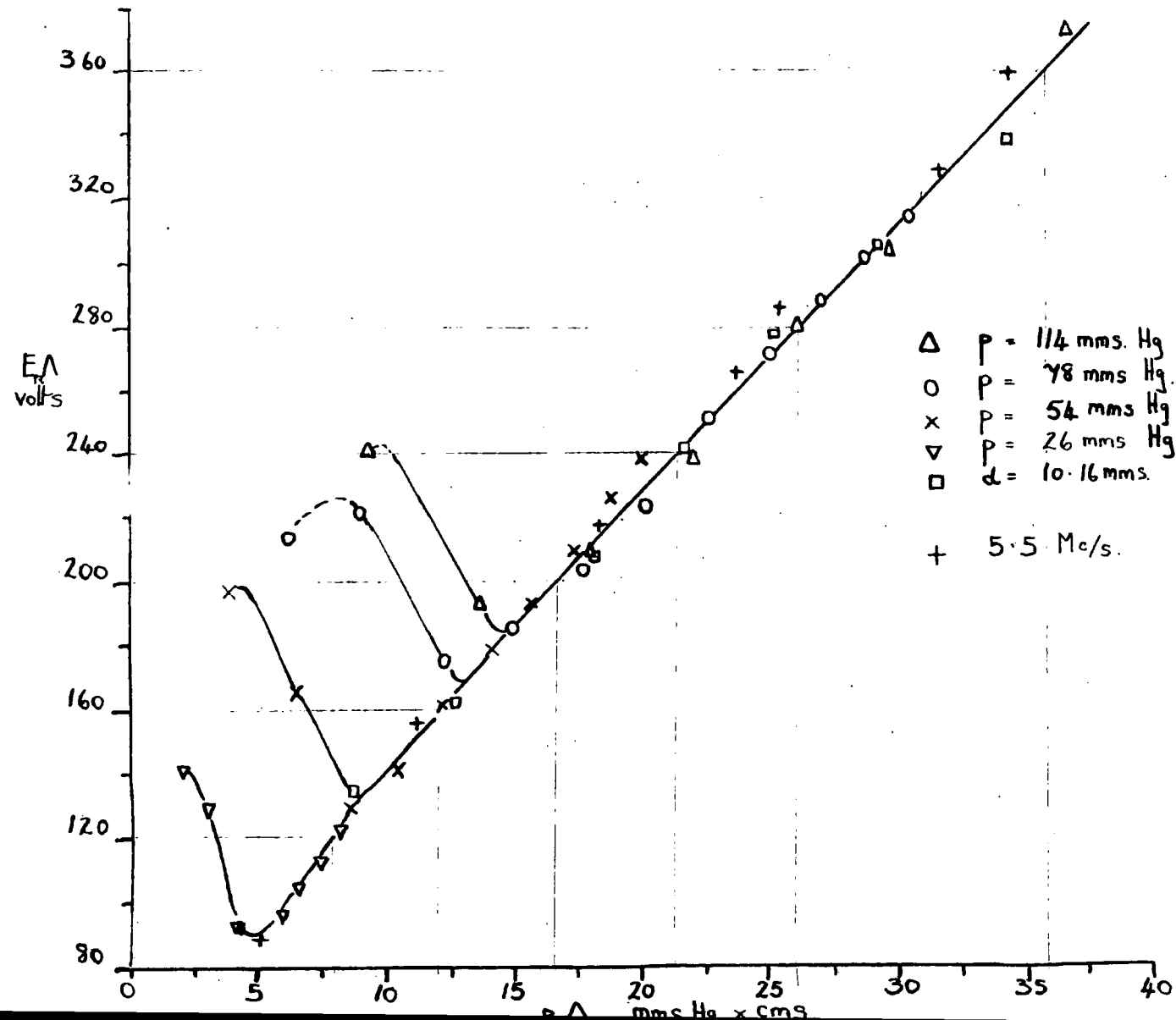
hydrogen at 9.5 Mc/s is controlled by diffusion processes.

Variation of E Λ with p λ

At high frequencies a further variable must be considered, the wave-length λ of the applied oscillations. This term may be included as the parameter p λ .

Where the data for a set of breakdown measurements includes frequency variation as well as variation of p & d, a three-dimensional plot may be made of the variables E Λ, p Λ and p λ, and the data may be represented by a single surface. Within the u.h.f. frequency range, bounded at one end by the collision frequency transition and at the other by the electron ambit limit, there is no reason to expect any variation of E Λ with p λ . This has been demonstrated by several workers, and is clearly shown on the solid model constructed by Brown (1955).

The frequency variation was not included in the hydrogen results, but a set of measurements, Fig.22, were taken at a constant frequency of 5.5 Mc/s showing the same pattern as those at the higher frequency. Spot values from the 5.5 Mc/s results are included in Fig. 21, these are seen to lie on the general curve, and indicate that breakdown in the radio frequency region is independent of λ .

Fig. 22. Hydrogen, 5.5 Mc/s.

Variation of Breakdown Stress with Electrode Separation.
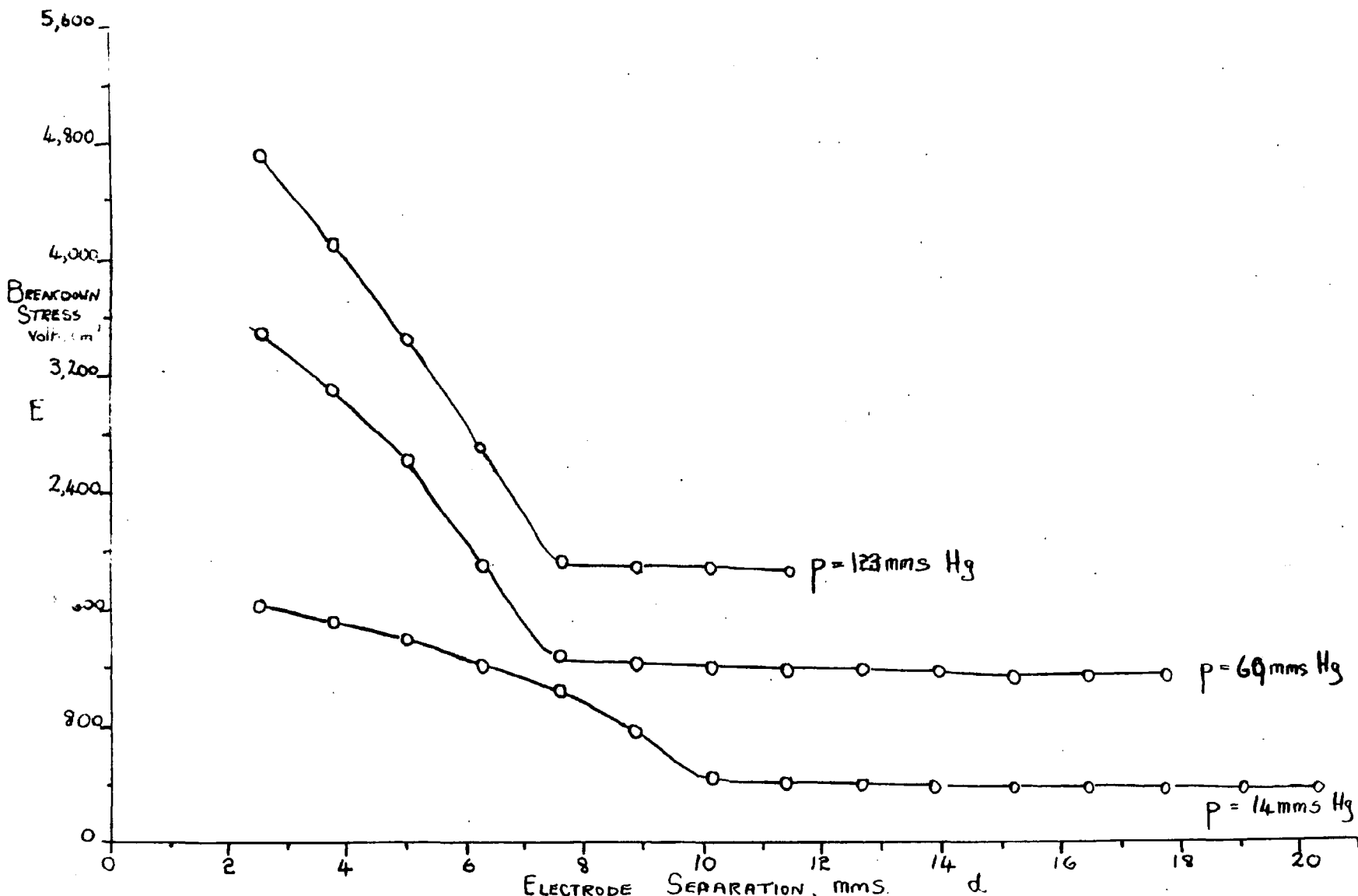
3.6.   <u>Effect of varying the electrode size</u>

3.6.1.   <u>Importance in view of previous results</u>

The results of varying the gas pressure and electrode separation, discussed in Sections 3.2 - 3.5., indicated that breakdown in hydrogen in the v.h.f. region is controlled by diffusion. In these experiments one important parameter, the size of the electrodes, was kept constant. Since the magnitude of the electrode radius plays an integral part in controlling the lateral diffusion of electrons, particularly at large plate separations, it was considered that a series of breakdown measurements involving electrodes of various sizes was essential as a confirmation of the applicability of the diffusion theory in the u.h.f. frequency range.

3.6.2.   <u>Experimental considerations</u>

Electrodes of four different sizes were employed, all profiled to the Rogowski pattern.   Their method of construction has been described in Section 2.2.   The difference in size between the largest and smallest pair of electrodes used was made as great as possible, the upper limit being restricted by the diameter of the Pyrex discharge chamber.

Table 3 tabulates the dimensions of the
electrodes employed, the letters appearing
in the left-hand column are introduced to
discriminate between separate pairs.

TABLE 3.   ROGOWSKI - PROFILED ELECTRODES

Electrode Material – brass		
Electrode Type	Maximum diameter Cms. _radius_	Uniform field, diameter Cms.
A	3.69 _1.38_	2.67 _0.72_ _0.66_
B	3.15 _1.53_	2.06
C	1.58 _1.76_	0.90 _0.57_
D	0.63 _1.61_	0.39 _0.62_

It was decided to observe breakdown as a function of
pressure at two gap separations, 7.62 mms and 10.16 mms.,
for each pair of electrodes, making a total of eight
sets of readings.   The characteristic diffusion
length for each set of conditions was calculated by
transforming equation 3.6 into the form:

$$\Lambda = \frac{1}{\sqrt{\left(\frac{\pi}{d}\right)^2 + \left(\frac{2\cdot405}{a}\right)^2}}$$

and the calculated values shown in Table 4.

Fig. 23. Hydrogen, 9.5 Mc/s. Breakdown at Fixed Gap Width for varying Electrode Diameters. Electrode Separation = 7.62 mms
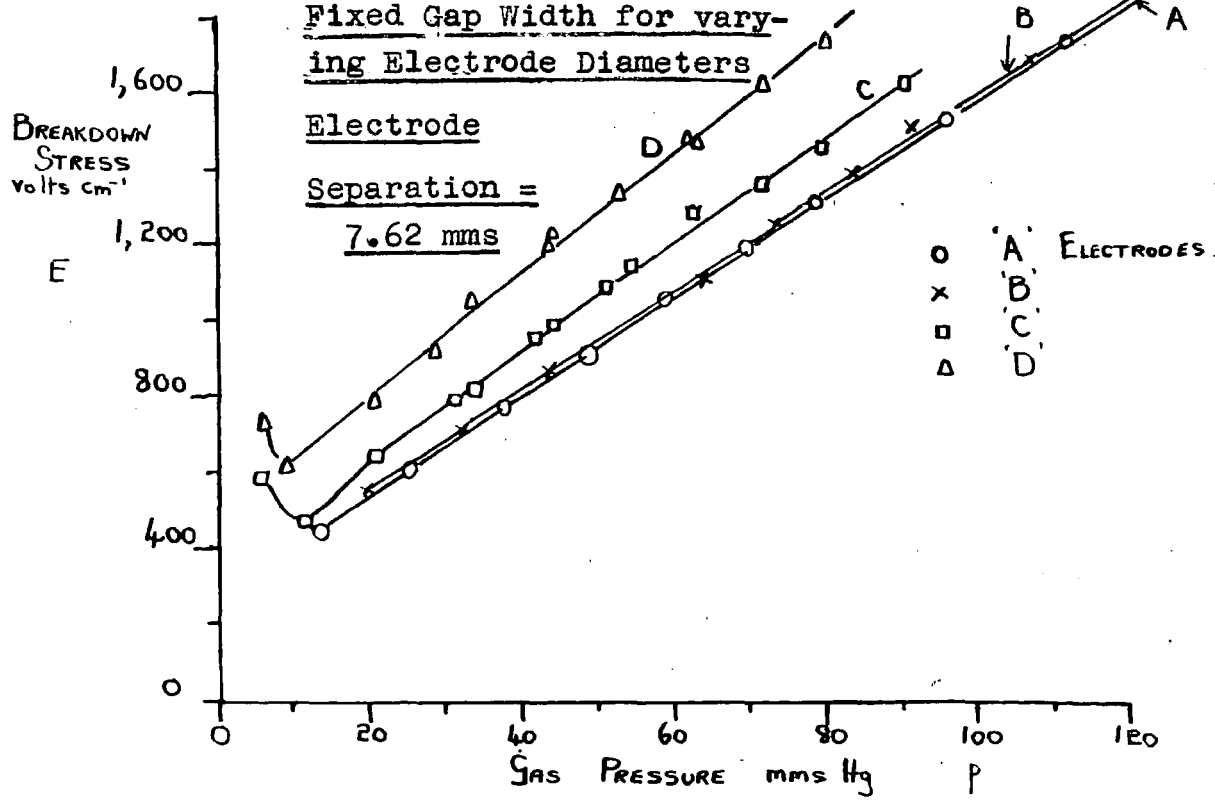
Fig. 24. Breakdown at Fixed Gap Width for varying Electrode Diameters. Electrode Separation = 10.1
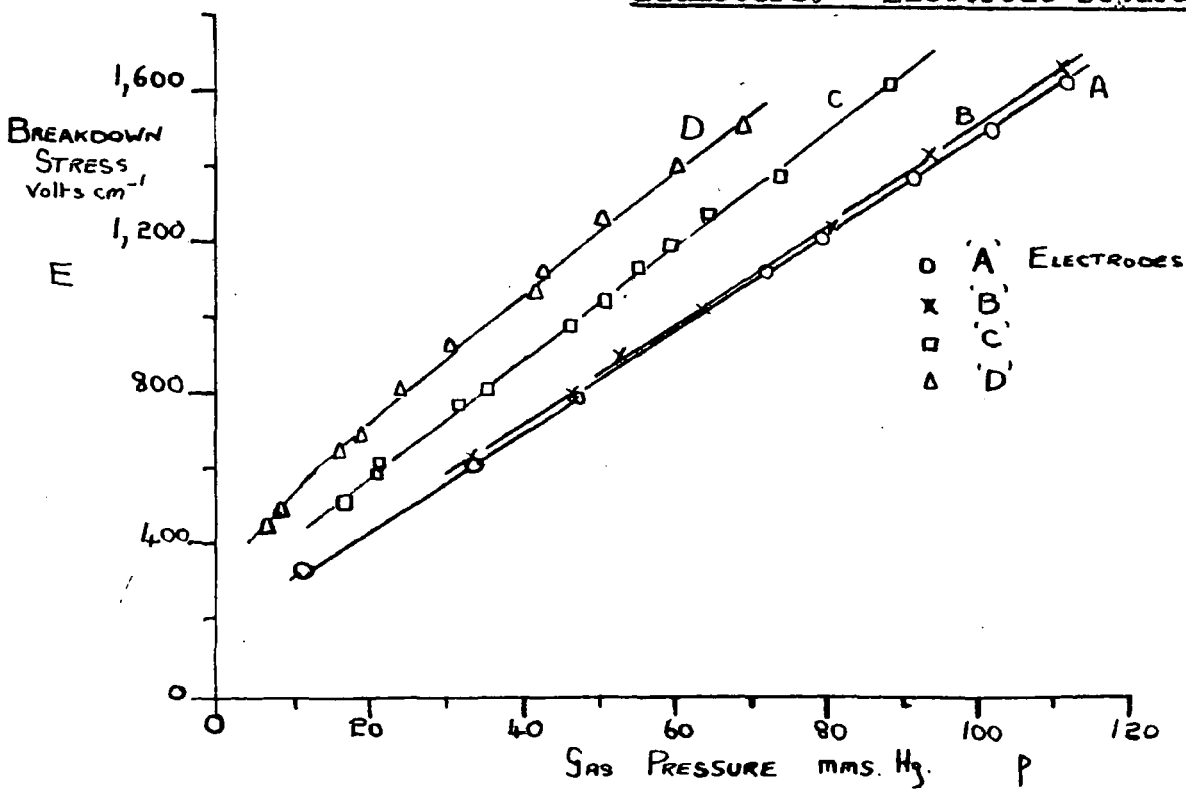
TABLE 4. CHARACTERISTIC DIFFUSION LENGTHS

Electrode Type	Λ, cms (d=7.62 mms.)	Λ, cms (d=10.16 mms.)
A	0.215	0.2792
B	0.205	0.2585
C	0.146	0.162
D	0.0748	0.0775

3.6.3. Experimental results

(1) At d = 7.62 mms. The family of curves shown in Fig.23 are the runs taken for the different electrode sizes at a constant electrode separation of 7.62 mms. The voltage required to break down the gap at constant pd is seen to increase progressively with decreasing electrode diameter. This is an expected trend in a system governed by diffusion; electron losses by lateral diffusion being necessarily greater from the smaller sized plates, a greater stress is needed to initiate a discharge.

(ii) At d = 10.16 mms. Similar sets of measurements, Fig 24, were observed when the separation was increased to 10.16 mms. A comparison of breakdown fields

Fig. 25. **Variation of E_aΛwith pΛ for Different Electrode Diameters and Gap Separations.**
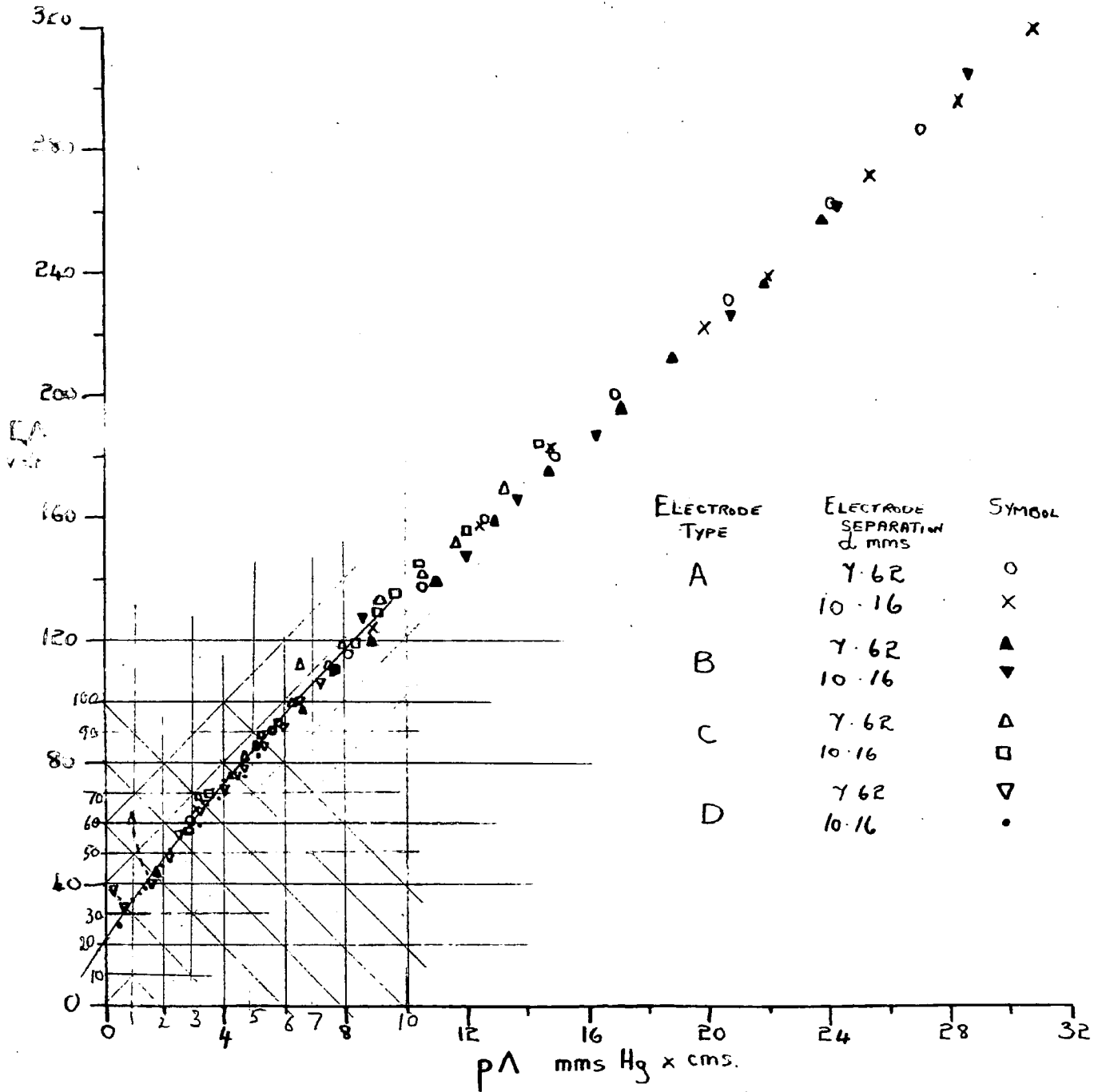
between similar electrodes separated by the
different gaps shows that a smaller stress was
necessary to initiate breakdown in the larger
gaps.   This phenomenon has already been
encountered - Fig 18   - and may be explained by
considering relative diffusion losses to the
electrodes.

3.6.4.   Presentation of results with respect to the proper variables.

When the breakdown measurements are
presented as functions of $E \Lambda$ and $p \Lambda$, Fig. 25,
the data lie on a continuous curve within the
limits of experimental error (Section 7).
Results taken for the different electrode sizes
and separations over-lap one another over a
considerable range.

These results confirm that u.h.f. breakdown in
hydrogen at u.h.f. frequencies is governed by
a mechanism in which the growth of electron
population within the gap due to collision ionisation
is restricted by the diffusion of electrons, (a) to
the electrode faces and (b) laterally out of the
intense field region into the surrounding gas
and ultimately to the walls of the discharge
chamber.   The relative magnitudes of effects (a)

and (b) are functions of electrode size and
separation.

3.7. Low pressure breakdown

3.7.1. Value of low pressure data

The range of gas pressure studied
in the experiments described, 10 mms - 130 mms.,
enabled an interpretation of breakdown to be
made over a wide range of the variables involved.
A further parameter frequently used in gas discharge
studies is the reduced value of the electric field,
E_R/p, and it is useful to discuss breakdown in
terms of this quantity. This applies in particular
to studies of ionisation coefficient. At high
pressures, E/p at breakdown was found to change
only slowly for considerable changes of p,
and at the highest pressures used approached the
constant value $E = 10\ p$. Studies of ionizing
efficiency were therefore confined to a range
E^R/p limited from 10 - 20, and graphical
presentation of such results were unsatisfactory
owing to the insensitive nature of the curves.
Breakdown measurements were thus recorded at
relatively low pressures, where small changes in
p would cause substantial variations in E_R/p.

Fig. 26. Hydrogen, 9.5 Mc/s.

Breakdown at Low Pressures.
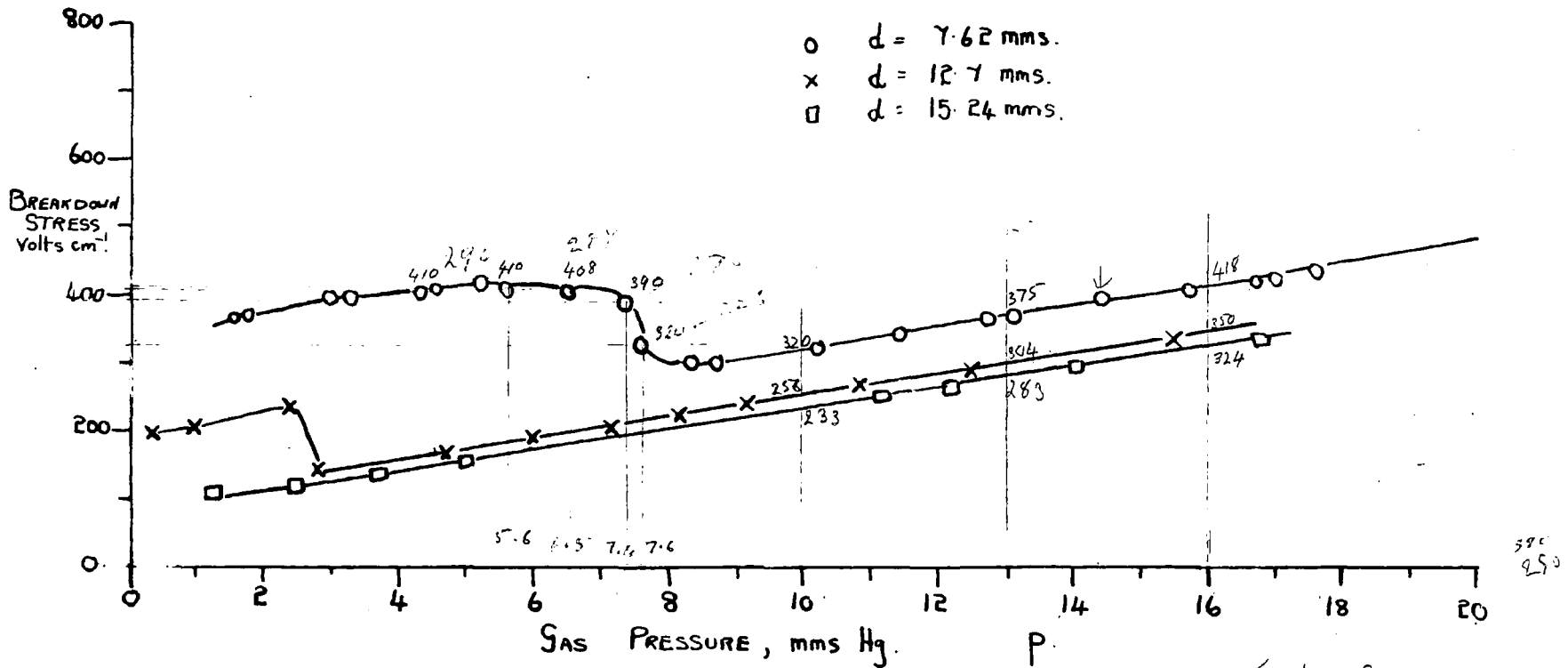
3.7.2. Experimental details

The Bourdon Gauge, normally used
for pressure measurements, proved unsuitable
for recording low pressures, being rather
insensitive below 15 mms.Hg (See calibration
curve, Section 2.3.3.). As a result, a new
gauge was fitted to the vacuum system - the Pye
CG.1 Dial Model. The scale, calibrated from
0-40 mms.Hg., was linear throughout the range.
Below 3 mms.Hg., the irradiating spark in the
side-arm of the discharge chamber became diffusive
in nature and spread considerably. The intensity
was reduced by adjusting the output impedance
of the multivibrator circuit (Section 2.6.2.)
and so lowering the amplitude of the irradiator
pulse. Subsidiary observations, described in
Section 2.6.1., established that the breakdown
field remained unaffected by these changes.

3.7.3. Results of low pressures

Breakdown measurements at three
electrode separations are presented in Fig. 26,
as functions of gas pressure in the range 0.3 mms.Hg
- 20 mms.Hg. The curves exhibit the same general
pattern as those at higher pressures. Minima

correspond to the electron ambit just
filling the tube; the progressive
lowering of onset field with increasing gap
separation is again a result of the slower
removal of electrons by diffusion.

3.7.4. High-frequency ionisation coefficient

The efficiency of ionisation in a
gas subjected to an electric field is conveniently
described in terms of an ionisation coefficient.
In a d.c. field the primary coefficient of
ionisation (Townsend's α) is defined in terms of
the electron drift motion towards the positive
electrode, by the number of new electrons
created by an electron travelling one centimeter
in the field direction.

i.e. $$n = n_0 e^{\alpha x}$$

α is thus the
number of new
electrons produced
(by collision
processes) in each
cm. of the gap, and
hence may be written
as:

$$\alpha = \frac{v}{\bar{v}}$$

Where
$\bar{v}$ = Average electron
    drift velocity
And
v = ionisation rate
    per electron

Rewriting this as ionisations/volt: $$\zeta = \frac{\alpha}{E_R} = \frac{v}{\bar{v} E_R}$$

But since $$\bar{v} = \mu E_R$$

$$\zeta = \frac{v}{\mu E_R^2}$$

... 3.7.

Fig.27. Hydrogen, 9.5 Mc/s.

High Frequency Ionisation Coefficient.
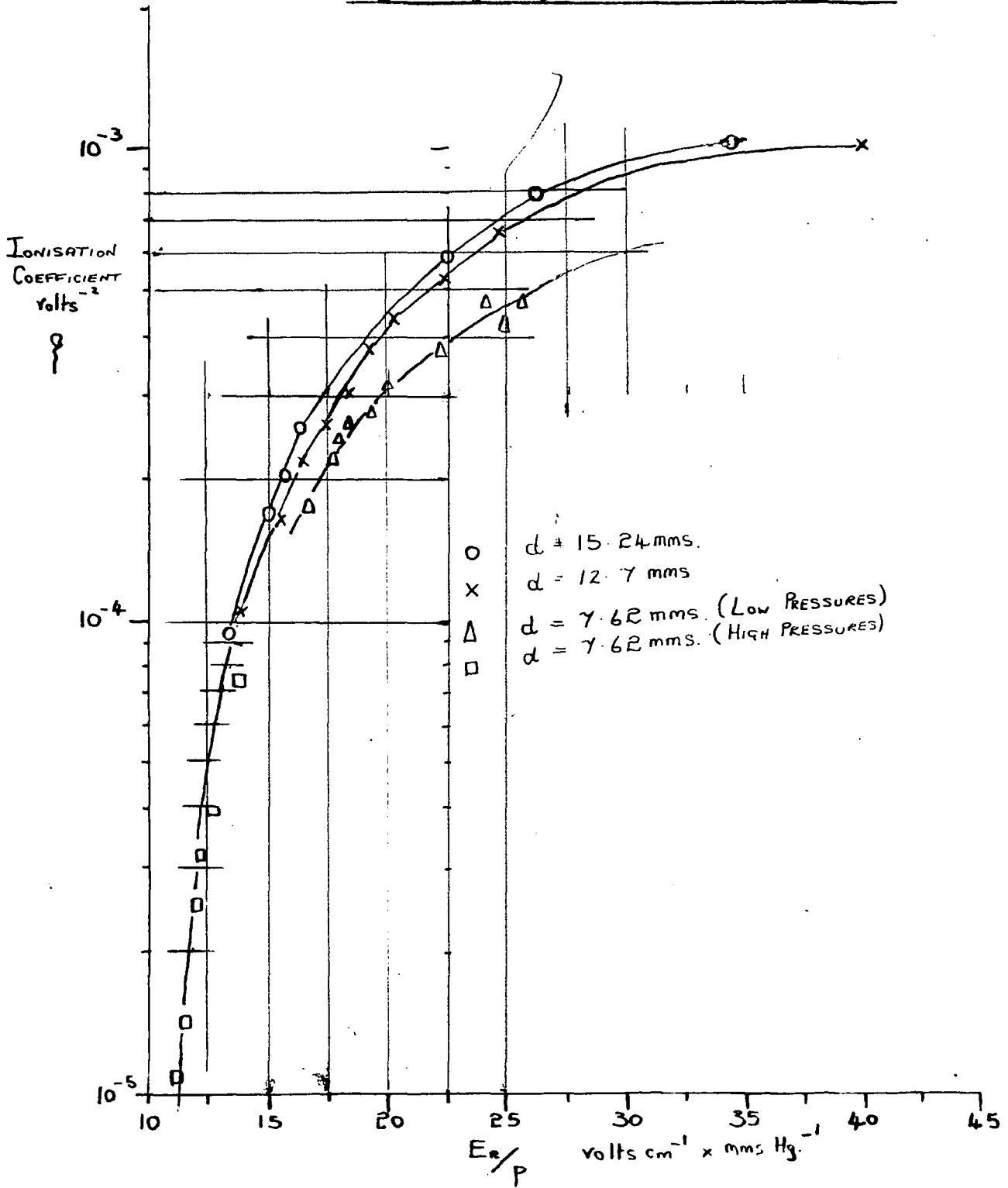
Under u.h.f. conditions, the drift velocity
of electrons is produced by diffusion instead
of mobility motion, and a 'high frequency'
ionisation coefficient may be introduced (Brown
1951), analagons to the first Townsend
coefficient: ζ .

$$\text{i.e.} \quad \zeta = \frac{\nu}{D \, E_R{}^2}$$

For parallel plate electrodes:

$$\frac{\nu}{D} = \left(\frac{1}{\Lambda}\right)^2$$

Hence: $\quad \zeta = \frac{1}{E_R{}^2 \Lambda^2} \quad$ with units Volt^{-2} ... 3.8.

Numerical values of ζ were computed from the
low pressure breakdown data, and are presented
in Fig 27., as a function of E_R/p.   The curves
correspond to breakdown at the three different
gap widths.   A further set of values is
included, taken from the higher pressure
measurements, Section 3.2.
The curves form a common envelope at low values
of E_R/p, corresponding to high pressures when
the electrons make many collisions/oscillations.
As E_R/p increases the curves begin to diverge;

for a given value of E_R/p the ionising efficiency
is greater at the largest value of plate
separation, indicating once again the relative
decrease in diffusion losses with increasing d.
Typical cases are illustrated in Table 5.

TABLE 5.   HIGH-FREQUENCY IONISATION COEFFICIENT

E_R/p	ς) Volts^{-2}		
	d = 15.24 mms	d = 12.7 mms.	d = 7.62 mms.
13	7×10^{-5}	7×10^{-5}	7×10^{-5}
16	2.2×10^{-4}	1.9×10^{-4}	1.5×10^{-4}
20	4.6×10^{-4}	4.2×10^{-4}	3.1×10^{-4}
25	7.2×10^{-4}	6.7×10^{-4}	4.6×10^{-4}

These curves may be used to predict breakdown in
system using different field configurations.

3.7.5.   Low values of breakdown field

Examples are given in Table 6 of typical
measurements of breakdown stress and voltage
recorded in the low pressure measurements.

TABLE 6   VALUES OF BREAKDOWN FIELD

$d = 12.7$ mms.			$d = 15.24$ mms.		
P mm Hg	E_R Volts cm^{-1}	V_R Volts	P mm Hg	E_R Volts cm^{-1}	V_R Volts
2.4	96	122	1.25	77	117
4.75	118	150	2.5	86	131
6.0	133	169	3.7	97	148
7.2	145	185	5.0	113	172

These values are considerably smaller than are normally associated with spark discharges in hydrogen. From a technical point of view a more thorough investigation of optimum breakdown in this region may be of interest, and given the correct conditions it is thought likely that breakdown will occur at very low voltages. This problem is discussed more fully in the case of breakdown in air (Chapter 6).

3.8.   Comparison of results with those of other workers.

High frequency breakdown measurements have been recorded in hydrogen by a number of workers over a frequency range varying from 10 mc/s to the microwave region. When these results lie within the prescribed limits for a diffusion-controlled breakdown, a direct comparison of data may be made.

Fig. 28. Hydrogen, 9.5 Mc/s to 10,000 Mc/s.

Effective Breakdown Voltages as a Function of E_R/p

Calculated for Several Workers.

Legend:
- • $d = 6.35\ mms$ 5.5 Mc/s
- ▼ $d = 7.62\ mms.$
- + $d = 10.16\ mms$
- ⊙ $d = 15.24\ mms$ 9.5 Mc/s
- ▽ $p = 54\ mms\ Hg$
- ▲ $d = 12.7\ mms$

- × J. Thomson
- □ S. Githens
- △ S. C. Brown etc. (M.I.T.)

Vertical axis: Effective Breakdown Voltage, $E_R\Lambda$ volts, from 0 to 500.

Horizontal axis: E_R/p, volts cm^{-1} × mms Hg^{-1}, from 0 to 60.
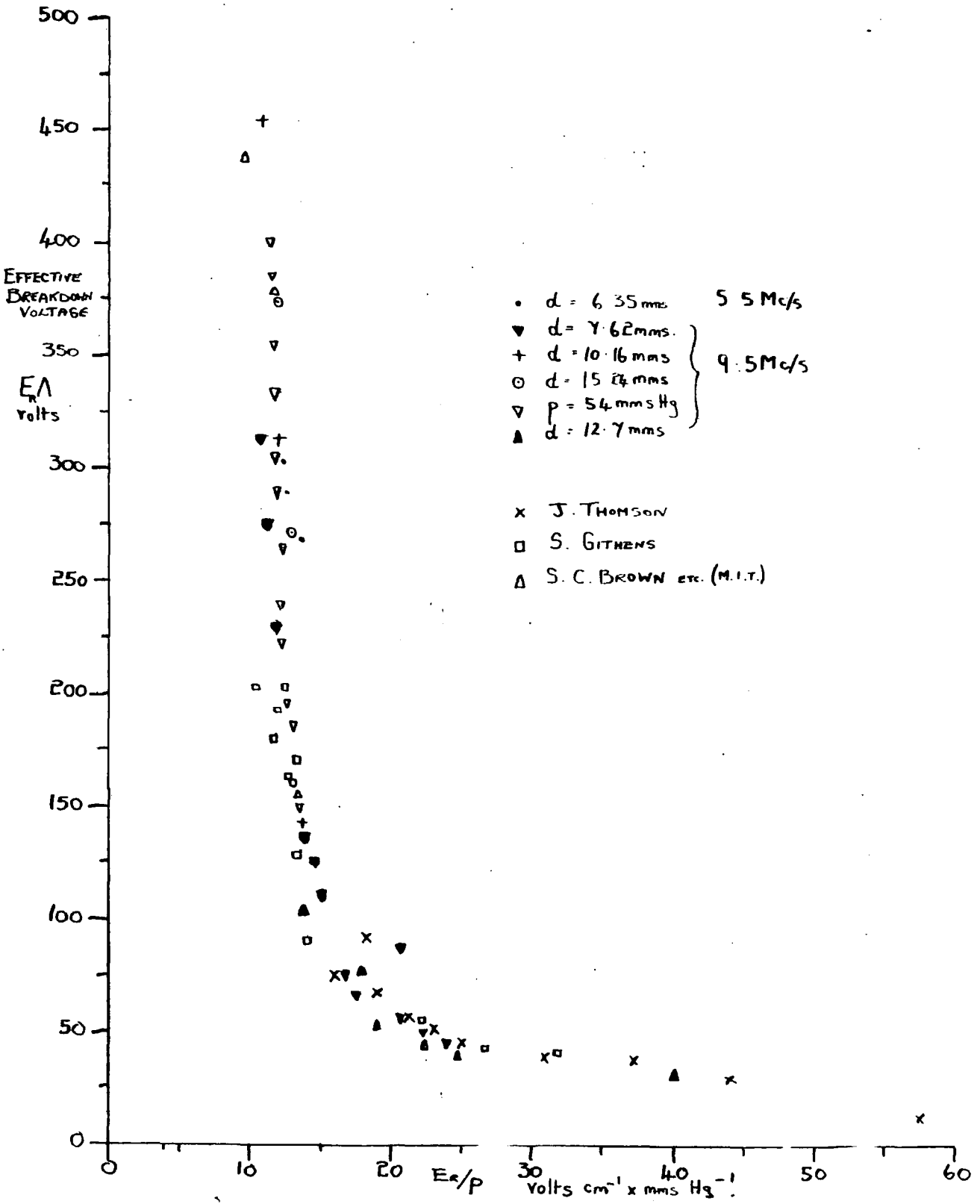
The results described at 9.5 Mc/s conform with those of McDonald and Brown (1949), J. Thomson (1937) and S. Githens (1940); this agreement is clearly illustrated in Fig 28., in which breakdown has been computed as a function of E_R/p. The points lie on a smooth curve, with E_R/p tending to a constant value at high pressures given by $E = 10\ p$. This is in agreement with the value derived by McDonald and Brown (1949). From the evidence presented, based on a quantitative prediction from the Diffusion Theory, and by comparison with the results of a number of independent workers, it is concluded that the breakdown mechanism of discharge in hydrogen at u.h.f. is controlled by diffusion processes.

3.9.   Visual appearance of the discharge

3.9.1.   General observations

The form of the discharge was observed to exist in one of four possible modes. Each mode was characterised by such visible features of the discharge as colour, intensity and extent. A tabulated description of these modes is given in Table 7.

TABLE 7   CLASSIFICATION OF DISCHARGES

Mode	Diffuse or Intense	Colour of discharge	Extent of Discharge
A	Intense	Milky-white	Thin pencil, broadening a little at electrode faces
B	Diffuse	White with trace of blue	Confined to inter-electrode space, diameter $\propto \frac{1}{p}$
C	Diffuse	Pale, Milky	Fills inter-electrode space and extends little beyond it.
D	Diffuse	Light Purple	Extends into surrounding gas

Another striking difference existed.   The onset of
the intense Mode A discharge was always accompanied
by large and sudden drop in the voltmeter reading
whereas the diffuse discharges, B, C & D, caused
only a small reduction.   This drop in voltage, due
to the external circuit being loaded by the gap, is
referred to by Llewellyn, Jones & Morgan (1951),
in a study of maintainence and extinction potentials.
Further, when the gas broke down in the form of Modes
B or C, an increase in the power supplied usually
caused an abrupt change to Mode A.

Fig. 29. **Hydrogen, 9.5 Mc/s. Form of Discharge as a Function of Gas Pressure and Electrode Separation.**
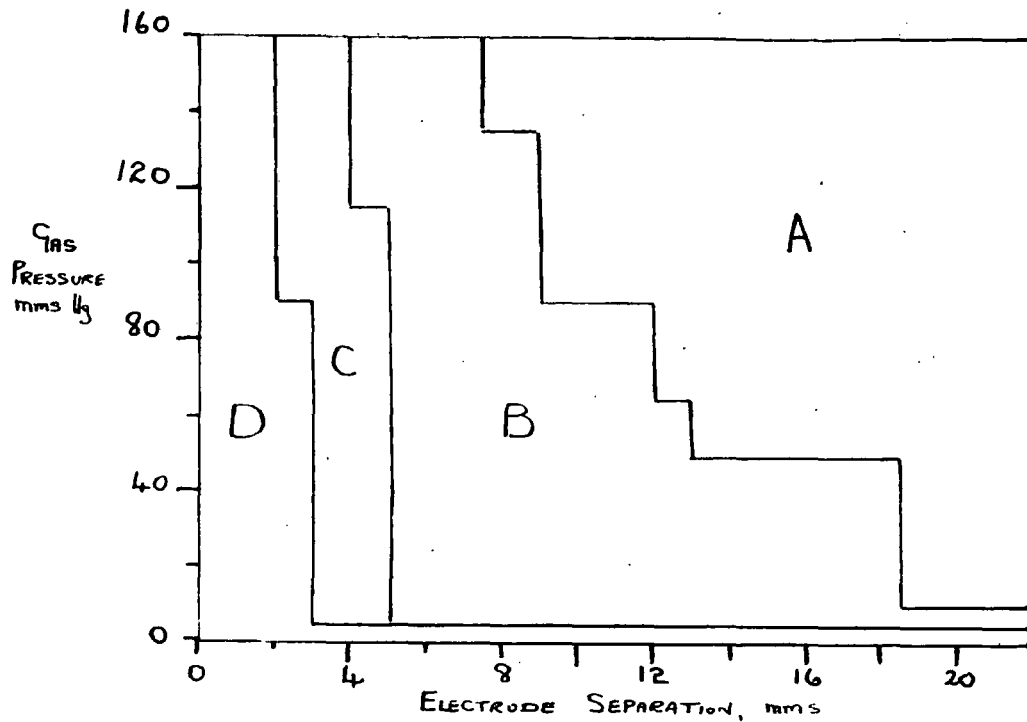
Fig. 30. **Hydrogen, 114mm Hg. Form of Discharge as a Function of Frequency and Electrode Separation.**
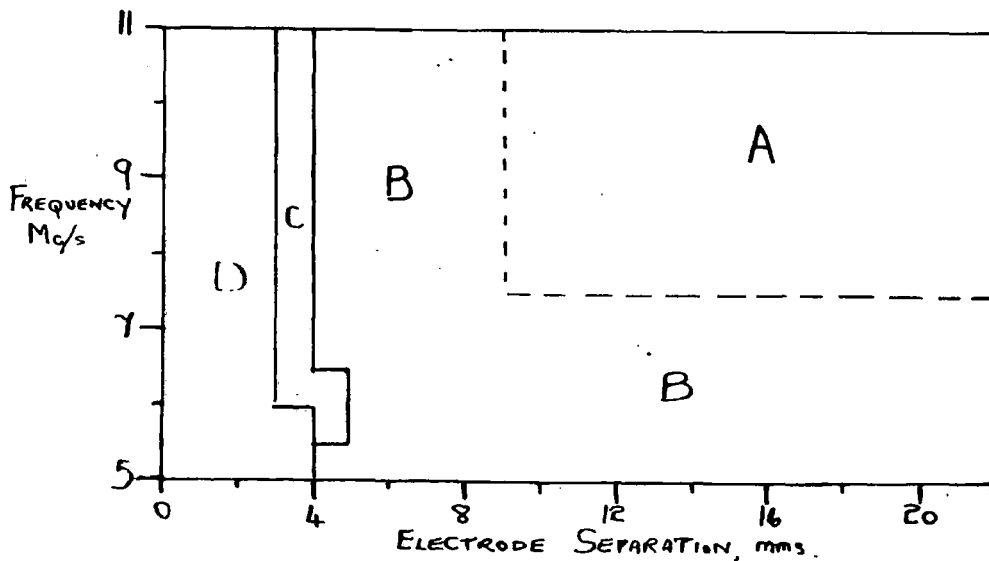
A record was kept, for each of the several hundred
discharge measurements in hydrogen, of the form
of the discharge; the mode appearing under a given
set of conditions was found to be a function of
gas pressure, electrode separation and frequency.
In terms of the above parameters, it was found
possible to construct phase diagrams, indicating
the mode of the discharge at any given value of
p, d, or f.
In Fig. 29, the appearance of the discharge as a
function of pressure and electrode separation
is shown at a constant frequency at 9.5 Mc/s.
The boundaries indicating transitions from one
mode to another have been marked as accurately
as possible using the available data. A similar
surface, Fig. 30, was constructed at a constant
pressure of 114 mms.Hg., giving the form of the
discharge as a function of frequency and electrode
separation. Fewer measurements were available
for this second surface, and consequently the
boundaries could not be defined so clearly.

3.9.2. <u>Qualitative interpretation of visual effects</u>

The mode of the discharge in relation
to the change from h.f. to u.h.f. conditions is now
examined, and reference made to the typical E - d curves

Fig. 31. Hydrogen, 9.5 Mc/s. Visual Characteristics of Discharges.
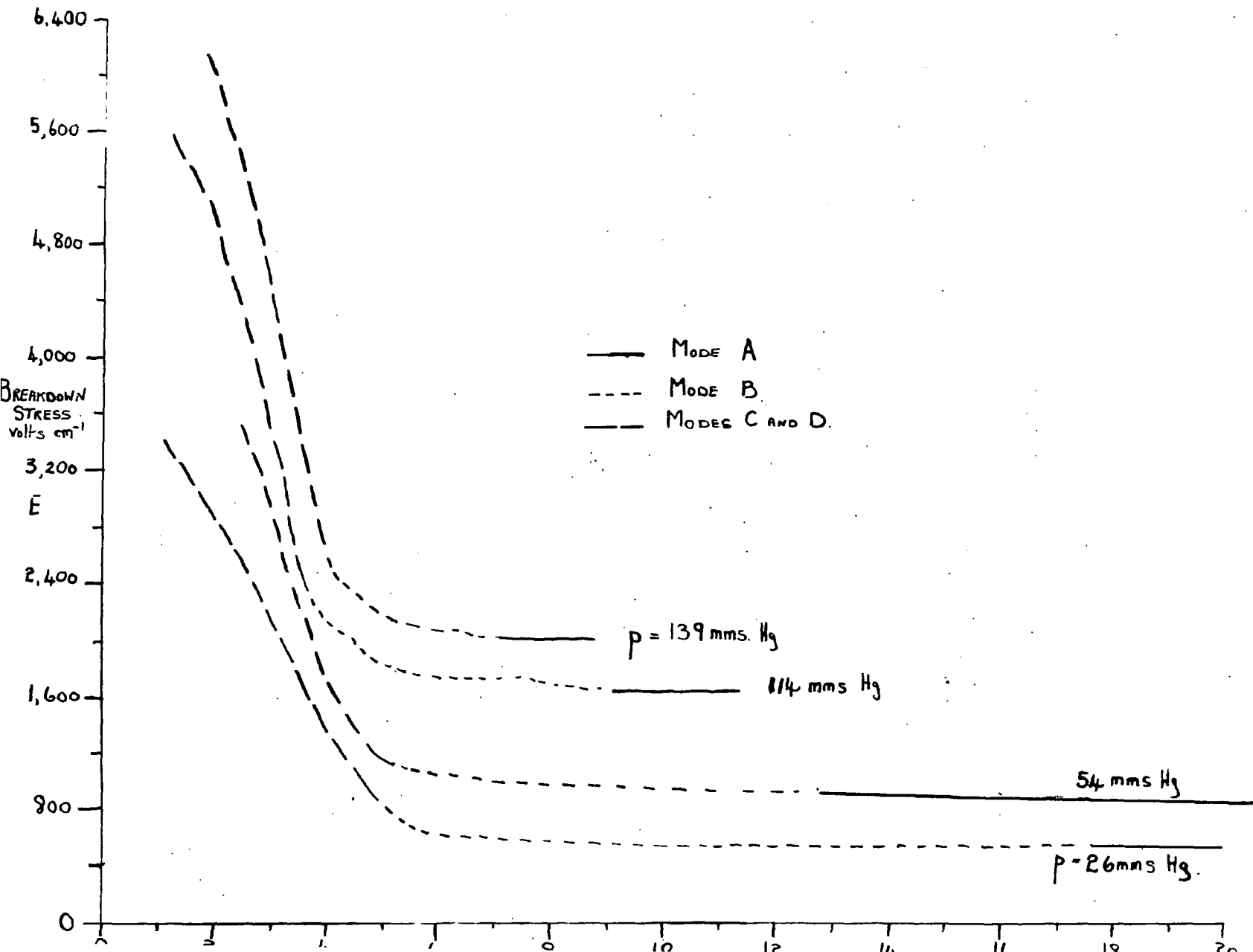
in Fig. 31. An inspection of the curves indicates
that at separations just larger than the critical
gap, the form of the discharge changes from Mode B
(Diffuse) to Mode A (Intense). It would, therefore,
appear that the change in intensity and extent of
the discharge is related in some way to the physical
transition from h.f. to u.h.f. conditions. A
qualitative interpretation of this transition is
now considered in terms of the mechanisms controlling
a maintained discharge. On the h.f. (low gap)
side of the transition, electrons are removed from
the system by electrode capture. At u.h.f. (large
gap), some at least of the electrons are not lost
to the electrodes, and in a non-attaching gas
recombination is necessarily the removal mechanism.
Ambi-polar diffusion (Townsend 1928) will restrict
the outward movement of electrons, but the situation
is distinguished from that in a discharge restricted
by the walls of the tube in that no question of
surface recombination enters (except at the
electrodes). It is thus considered that volume
recombination in the plasma is the removal
mechanism for most of the length of the tube.
Measurements by Biondi and Brown (1949 (a) and (b))
have shown that at pressures greater than a few
mms.Hg. electron losses are mainly of the

recombination type. This case has been studied theoretically by Davydov (1943), whose studies are exemplified by a characteristic curve, reproduced in Fig. 32.
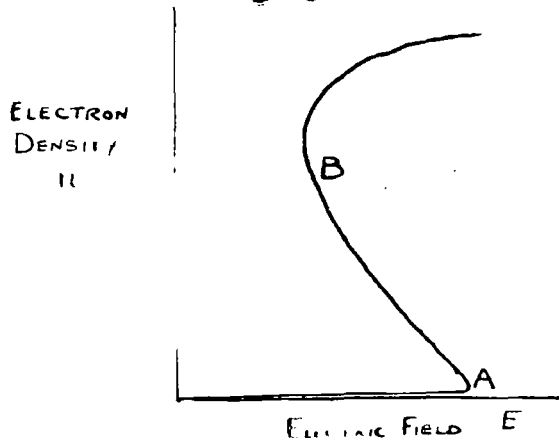
Fig.32.
Davÿdov,(1943)
Change in electron density in a homogeneous electric field.

It is seen that the electron population increases slowly with E up to a critical value A, (depending on the conditions of the experiment), upon which breakdown occurs. The magnitude of n then increases rapidly along AB. It is to be expected that when the total number of ions rises beyond a critical value, the current density must show a sudden increase. With a given power supply this should cause a decrease in the discharge column. Although visual indications are not to be relied upon as precise evidence of current density, nevertheless the co-existence of a narrow bright column with a non-luminous surrounding (the column being narrow with respect to the electrode size) is sufficient evidence of the contraction required

by Davydov's theory.

The quantitative considerations in Davydov's paper are based on the occurrence of stepwise ionisation, and indicate that without such processes the instability referred to would not occur.   The contraction of the luminous column is therefore considered to be evidence of existence of stepwise ionisation processes in this kind of discharge.

CHAPTER 4 - BREAKDOWN IN NITROGEN

Breakdown studies in nitrogen were conducted at
pressures up to 80 mms.Hg. using various electrode
separations from 2 to 20 mms.   The same pair of
electrodes (Type A) were used throughout the
experiments.

4.1.   Experimental procedure

The experimental techniques employed
in recording breakdown measurements in nitrogen
were very similar to those described for the
hydrogen experiments.   Statistical lags were
evident; at the higher pressures particularly
these sometimes approached a minute in duration.
Due to this factor great care was necessary to
pinpoint accurately the threshold potential of
the discharge, and a run in the gas required
several hours' recording.   As with hydrogen,
the visual appearance of the discharge was
observed to transfer successively through a series
of well-defined modes during each set of
measurements; the appropriate characteristics were
recorded.

4.2.   Results at 9.5 Mc/s

4.2.1.   Variation of breakdown stress with electrode separation

Typical results, with peak breakdown

Fig. 33. Nitrogen. Variation of Breakdown Stess with Electrode Separation.

P = 57 mms Hg.

P = 39 mms Hg

P = 14 mms Hg.
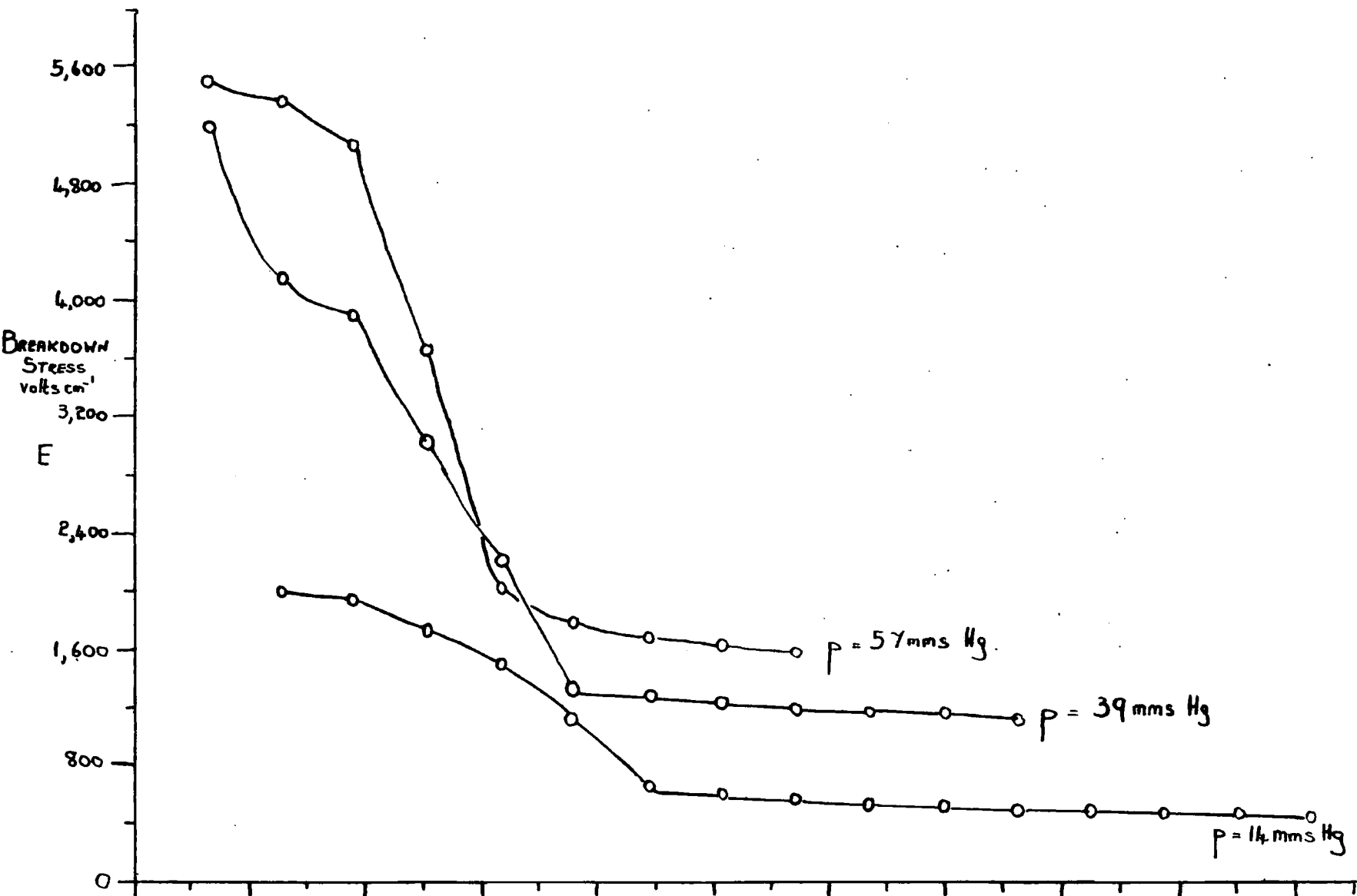
stress plotted as a function of electrode separation, are given in Fig.33. Each curve represents breakdown at a given value of gas pressure. The familiar sharp drop in the field E as it approaches a critical value, followed by a gentle lowering of the stress with increased electrode separation, is again observed.

In order to establish that conditions in gaps greater than the critical value correspond to true u.h.f. breakdown, it is necessary to show that within this region the amplitude of electron oscillation is always numerically less than the electrode separation. The electron ambit at and beyond the critical value of gap width may be calculated by inserting the appropriate data in equation 3.1. The required relationship between electron drift velocity and E/p is obtained from measurements by Nielson (1936), which show that:

$$V = 3.22 \times 10^5 \times E/p$$

Since $de = \dfrac{V}{\pi F}$

then at 9.5 Mc/s, $de = \dfrac{3.22 \times 10^5}{\pi \times 9.5 \times 10^6}$ cms $= 1.08 \times 10^{-1} \times \dfrac{E}{p}$ mms.

Table 8 (a) compares the observed values of gap width at which the curves begin to smooth out with the

calculated values of d.c. at these points.

TABLE 8 (a)

d.e near critical values of
electrode separation

P mms	E volts cm.$^{-1}$	E/p	de calcu lated mms	d observed mms
14	660	47.3	5.1	8.9
39	1,340	35.7	3.9	7.6
57	2,000	35.0	3.8	6.36

TABLE 8 (b)

Values of de with-within u.h.f.
region

p = 14 mms.Hg

E volts cm.$^{-1}$	E/p	de mms	d mms.
600	43	4.64	10.16
500	35.7	3.85	15.24
470	33.5	3.61	20.32

It is seen that in each case the amplitude of
electron oscillation is considerably less than
the electrode separation, showing that breakdown

at these points is within the u.h.f. region.
The gaps at which electrons are just removed
from the system, corresponding to the change
from h.f. to u.h.f. conditions, are not
clearly indicated in the E-d results in nitrogen.
In Table 8 (b) the amplitude of electron
oscillation at gaps well beyond the critical
value is shown for the typical run at
14 mms.Hg., and demonstrates that under these
circumstances electrons move only a small
fraction of the distance between the plates
before their direction of motion is reversed
by the field.

Results at lower field frequencies were
restricted. $d_{c c.}$ rises sharply with decreasing
frequency $\left(d_{c c.} \propto \dfrac{1}{f} \right)$ and consequently either

high pressures or large gaps were required to
fulfil u.h.f. conditions. The electrode separation
could not be increased beyond 20 mms., and at high
pressures (80 mms.Hg) even the maximum potential
available, nearly 3 Kv., was insufficient to break
down the gap. However, the limited measurements
taken indicated that the general pattern of breakdown
was similar to that at the higher frequency.

Fig. 34. Nitrogen. Variation of Breakdown Stress with Pressure
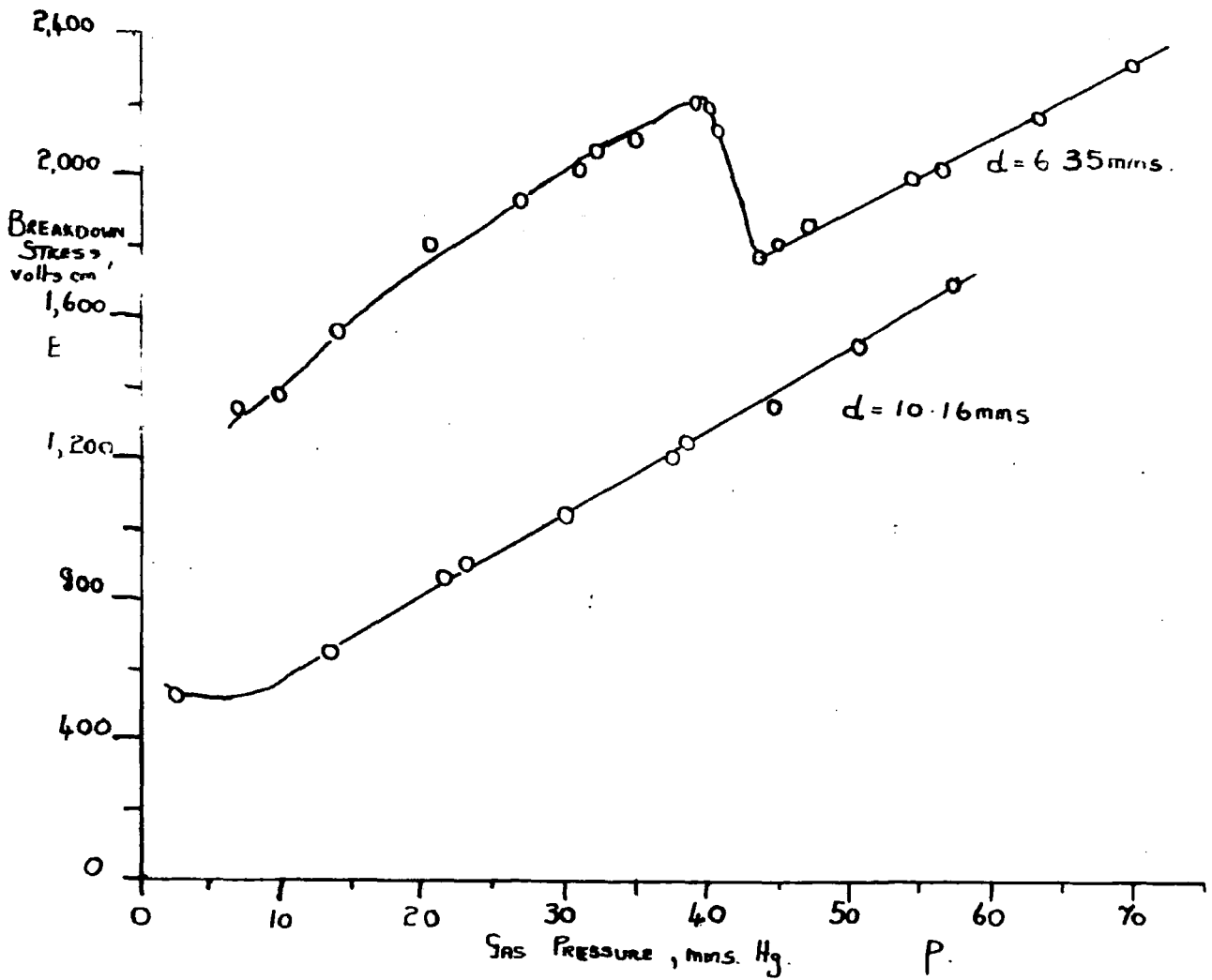
4.2.2. Variation of breakdown stress with gas pressure.

Results of breakdown observations at two fixed gaps for various gas pressures is shown in Fig. 34. At the plate separation of 6.35 mms. , the sharp drop in field occurring at 39 mms. Hg readily shows the transition from h.f. to u.h.f. conditions, and 39 mms. Hg may be defined as a critical pressure Pc, analagous to the critical electrode separation.

When the pressure is increased to 43.5 mms. Hg., all electrons oscillate within the inter-electrode space. In the larger (10,16 mms) gap, u.h.f. breakdown persists to a much lower pressure, the minimum being at about 7 mms. Hg. Equation 4.1 can be altered to the form:

$$P = 1.08 \times 10^{-1} \frac{E}{d} = Pc \text{ (at transition)}$$

and used to calculate Pc. This gives a value of Pc = 37.2 mms. Hg., compared with observed pressure of 39 mms. Hg. In view of the approximations used in deriving the above equation (Section 3.2.) the agreement is considered quite satisfactory.

4.3. Breakdown mechanism in nitrogen

4.3.1. Breakdown potential as a function of Pd.

Both nitrogen and hydrogen are non-

Fig. 35. Nitrogen. Breakdown Potential as a Function of pd.
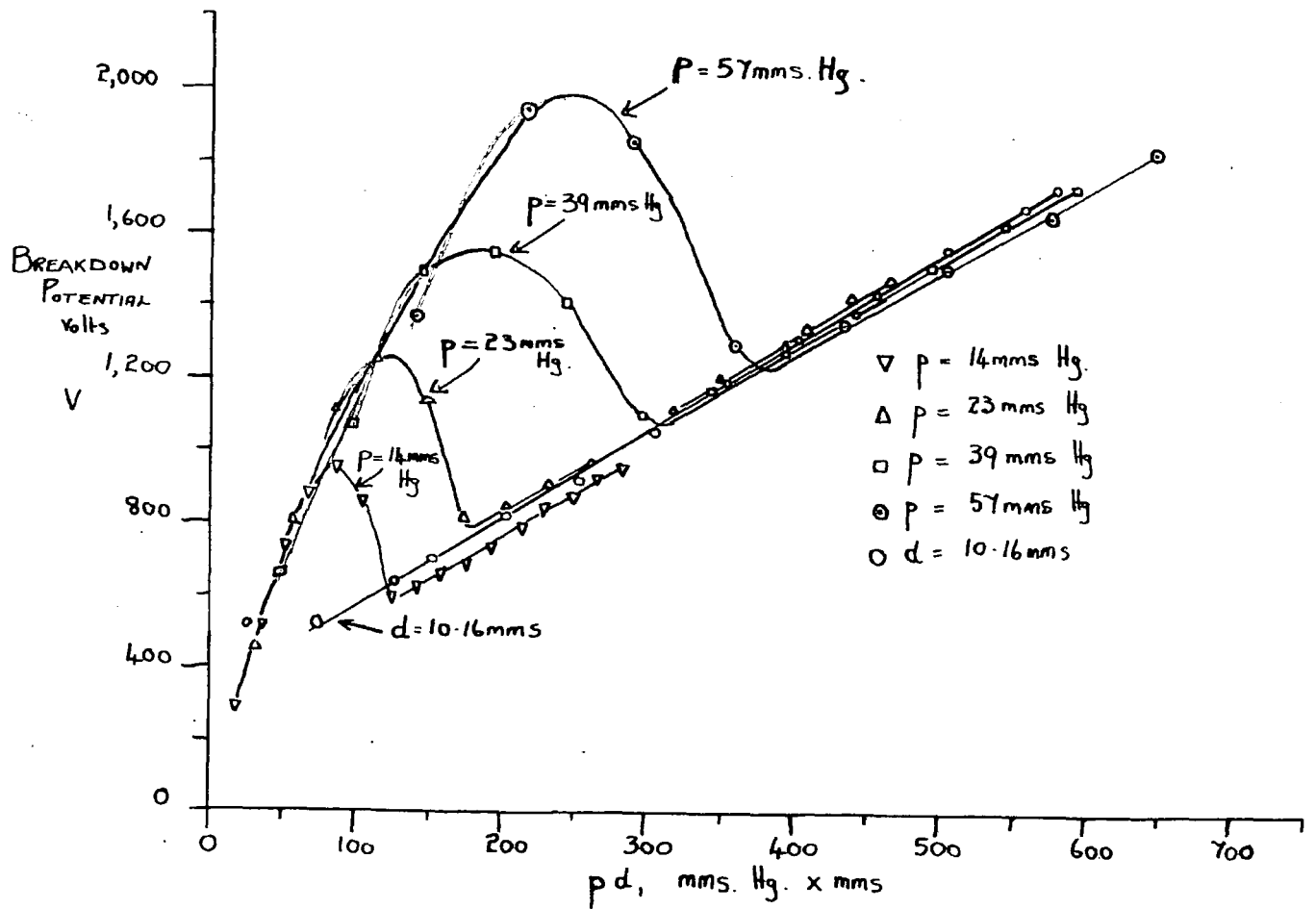
attaching diatomic gases, and the close
similarities in breakdown behaviour observed
in the two gases at once suggests a similarity
in breakdown mechanism, namely diffusion.
The dependence of breakdown field on electrode
separation is clearly indicated in Figs. 33 and
34.   Further information can be obtained by
computing breakdown as a function of Pd.   This
is shown in Fig. 35; in four of the curves d
is varied at a constant pressure; a typical
run at a fixed plate separation is also included.
Minima correspond to electrons just in the gap
each half-cycle of the field; breakdown at
greater values of Pd is in the u.h.f. region.
At a fixed value of Pd. in the u.h.f. part of the
system it is seen that breakdown voltage lowers
progressively as the pressure is increased.
(This difference, though small, is significant).
The value of V required for breakdown is governed
by the rate at which electrons are removed from
the gap, and the fact that the observed values
of V for each curve do not coincide at a given
Pd indicates that electron losses vary in each case.
Since the value of d is unique in each curve at the
same pd, the differences in electron losses may be

Fig. 36. Nitrogen. Variation of $E_s \Lambda$ with $p\Lambda$.
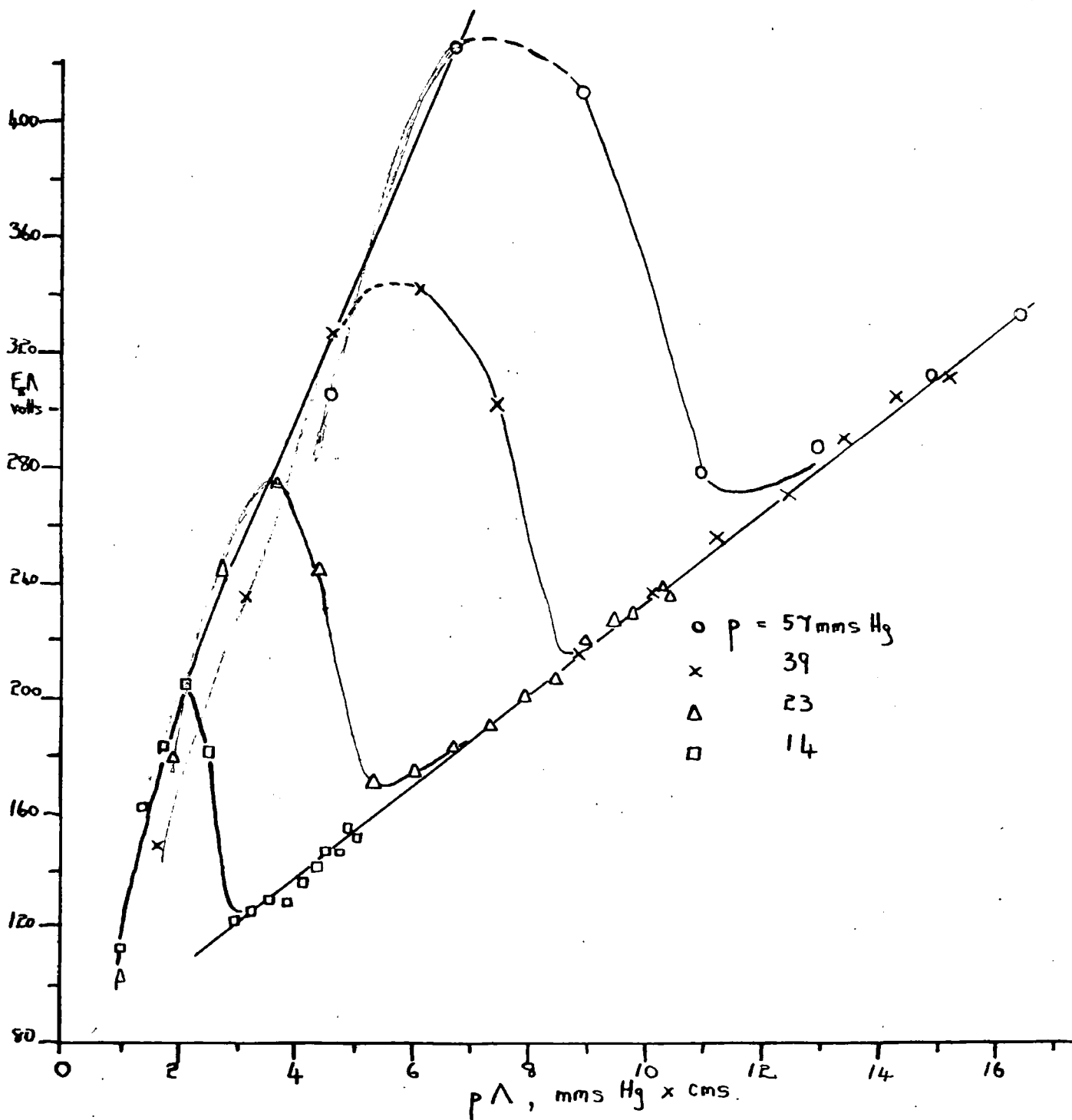
attributed to differences in electrode separation.
This is consistent with the demands of the
diffusion theory, in that removal of electrons is
a function of electrode separation (equation
3.6).

4.3.2.   Interpretation of results on the diffusion
theory

The most effective way of testing the
conformity of the nitrogen results to the diffusion
theory is by calculating values of Λ (the characteristic
diffusion length) on the assumption that diffusion is
the controlling removal mechanism, and transferring
the breakdown data to the variables $E\Lambda$ and $p\Lambda$.
As described in Section 3.5.3., in considering
u.h.f. discharges in hydrogen, the diffusion
theory requires that when breakdown measurements
in a particular gas are plotted in terms of these
parameters, all points shall lie in a continuous
curve.

This relationship is tested in Fig. 36.,
in which effective breakdown voltage $E\Lambda$ is plotted
as a function of $p\Lambda$ for four separate runs
at pressures varying from 14 - 57 mms.Hg.   Points
in the u.h.f. region are seen to lie on a smooth,
almost linear, curve, the scatter of the points being
very small.

As previously stated, Section 4.2., it
was not possible with the apparatus employed to
record series of u.h.f. measurements at frequencies
far removed from 9.5 Mc/s. However, in view of
the close similarity in form between the hydrogen
and nitrogen results, it is not considered likely
that the pattern of measurements in nitrogen would
vary with frequency. It is concluded that under
u.h.f. conditions the controlling factor restricting
the cumulative growth of ionisation in nitrogen
is diffusion of the electrons, either to the
electrodes or sideways out of the intense field
region.

4.4.   High-frequency ionising co-efficient

Owing to the relatively high pressures
used in the nitrogen experiments, the range of E_R/p
encountered was rather small, varying from $E_R/p = 34$
(at the lowest pressure) to a limiting value given
by $E_R = 21 p$ at high densities. Values of ^{c}
the high frequency ionising co-efficient φ
(ionisations/volt^2) in this region are given in
Table 9., and indicate the efficiency of ionisation
in nitrogen as a function of E_R/p for two typical
electrode separations.

TABLE 9.   VALUES OF γ . IONISATIONS. VOLT^{-2}

d = 6.35 mms		d = 10.16 mms	
E/p	γ	E/p	γ
35.7	1.34×10^{-5}	33.8	6.2×10^{-5}
23.7	1.24×10^{-5}	28.2	3.52×10^{-5}
22.8	9.8×10^{-6}	26.0	2.11×10^{-5}
22.0	8.55×10^{-6}	22.4	1.82×10^{-5}
21.2	7.53×10^{-6}	21.2	1.13×10^{-5}

No comparison between γ and the corresponding d.c. co-efficient is possible, as values of β are not available in the range of ER/p used.

4.5.   Visual aspects of the discharge

The visual form of a discharge was observed to fall into one of several discrete modes. Each form differed from its neighbours in colour, volume, and intensity. Table 10 classified the various modes and describes the visual characteristics.

Fig. 37. Nitrogen. Visual Form of Discharge as a Function of Gas Pressure and Electrode Separation.
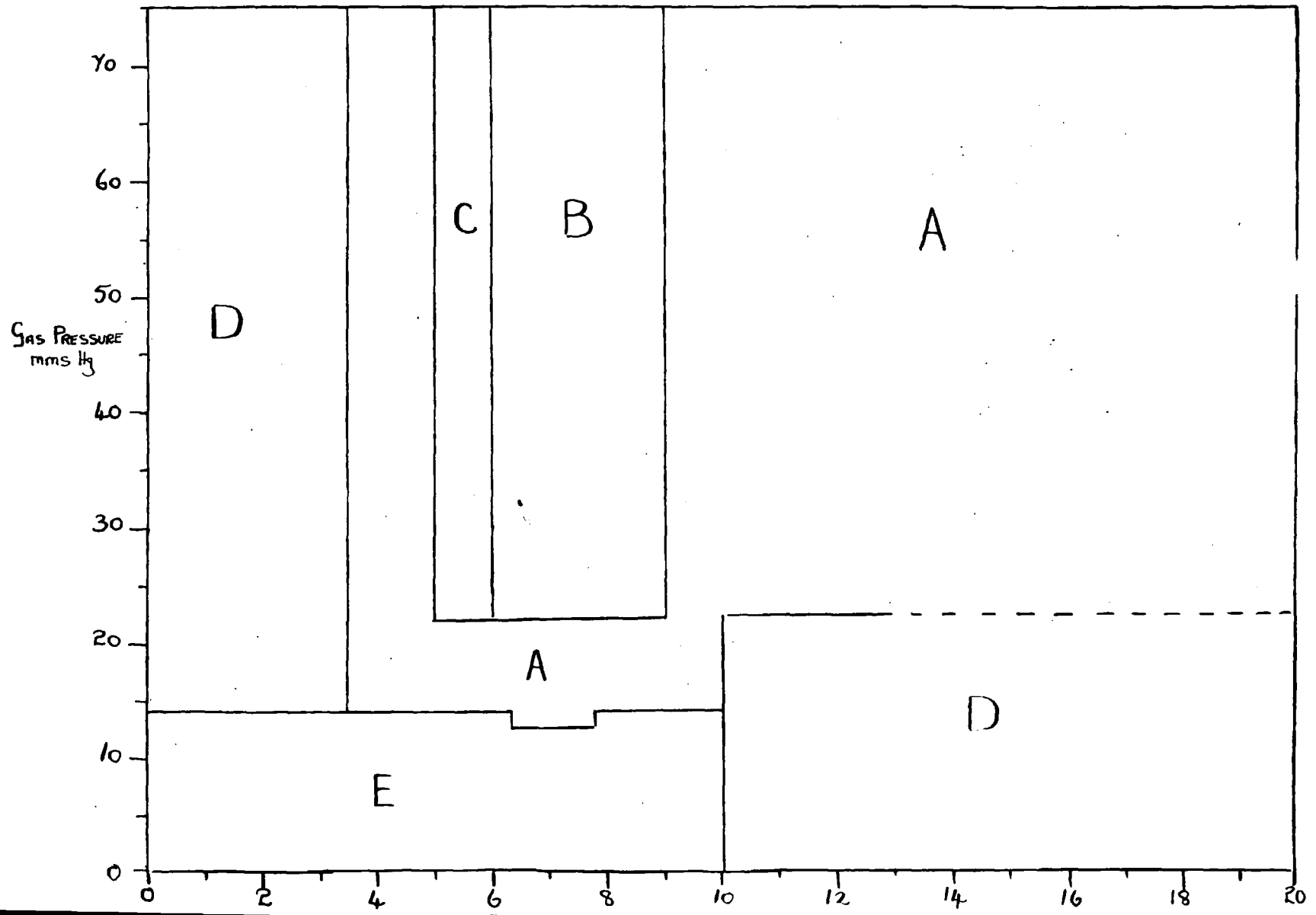
TABLE 10. DISCHARGE CHARACTERISTICS.

Mode	Diffuse or Intense	Colour	Volume of Discharge.
A	Intense	Purple near electrode, orange-red between.	Intense filament, confined to fairly narrow channel near centre of electrodes.
B	Diffuse	Milky-blue	Narrow channel within inter-electrode space
C	Intense	Purple	Four luminous segmental bands near electrode edges
D	Diffuse	Milky-blue	Fills inter-electrode space
E	Diffuse	Purple	Extends into volume of surrounding gas.

It was noticed that, as in hydrogen, the mode of discharge appearing was a function of gas pressure and electrode separation, and it was again found possible from the considerable number of observations taken to construct a 'phase' diagram, Fig. 37., relating the form of the discharge to p and d.

The general pattern can be seen to indicate that
at the high values of pd, corresponding to
breakdown within the u.h.f. region, the form
of the discharge changes from a diffuse glow
to an intense conducting filament.   Any
interpretation made from the above observations
regarding physical conditions in a maintained
nitrogen discharge must necessarily be
tentative and qualitative in manner.   Nevertheless,
it is considered likely that the suggestion made
in Section 3.9.2. in discussing the relationship
between the form of the discharge in hydrogen
and the physical mechanisms maintaining it,
apply similarly to breakdown in nitrogen.

Fig. 38. Neon. Variation of Breakdown Stress with Electrode Separation.
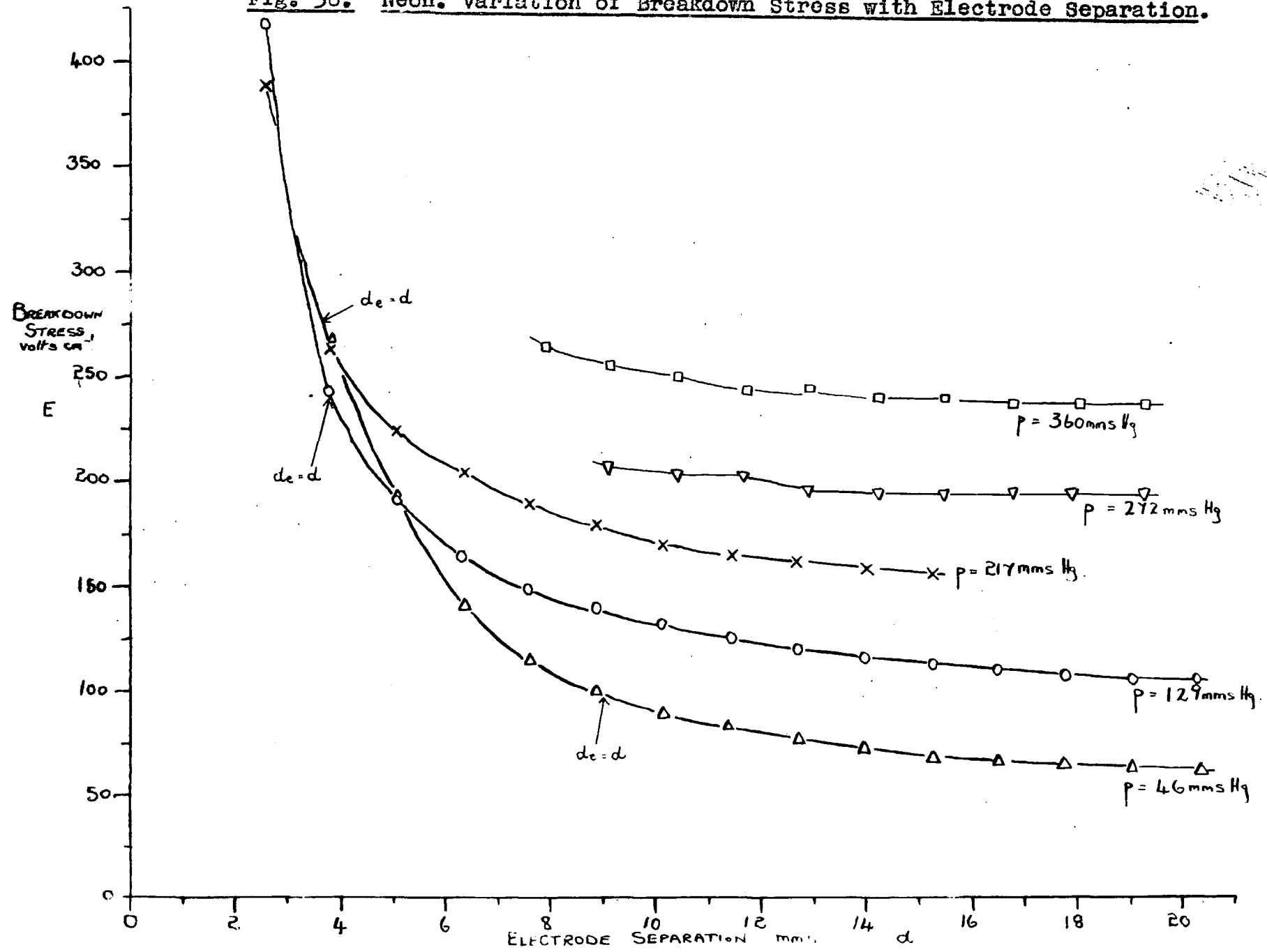
CHAPTER 5 - BREAKDOWN IN NEON

Measurements in neon were conducted at a constant frequency of 9.5 Mc/s, over a wide range of pressure varying from 40 - 350 mms. Hg., and using the 'A' type Rogowski-profiled electrodes.

5.1. Experimental procedure

Owing to the low values of breakdown potential encountered, slight modifications to the apparatus were necessary. In the voltage-measuring circuit a new electrostatic voltmeter was installed, reading 0-130 v. (See Section 2.5.) The irradiating spark tended to spread too much at low pressures. This was counteracted by reducing the current through it. Discharges at the shorter gap separations were difficult to see, being characterised by a glow of very faint luminosity. For this reason all the neon results were recorded with the room darkened.

5.2. Breakdown measurements

Curves showing the variation of breakdown stress with gap width are given in Fig. 38.

The low-range voltmeter was available only
for later measurements in neon;   results
previous to this were restricted to conditions
in which breakdown occurred at potentials
200 volts. peak, corresponding to high pressures
and large plate separations.   The breakdown
curves at 272 mms. and 360 mms.Hg. are
typical of such results, and exhibit the
familiar gentle decrease in field as the
electrode separation is increased.   When it
became possible to record smaller voltages
breakdown studies were extended to lower
pressures and smaller gaps;   three such runs
are included in Fig. 38 .   The form of these
curves at short gaps is somewhat different from
the other gases investigated, E changing
quite rapidly with d.   An explanation of this
phenomenon, in terms of ionising efficiencies,
is considered in Section 5.5.   Values of the
electron ambit at specified points may be
calculated from a knowledge of the electron
drift velocity at the appropriate values of
E/p, and using the equation:

$$de = \frac{v}{\pi F}$$

The most accurate determinations of

in neon, made by Nielson (1936) only cover a

range of E/p from 0-1.6. Extrapolation of

this graph is necessary to determine ν

at the experimentally determined values of

E/p, values of de calculated in this manner are

given in Table 11, and compared with the

observed values of electrode separations at the

points considered.

TABLE 11   ELECTRON AMBITS IN NEON

p power of $10^?$

Nielson (1936) (Extrapolated) de = 0.537 x E/p ι				
p mms.	E	E/p	de mms.	d (observed) mms.
46	265	5.76	3.1	·3.8
46	177	3.84	2.1	·5.1
46	137	3.0	1.6	·6.35
217	386	1.78	0.96	2.54
129	417	3.24	1.74	2.54

The calculations indicate that in each case the

amplitude of electron oscillation is less than the

gap width. These values, however, must be

treated with considerable reserve since the

ν - E/p curve was only approximately linear, and

Fig. 39. Neon. Variation of Breakdown Voltage with Electrode Separation.
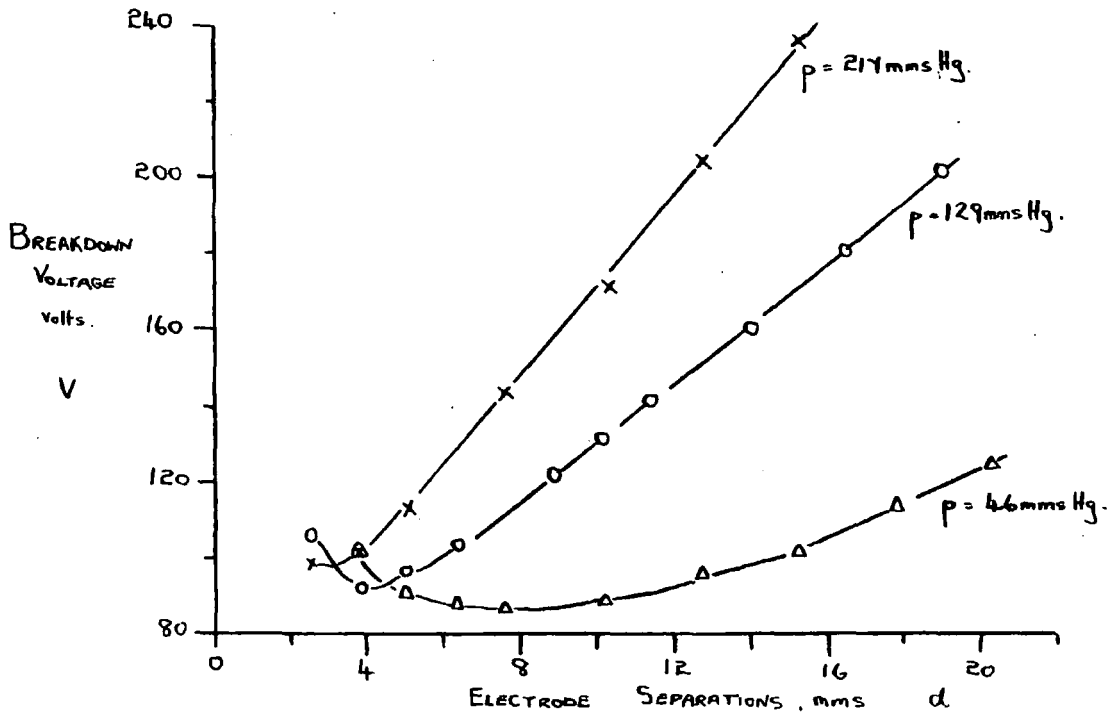
Fig. 40. Neon. Variation of Breakdown Stress with Gas Pressure.
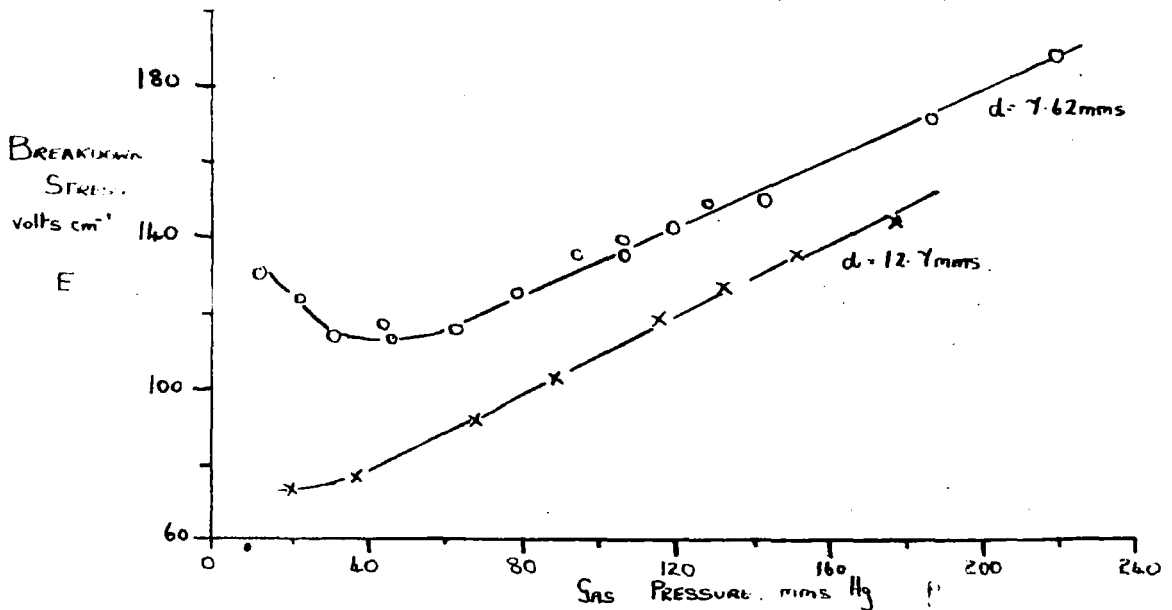
the straight-line extrapolation must necessarily
lead only to fairly approximate results.

Critical values of electrode separation
may also be found by plotting breakdown
potential as a function of gap width.   This is
done in Fig. 39.   Voltage minima on these
curves represent electron capture by the
plates and indicate approximately the values of
d_c.   These transitions are marked in Fig 38.,
and it is evident that in neon the breakdown
field at separations immediately beyond the
critical value shows a sharp drop before
smoothing out to the pattern familiar in the
other gases.   An interpretation of this
phenomenon in terms of the rate of growth of
ionisation is given in Section 5.5.

Breakdown at constant electrode separation
is illustrated in Fig. 40 and shows E as a
function of p for two separations,
7.62 mms and 12.7 mms.   At 42 mms. Hg. a
minimum occurs in the 7.62 mms. plot, indicating
a critical value of pressure.

5.3.   <u>Qualitative examination of results</u>
Breakdown occurs when the ionisation

Fig. 41. Neon. Variation of Breakdown Potential with pd.
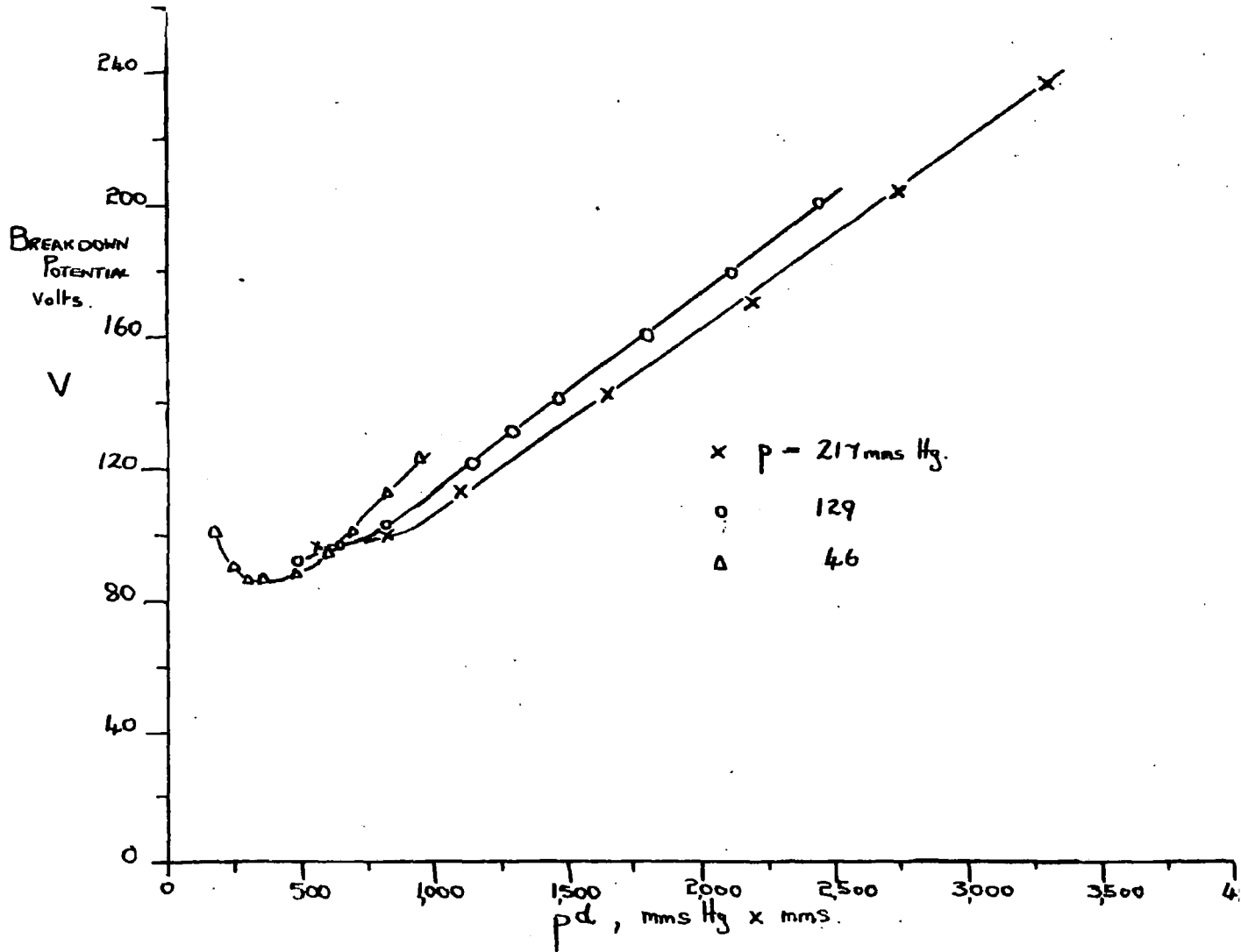
produced by the field just exceeds the net loss of electrons from the gap. In a diffusion-controlled system, this loss results from diffusion, both to the electrodes and laterally out of the intense field region. The _rate_ of removal under such conditions is governed by the mean lifetime, t_D, of an electron in the gap. In experiments conducted with electrodes of constant size t_D is a function of d alone. Under such conditions the breakdown stress is thus a function of electrode separation. Neon is a non-attaching, monatomic gas, and for a given value of p, Fig 40, a decrease in E is observed as the plate separation is increased, immediately suggesting diffusion as the electron removal factor. Similar evidence is provided by plotting breakdown potential against pd to form the familiar Paschen Curves. In Fig. 41, V - pd plots have been constructed from data at 46-, 129-, and 217-mms Hg. Unlike the d.c. case, it is seen that the breakdown curve is not unique, but differs for each pressure run, indicating that V at a given value of pd is dependent upon the parameter d, as required by the diffusion theory.

5.4. Applicability of Diffusion Theory

The applicability of the diffusion theory to u.h.f. breakdown in neon may be tested, in a similar manner to hydrogen, by computing effective breakdown voltage, $E\Lambda$, as a function of $p\Lambda$ for a number of sets of breakdown

Fig. 42. Neon. Variation of $E_R\Lambda$ with $p\Lambda$.
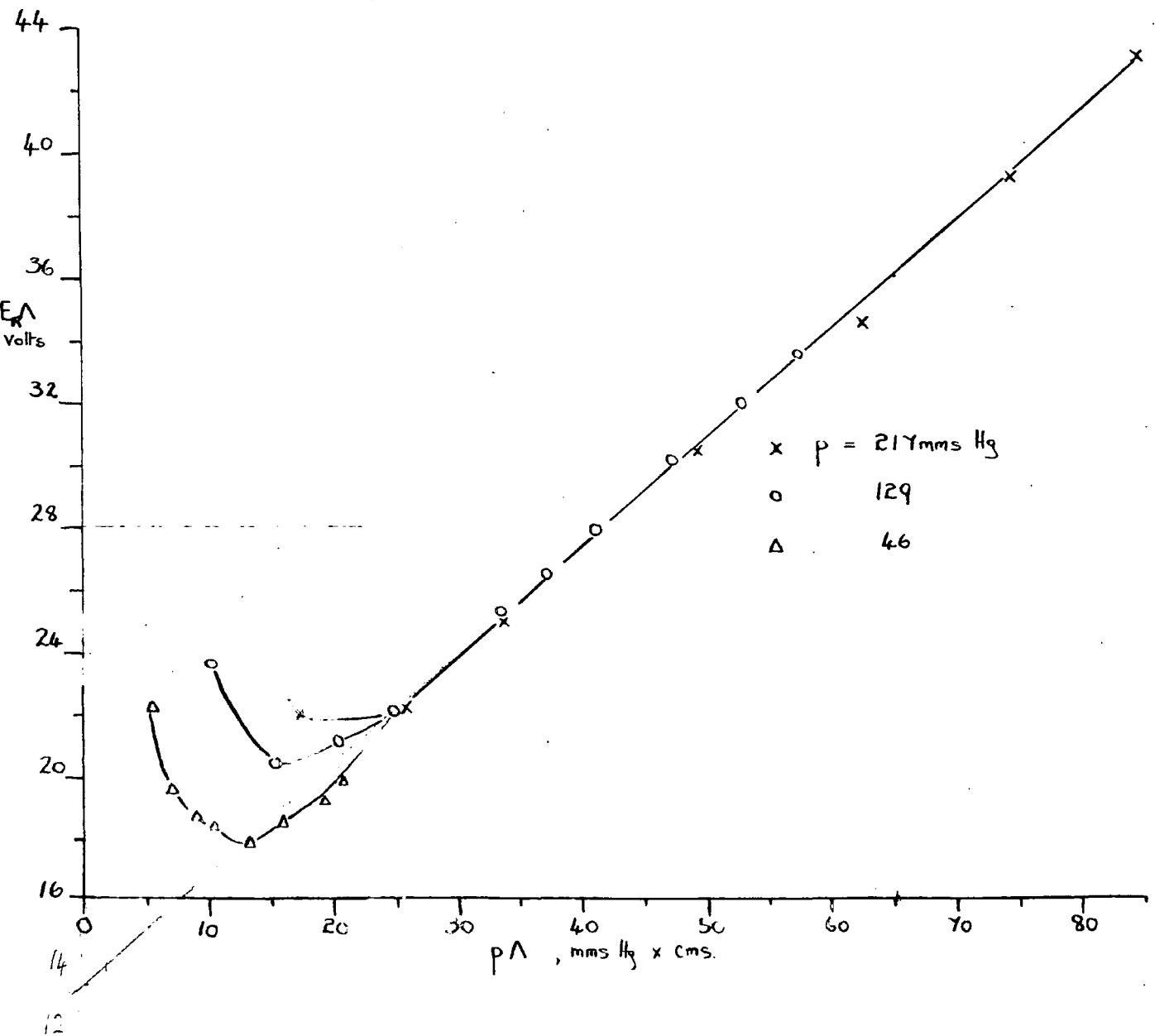
measurements, using values of Λ determined on the assumption that the mean life of an electron within the gap is limited by diffusion processes alone. Since "A"-type Rogowski electrodes were used in all the neon measurements, values of Λ in terms of the electrode separation were calculable directly from Fig. 20.

The $E\Lambda - p\Lambda$ plots are shown in Fig. 42. Although the overlap of data from different runs does not cover a very wide range, points in the u.h.f. region lie on the same smooth curve; from this evidence it is concluded that breakdown in neon under u.h.f. conditions occurs when the gain in electron population by ionisation just exceeds the loss due to diffusion.

5.5. Ionisation in Neon

As mentioned in Section 5.2, the rate of lowering of E with d is seen to be relatively greater in neon (reference to Fig. 38), than in hydrogen, nitrogen, or air. An explanation of this is now considered. In the discussion an important factor is a comparison of ionising efficiencies, as a function of E/p, between neon and the other gases examined. Values of ionisation coefficients calculated from the breakdown data at 9.5 Mc/s are restricted owing to the short ranges of E/p encountered. Measurements over extended ranges of E/p are, however, available from the results of other workers. d.c. measurements, in terms of

Neon, Air DRUYVESTYN (1940)
HYDROGEN. VARNERIN. (1950)
NITROGEN von ENGEL (1932)

10^{-2}

η
Ion PAIRS/Volt

x x BREAKDOWN RATIO ... E/P

10^{-3}

NEON

HYROGEN

AIR

NITROGEN

10^{-4}

1   10   100   1,000

E/P , Volts cm^{-1}, mms Hg^{-1}

<u>Fig.43(a)</u>.

10^{-2}

HYDROGEN, AIR. BROWN (1951)
NEON   MacDONALD (1955).

HYDROGEN

AIR

10^{-3}

ξ
Volts^{-2}

10^{-4}

NEON

10^{-5}

1   10   100   1,000

E/P volts cm^{-1}, mms Hg^{-1}
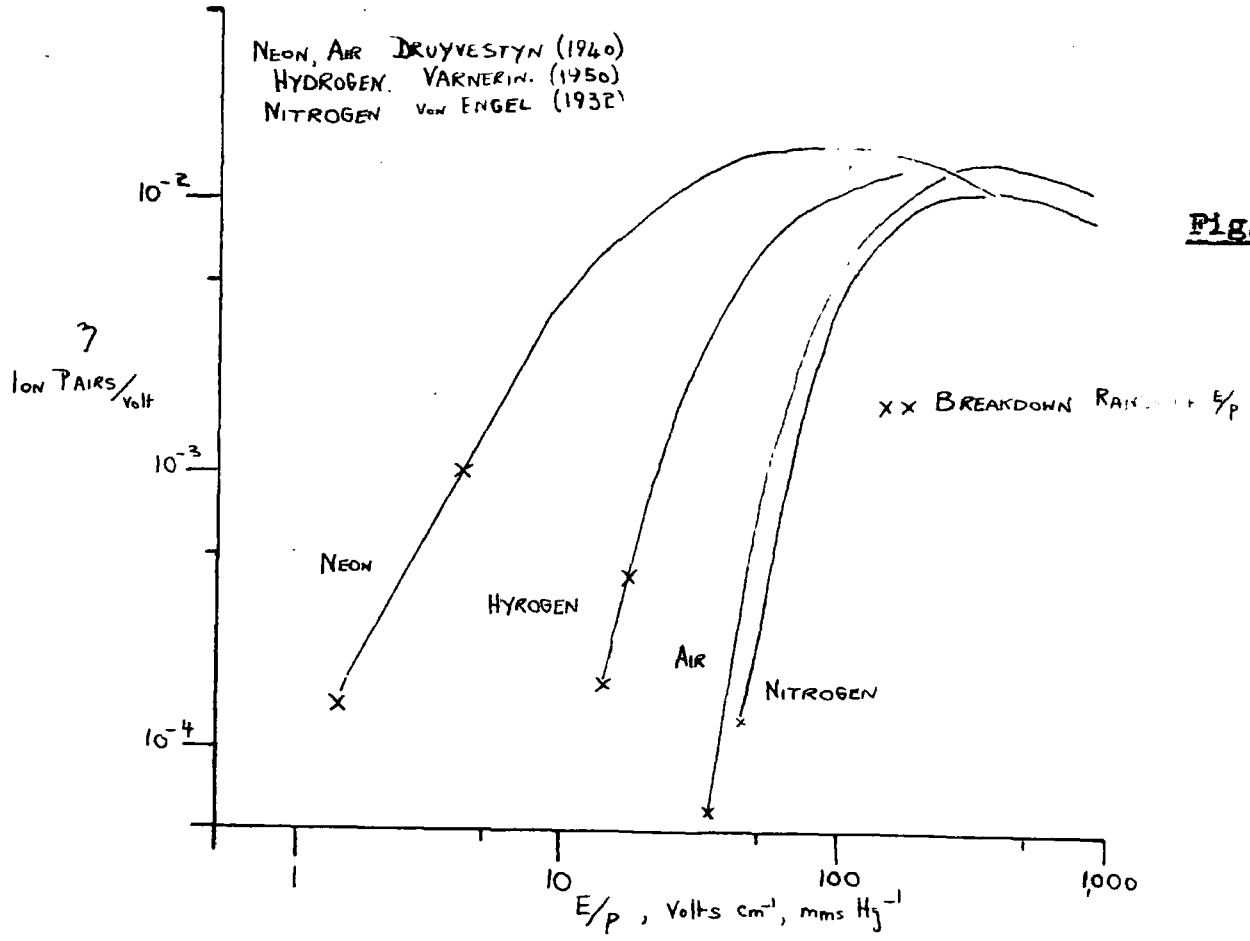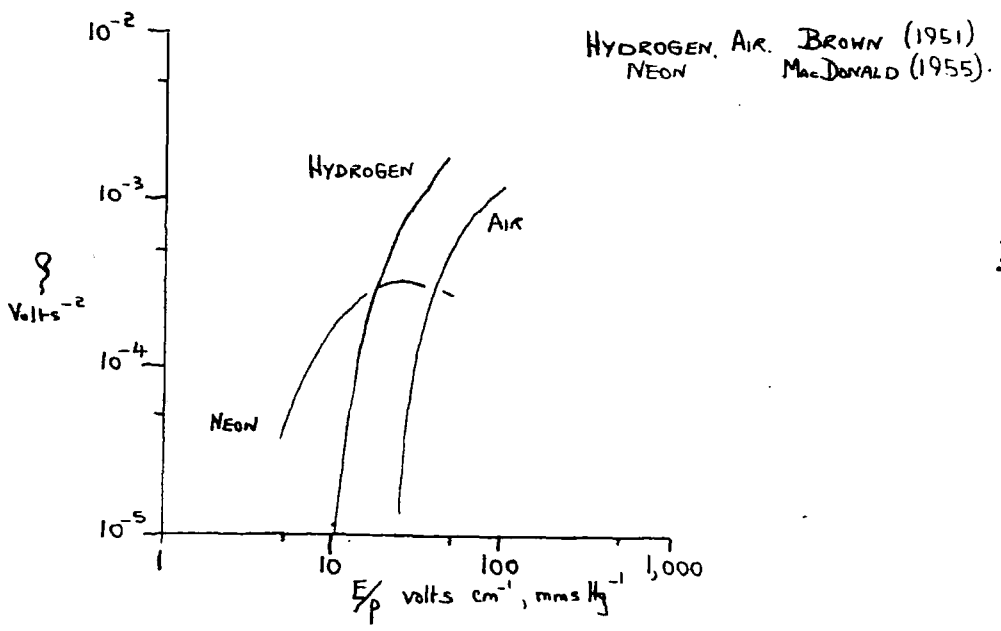
<u>Fig.43(b)</u>.

ion pairs/volt 3, are compared for the four gases in
Fig. 43(a), and the corresponding high frequency
coefficients γ similar in form to the above, in Fig. 43(b).
The range of E/p encountered during breakdown studies in
each gas is marked in Fig. 43(a); it is evident from the
curves that in the neighbourhood of breakdown the ionising
efficiency rises more sharply with E/p in the polyatomic
gases than in neon.

The condition for a favourable increase in electron
population leading to breakdown is that an electron must
create one new ion pair during its life-time as limited
by diffusion.

This may be expressed as

$$Vi \ t_0 = 1 \quad \ldots \ldots \quad 5.1.$$

where t_0 = mean life of electron, secs.

Vi = no. of ion pairs created/sec.

$Vi = \alpha \mu \ E;$ where μ = electron mobility

Therefore $Vi \propto \alpha$

The duration t_0 is governed by the electrode config-
uration, and for electrodes of constant size is a function of
electrode separation (Equation 3.6.)

In the polyatomic gases, where α/p rises sharply
with E/p in the neighbourhood of breakdown, a variation in
t_0 caused by a given variation in electrode separation will
require only a small compensating variation in E to satisfy
equation 5.1. Such a sequence has been observed in hydrogen

nitrogen and air.

In neon, however, a similar change in d would require
a relatively larger variation in the stress required to
initiatate breakdown; this would account for the form of
the E - d curves shown in Fig. 38.

Further evidence regarding the relatively slow rise of
α/p with E/p in neon compared with the other gases may be
deduced from the pulsed breakdown measurements of Labrum (1947),
and Prowse and Jasinski (1952). Measurements in neon
similar to those given in Fig. 38 have been recorded by
Rowbotham (1956).

Fig. 44. Air, 9.5 Mc/s.

Variation of Breakdown Stress with Electrode Separation.
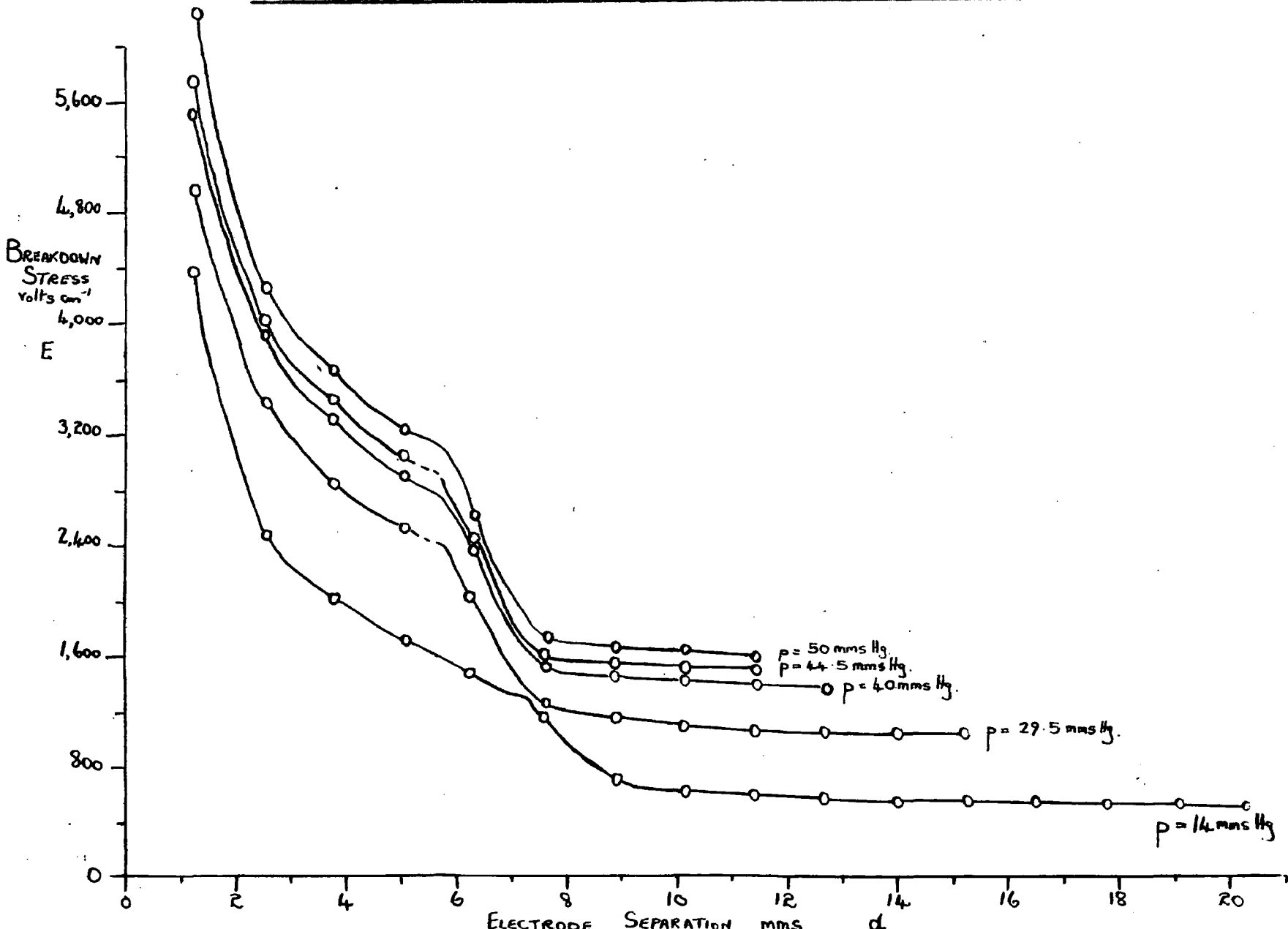
CHAPTER 6

BREAKDOWN IN AIR

The breakdown investigations in air may conveniently be divided into two sections:-

(a) Breakdown as a function of p and d in the pressure range 15 mms.Hg - 70 mms.Hg.

(b) Low pressure measurements at fixed gaps.

"A" - type Rogowski electrodes were used. The field frequency, unless otherwise stated, was kept constant at 9.5 Mc/s.

6.1 Experimental procedure

The gas samples used were drawn from the atmosphere, and carefully dried as indicated in Sect. 2.3.2. Statistical lags associated with the discharge varied in duration from a few seconds to upwards of a minute, and were more pronounced at the higher pressures. A feature of the low pressure measurements was the small stress required to initiate a discharge; the significance of this is discussed in Sect. 6.5.2.

6.2. Variation of breakdown stress with electrode separation

A typical family of curves relating peak breakdown stress and electrode separation is shown in Fig. 44. At

small gaps E drops sharply as d is increased until the
separation reaches a critical value, different for each
curve, beyond which an abrupt "step" appears. As d is
still further increased, E falls off gently in the familiar
manner. The "step" in each curve gives a visible
indication of the change from h.f. to u.h.f. conditions;
this can be confirmed by numerical calculations of the
amplitude of electron oscillation at points bounding the
transition. An examination of Nielsen and Bradbury's (1937)
curve for values of E/p in terms of electron drift velocity
show that a fair approximation may be obtained from a
straight-line extrapolation of the form

$$V = 3.57 \times 10^5 \; E/p$$

Substituting for   in equation 3.1. at 9.5 Mc/s gives

$$de = .12 \; E/p \quad \ldots \ldots \ldots \quad 6.1.$$

In Table 12, this relationship is used to derive de at the
top and bottom of "steps" in typical E - d curves.

TABLE 12.   ELECTRON AMBITS IN AIR

Pmms Hg	Top or bottom of "step"	E volts/cm.	E/p	de mms	d observed mms
14	Top	1300	93	11	7.3
"	Bottom	640	45.7	5.5	9.5
29.5	Top	2380	81	9.7	5.8
"	Bottom	940	32	3.9	8.9
44.5	Top	2920	65	7.8	5.6
"	Bottom	1620	36	4.3	7.6

Fig. 45. **Air, 9.5 Mc/s.**

Variation of Breakdown Stress with Gas Pressure.

BREAKDOWN
STRESS
volts cm⁻¹

E

GAS PRESSURE, mms Hg

o   d = 7·62 mms
x   9·27
⊙   10·16

P
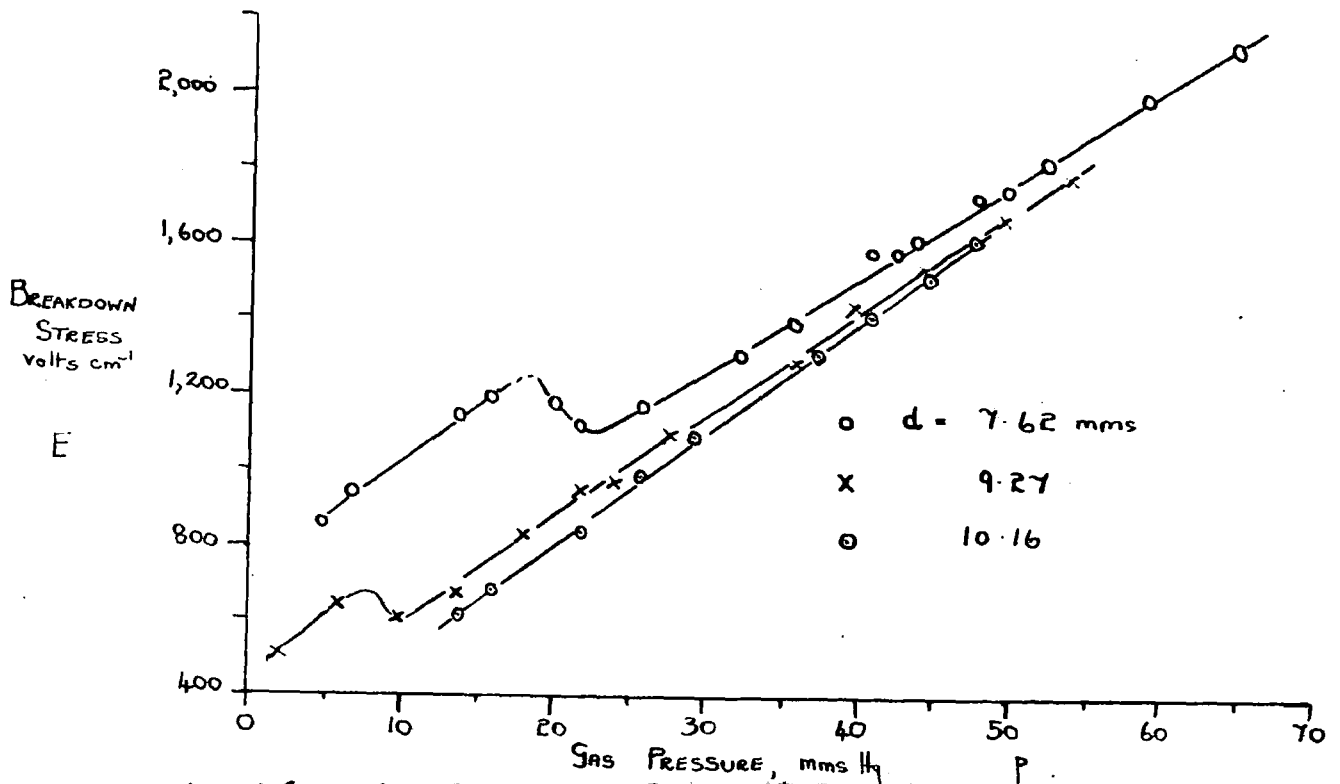
Fig. 46. **Air, Pressure of Gas 27.5 mm Hg.**

Variation of Breakdown Stress with Field Frequency.

BREAKDOWN
STRESS
volts cm⁻¹

E

d = 5·08 mms

d = 7·62mms

d 10·16mms

FIELD FREQUENCY, Mc/s

f
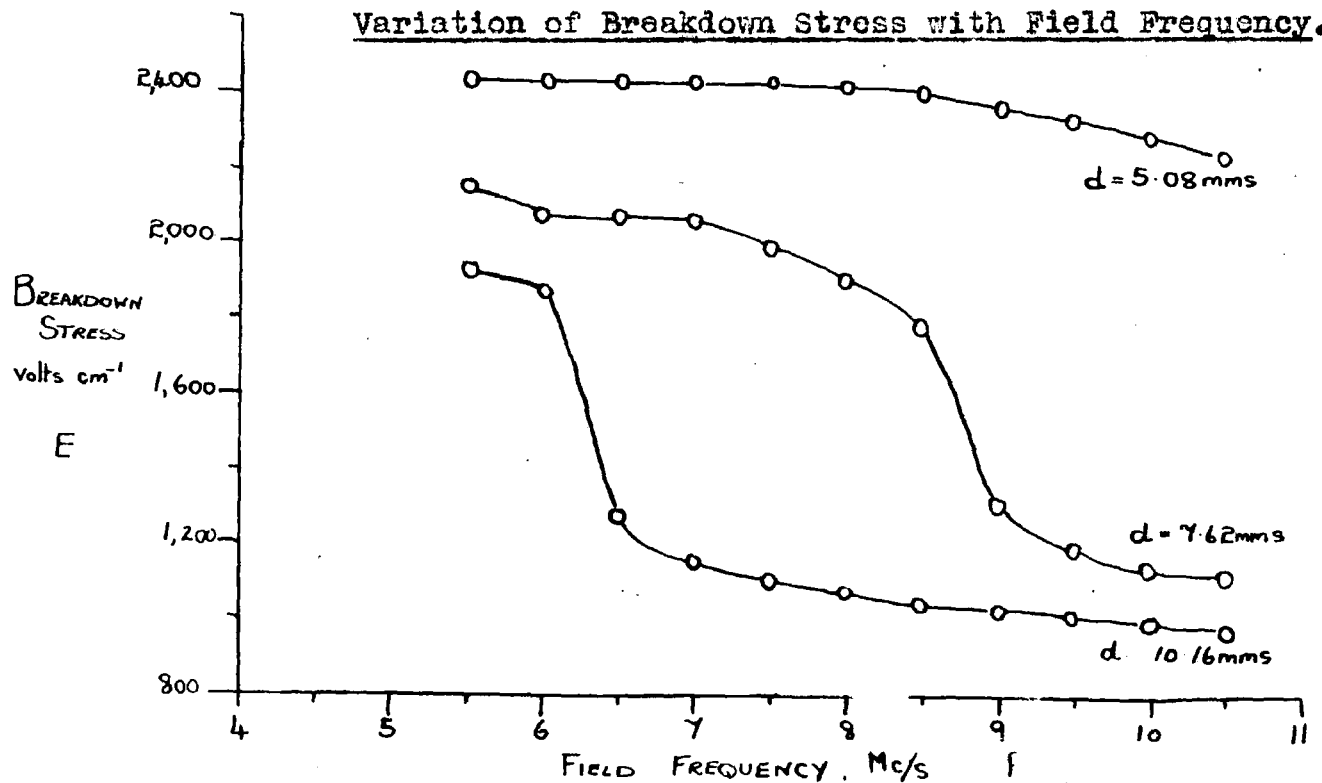
The calculations confirm that at the top of each "step" the amplitude of electron oscillation is very close to the gap spacing; at the bottom electrons are free to oscillate within the gap each half-cycle of the field. Discharges at separations exceeding this value constitute true u.h.f. breakdown.

6.3. Variation of breakdown stress with gas pressure and field frequency

The effect on E of varying the pressure at fixed plate separations is shown in Fig. 45. In the u.h.f. parts of the curves the onset field at a given pressure is seen to decrease with increasing gap width, a feature encountered in each of the gases investigated. In the runs at d = 7.62 mms. and 9.27 mms., critical pressures p, are indicated at 18.5 mmsHg and 8mmsHg respectively. These compare very closely with the values 18.3 mmsHg and 7.9 mmsHg as calculated from the equation

$$p_c = \frac{.12E}{d} \quad \text{(from 6.1.)}$$

The frequency variation for three electrode spacings at a pressure of 27.5 mmsHg is shown in Fig. 46. As f is increased the electron ambit de is correspondingly reduced, eventually just filling the gap; this accounts for the observed variations in E. Under conditions removed from this transition, the breakdown stress is affected only slightly by change of frequency over the range investigated.

Fig. 47. Variation of Breakdown Potential with pd.

$d_1 = 500/50 = 10 \text{ mm}$

$d_2 = 4500/445 = 11.25 \text{ mm}$
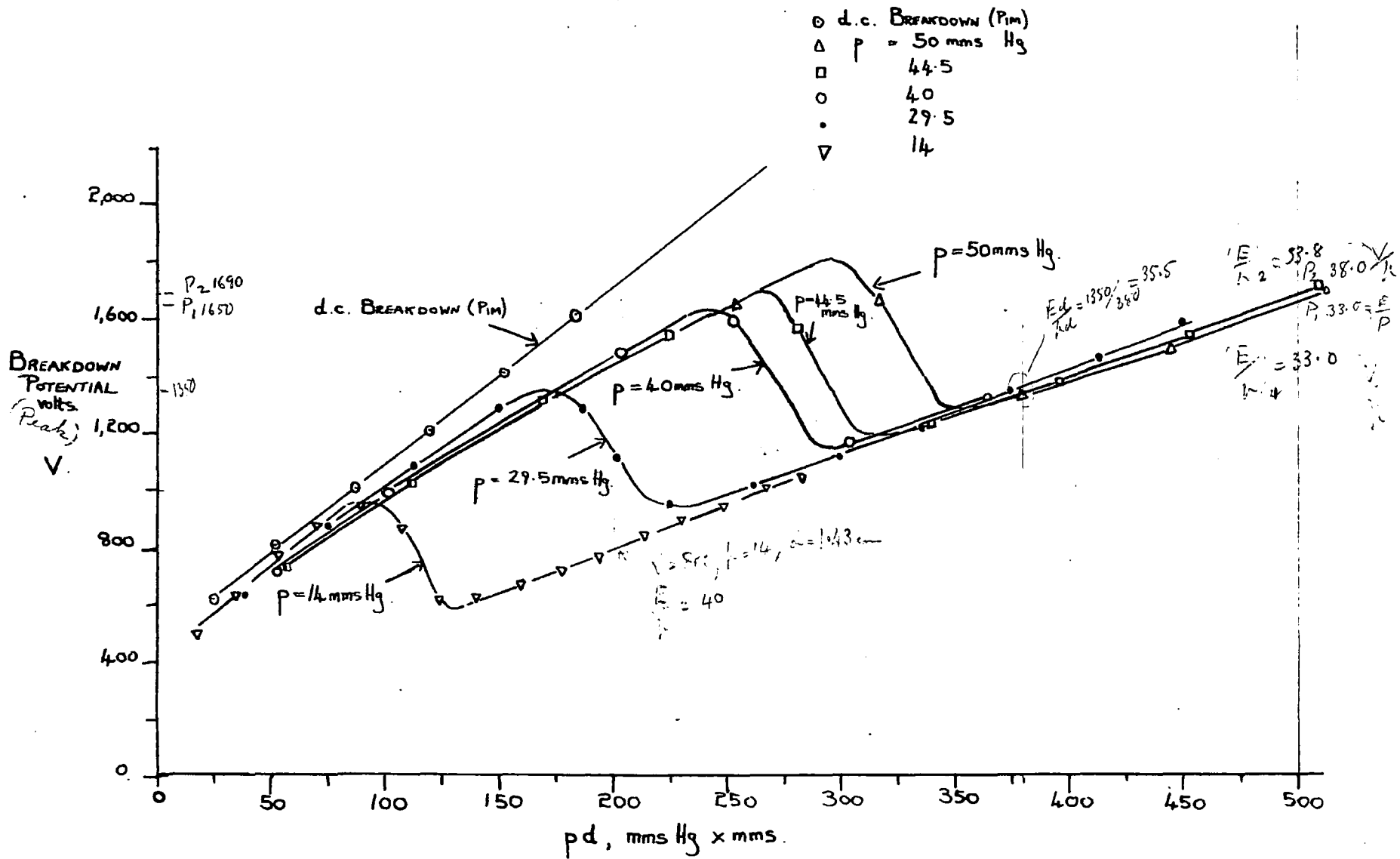
6.4. Breakdown mechanism in air

An encounter between a free electron and an oxygen molecule can lead to the formation of a negative ion. The possibility of such attachments must therefore be examined when considering factors controlling the growth of electron density preceding an electrical discharge in air. An analysis of the results at 9.5 Mc/s given below, shows that any removal process other than diffusion has little effect upon the build up of electron population within the gas. However, in view of the fact that the probability of attachment is a function of gas pressure, the conclusion that u.h.f. breakdown in air is diffusion-controlled must be reserved to pressure conditions not exceeding 70 mmsHg, the highest density used. In an attempt to deduce some positive information regarding the role of attachment in air, and also to explain some of the apparently anomalous results obtained in this gas by various workers, the problem is discussed more fully in Sect. 6.5.

The relationship between breakdown voltage V and the parameter pd for air is given in Fig. 47. Five curves have been drawn for different values of p at 9.5 Mc/s. In each case V increases steadily with pd until a critical value is reached at which there is an abrupt decrease in potential down to the u.h.f. part of the curve. The

Fig. 48. Variation of $E_R\Lambda$ with $p\Lambda$.
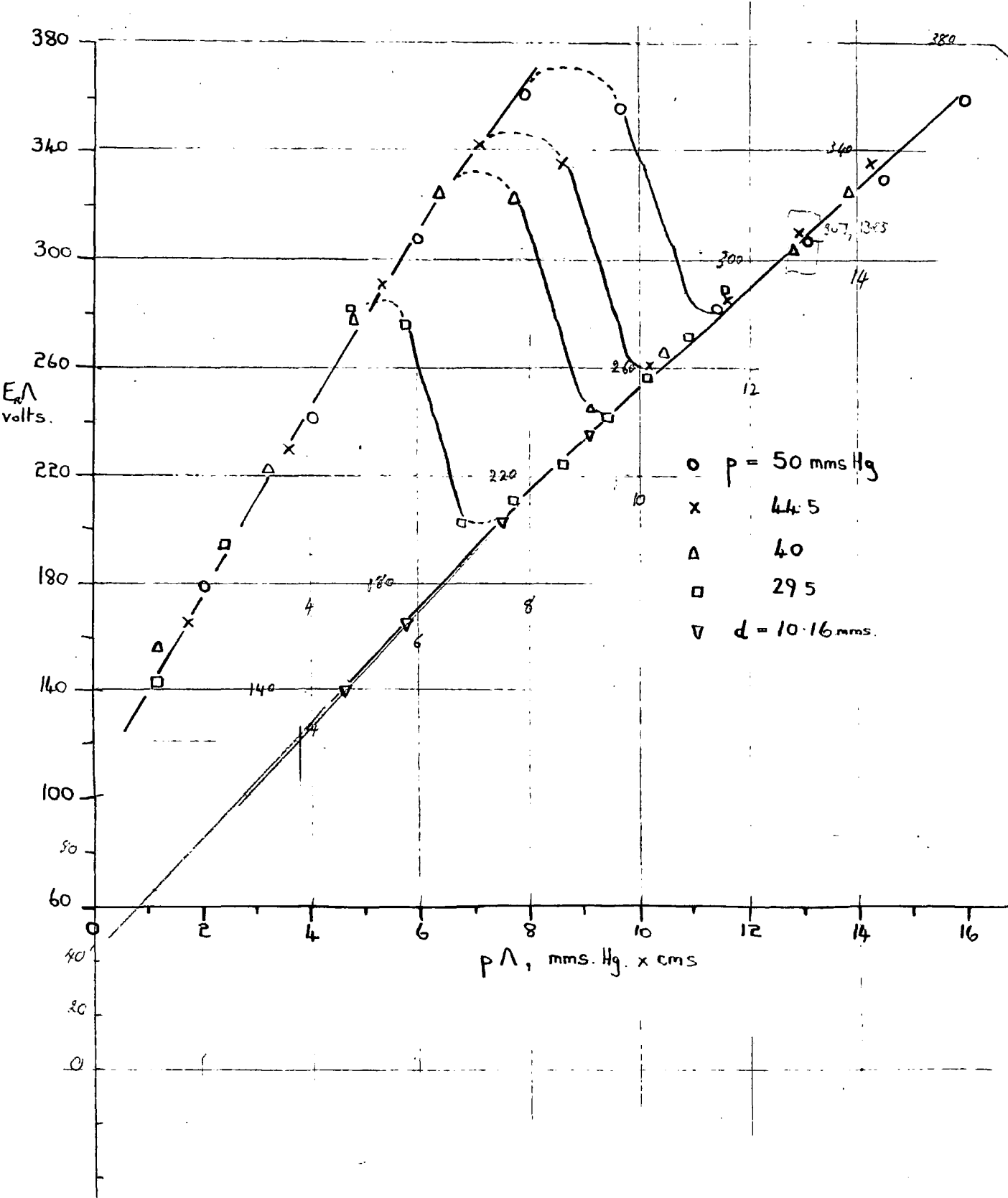
breakdown plots in this region are similar to those observed in the other gases; (the intersection of the separate curves with a chosen ordinate corresponds to different values of pd). The static (d.c.) breakdown curve for air, as measured by Pim (1949), is included for comparison; u.h.f. onset potentials are seen to be approximately half the d.c. values at similar magnitudes of pd (though it is seen that the two sets of curves are not parallel to one another); values in the h.f. region are also less than under d.c. conditions owing to the non-removal of positive ions from the gap.

When the data is transferred to the proper variables $E \Lambda$ and $p \Lambda$, points in the u.h.f. region fall on a single smooth curve, Fig. 48. This is in agreement with the requirements of the diffusion theory.

6.5. Comparison of results with other observers - consideration of electron attachment

The results described in the previous section are in quantitative agreement with those of Herlin and Brown (1948) at a frequency of 3,000 Mc/s. They appear to be at variance, however, with those of Pim (1948 and 49), and Prowse and Lane (1955), who observed constancy of breakdown stress with increasing plate separation for discharges in the u.h.f. region. It is impossible to reconcile this independence of E and d with a diffusive mechanism, in

which the two quantities are related, Eqn. 3.8. Electron attachment to oxygen molecules in air may, either wholly or partially, account for the differences in breakdown behaviour; this possibility is now considered.

If electron attachment is included as a possible loss mechanism in the build-up of ionisation in addition to diffusion, the continuity equation 3.2. may be modified, Brown (1955), to the form

$$\frac{dn}{dt} = (V - Va)n - \nabla \mathcal{J}$$

where Va = is the frequency of attachment

For a parallel plate electrode system, this leads to the breakdown criterion

$$V = Va + \frac{D\pi^2}{d^2} \quad \cdots \cdots \cdots \quad 6.2.$$

V may be written, in terms of the first ionisation coefficient $\propto$, and the average electron drift velocity, as

$$V = \propto \bar{V} \quad \text{(see Sect. 3.7.4.)}$$

Hence $V = \propto E_R \mu$

By analogy with the above equation, the probability of attachment $/cm$, β, is

$$Va = \beta E_R \mu$$

Hence by substitution in eqn. 6.2.

$$\frac{\propto}{p} = \frac{\beta}{p} + \frac{D\pi^2}{\mu} \cdot \frac{1}{(E_R/p)(pd)^2} \quad \cdots \cdots \quad 63.$$

Equation 6.3., though relating $\propto$ and β, was not found suitable for calculating the attachment efficiency under

experimental conditions owing to a lack of reliable information regarding numerical values of the related quantities. However, a comparison between eqn. 6.3. and experimental data in air has been made graphically by Brown (1955), in terms of E/p and pd. In the low pressure region, where E/p is shown to be a function of pd, electron diffusion controls the discharge. The high pressure results of Pim are also included. In this region of low E/p breakdown becomes practically independent of pd, interpreted by Brown as corresponding to to volume loss of electrons from attachment.

This qualitative analysis appears at first sight quite satisfactory in correlating the results of different workers. A close inspection of Pim's 200 Mc/s curves shows that at high pressures of atmospheric order, true constancy of breakdown stress exists for all gaps in the u.h.f. region, whereas at lower values of pressure, the breakdown field decreases slowly with increased electrode separation in a similar manner to the 9.5 Mc/s results and also those of Herlin and Brown, each of whose measurements were taken at pressures < 70 mmsHg. Thus an E – d curve at constant pressure is not typical of u.h.f. breakdown in air throughout the pressure range. Electron losses would therefore appear to be dominated at low pressures by diffusion and at high pressures by attachment.

Measurements of the attachment coefficient β have

been made by Geballe and Harrison (1953), and although
the numerical results are still somewhat uncertain, it
transpires that as E/p rises, β/p passes through a
minimum, at E/p = 30, and subsequently increases. This
somewhat surprising transition, which occurs at a value
of E/p near to the minimum encountered at breadown,
indicates that within the experimental range the attachment
probability decreases with increased pressure.

This is in the opposite sense to the general assumption
made above. It must be stressed, however, that Geballe
and Harrison's measurements are not conclusive and were
recorded over only a small range of E/p.

A partial explanation of the discordant results may
also lie in the choice of electrodes of the different
observers. Rogowski electrodes, used in the 9.5 Mc/s
results, are profiled to simulate an infinite pair of
parallel plates; the cylindrical cavities used by Herlin
and Brown also approximated conditions of infinite plates
with a uniform electric field. Pim, on the other hand,
used spark gaps, domed very slightly towards the centre,
whilst Prowse and Lane adopted a pair of plane-parallel
discs. The possibility of field distortion affecting the
breakdown measurements of these workers cannot be disregarded.

Fig. 49. Air, 9.5 Mc/s. Low Pressure Breakdown.
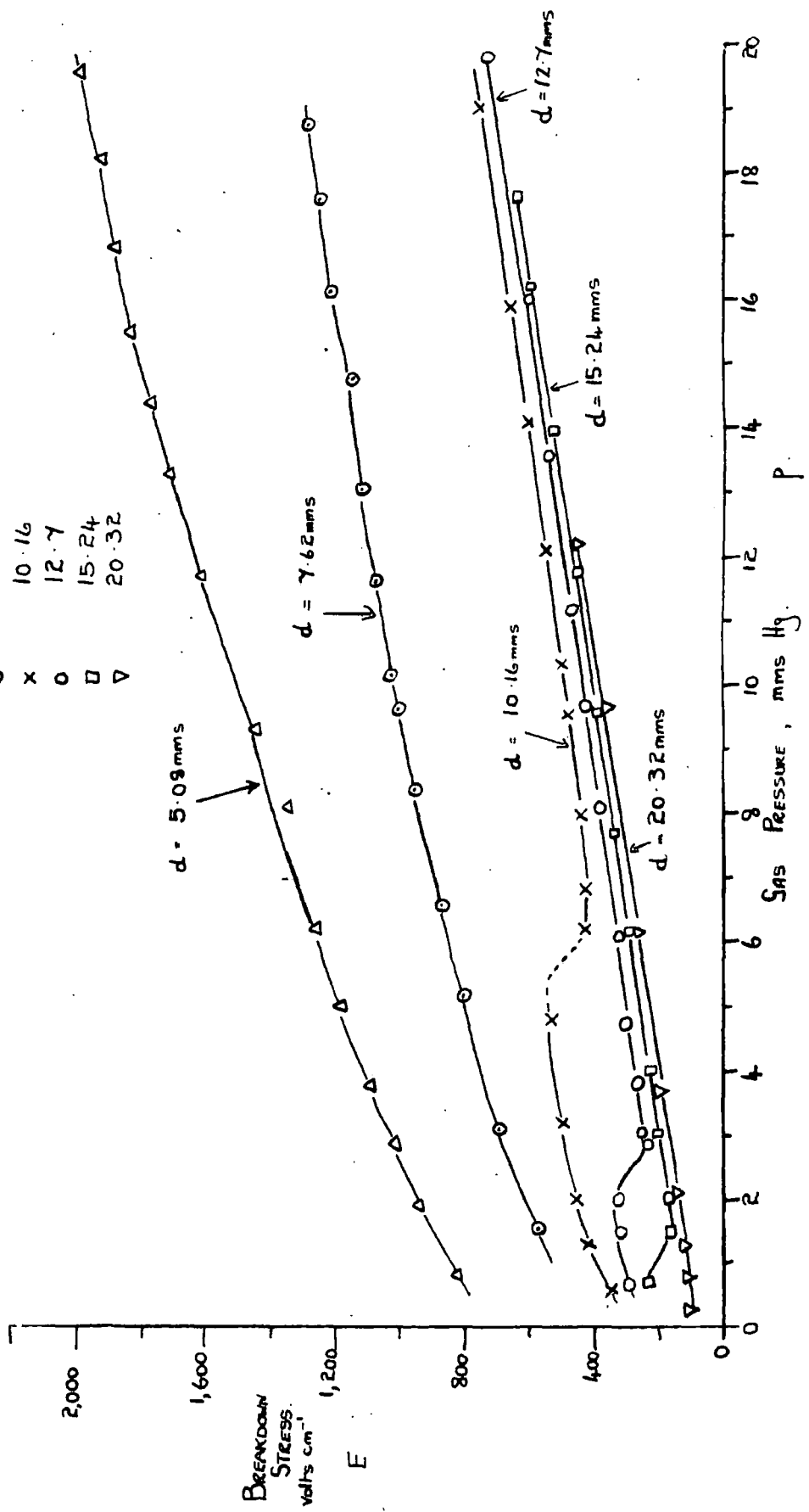
6.6. <u>Low Pressure results</u>

6.6.1. <u>Advantages of low pressure measurements</u>

At low pressure the reduced value of the breakdown field E/p changes quite rapidly for small changes in p. Between 1 mmsHg and 20 mmsHg the range of E/p encountered was quite considerable, and measurements in this region were particularly useful for determining quantities related to E/p, notably the ionisation coefficient. The numerical values of breakdown stress recorded were considerably smaller than have been observed at microwave frequencies. They are, however, in qualitative agreement with values reported by Paska (1955); their significance is discussed in the following section.

6.6.2. <u>Variation of breakdown stress with gas pressure</u>

The curves shown in Fig. 49 represent breakdown at a number of fixed gaps over a pressure range .3 mmsHg - 20 mmsHg. Discharges in the smaller gaps are confined to the h.f. region; at larger separations the u.h.f. transitions are clearly indicated.

The form of the curves is similar to those at higher pressures, being characterised by a fall in breakdown field at constant pressure with increasing separation of the plates. Only small values of field were required to break down gaps in the u.h.f. low-pressure region. Typical values of V and E are given in Table 13.

TABLE 13. U.H.F. BREAKDOWN AT LOW PRESSURES

d = 20.32 mms			d = 15.24 mms		
PmmsHg	V_R volts	E_R volts	PmmsHg	V_R volts	E_R volts
0.3	146	71	1.5	176	116
0.8	155	76	2.0	184	121
1.3	176	87	3.0	228	151

Even smaller breakdown potentials have been observed
by Paska (1955), who has studied the breakdown strength
of air between casual cylinders at a frequency of 77 Mc/s
within a pressure range 0.01 mmsHg - 5 mmsHg. These
values, lower than are obtainable using microwave
oscillations, are explained as follows. Using geometrically
similar systems, microwave breakdown voltages are somewhat
less than those for radio frequencies (Prowse (1950)). V
is determined by the electrode separation, gas pressure,
and field frequency, and limited by two main factors, the
collision frequency (Sect. 3.5.2.) and electron ambit
transitions. The electron ambit limit is seldom encountered
in microwave breakdown, (the electrons move only a fraction
of a millimetre before their velocities are reversed by the
field), and can be avoided at radio frequencies by using
sufficiently large gaps. However, the collision-frequency
transition at microwave frequencies occurs at a considerably

Fig. 50. Air, 9.5 Mc/s. High Frequency Ionisation Coefficient.
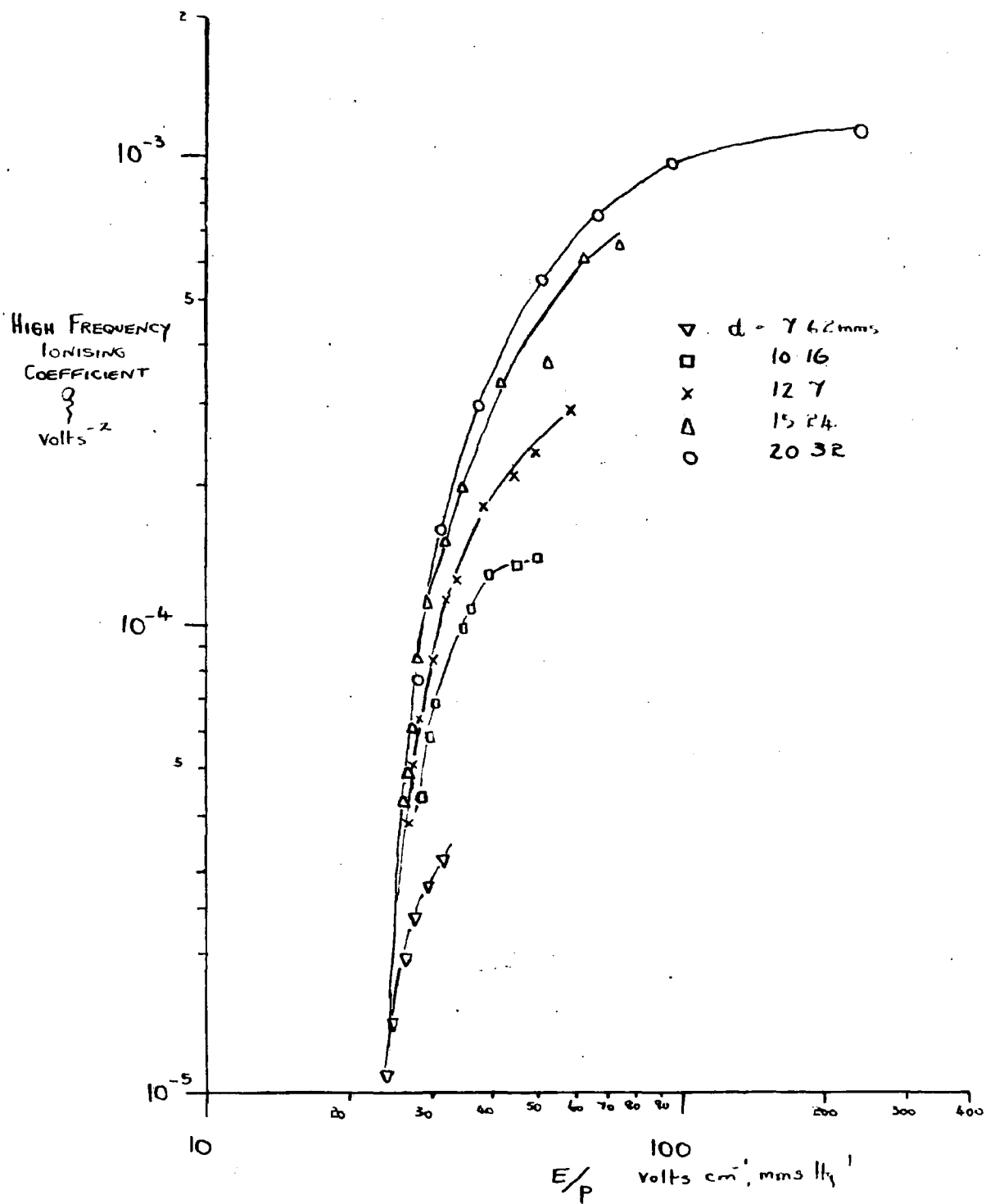
higher pressure than at radio frequencies, and since the
efficiency of ionisation is greater at lower pressures,
it is possible for r.f. breakdown voltages recorded near
the minimum to be lower than those obtainable at micro-
wave frequencies.

Thus, by careful choice of frequency, gas pressure,
and electrode separation, it seems likely that the break-
down potential of the gap would not be greater than a few
volts.   A thorough investigation of optimum breakdown in
the radio-frequency region may be of considerable technical
importance.

6.7. Ionising efficiency in air

The breakdown data in air were used to calculate
values of the high-frequency ionising coefficient ξ ,
using equation 3.8.

Plots of ξ as a function of E_R/p are given in Fig. 50;
each curve corresponds to a pressure run at constant
electrode separation.   On the high pressure (low E_R/p)
side, they come together to form a common envelope,
departure from this occurs at values of E_R/p determined by
the individual gaps.   For a given E_R/p the ionising
efficiency is seen to increase with electrode separation,
and may be attributed to the lengthening of the life-time
of electrons within the gap.   These curves could be used,
in conjunction with eqn. 3.8. to predict breakdown at
various pressures using different electrode configurations.

Fig. 51. Air, 9.5 Mc/s. Form of Discharge as a Function of Gas Pressure and Electrode Separation.
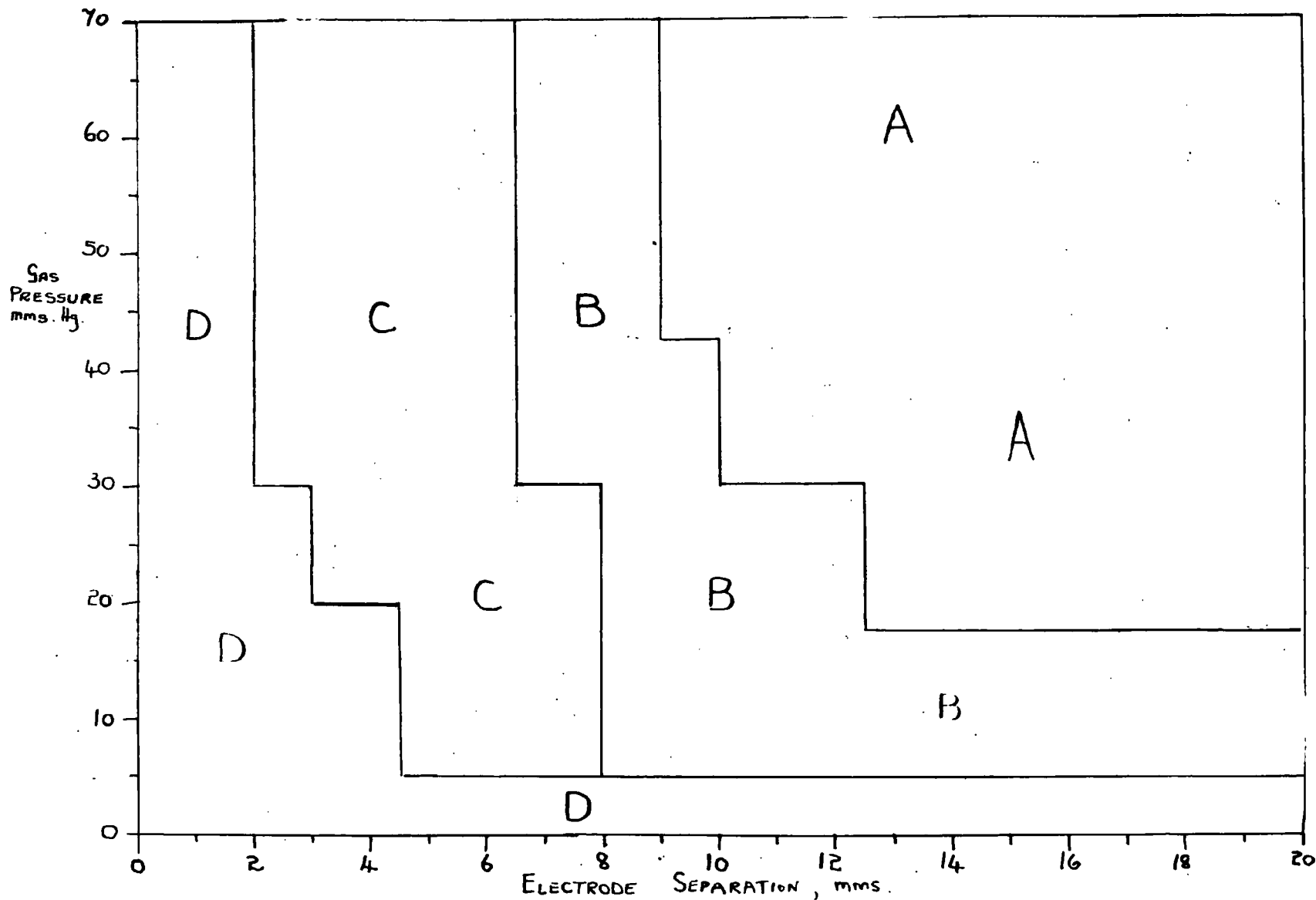
6.8.   Visual characteristics of the discharge

Observations of breakdown in air showed that under a prescribed set of conditions the discharge was visible in one of four different modes.   In Table 14 each mode is specified by its colour, intensity, and volume.

TABLE 14.   DISCHARGE CHARACTERISTICS IN AIR

Mode	Intense or Diffuse	Colour	Extent of discharge
A	Intense	Pink, white spots on electrode	Confined well within inter-electrode space.
B	Diffuse	Bright pink	Within inter-electrode space; dark spaces round electrodes.
C	Intense	Pink	Within inter-electrode space.
D	Diffuse	Faint pink	Extended beyond inter-electrode space but dark space in central region of gap.

In the neighbourhood of the u.h.f. transition, the form of the discharge changed from mode B to the intense mode A, and was accompanied by a sharp drop in the voltmeter reading, indicating a heavy loading of the circuit.   Fig. 51, constructed from a large number of observations, shows the change in form of discharge in relation to electrode separation and gas pressure.   This phase-diagram can be

used to predict the discharge appearance under a given
set of conditions.

An explanation similar to that given for hydrogen,
Sect. 3.9.2., is thought likely to explain the change in
nature of the spark in the vicinity of the u.h.f.
transition.

CHAPTER 7

EXPERIMENTAL ERRORS

In all of the diagrams, the values of electric stress
are based on indicated voltages. The meters used were
calibrated in terms of the electromotive force of two
standard cells.

In all cases the percentage error decreased with
increasing voltage, as shown in Table 15.

TABLE 15. VOLTMETER ERRORS

Meter	Instrument Range (Volts)	Error (per cent)
Pye Scale-Lamp e-static	1000 - 500	.3 - 1.2
Ayrton-Mather (high range)	530 - 110	.4 - 1.8
Ayrton-Mather (low range)	120 - 40	.6 - 1.4

It will be recalled that measurements of breakdown
voltage were made by using stepwise increases in the
applied voltages. In the higher voltage range the last

increase between no-breakdown and breakdown did not exceed 5 volts, and in the lowest range 2 volts.

Precautions were taken to ensure that the finite lengths of the connections to the electrodes and to the diodes should not introduce an error. A parallel-wire transmission line was connected between the final tuned circuit and the electrodes; the side-branch taken from points near the electrodes to the diodes was so adjusted that the total run to the electrodes was equal to the total run to the diodes. This total run was itself only a small fraction (5%) of the shortest wavelength used.

Pressures were read to ·5 mmsHg, in the higher range (above 15 mmsHg) by means of the modified Bourdon Gauge. The calibration (Section 2.3.3.) was repeated at regular intervals, and no point ever departed from the original curve by more than ·5 mm Hg. The diaphragm gauge used for the low-pressure measurements in hydrogen and air was subject to an error not exceeding $2\frac{1}{3}\%$ of the full-scale reading (40 mm Hg). In the figures the pressures used are indicated pressures not corrected for fluctuations in laboratory temperature, and this may account for occasional departures from regularity, such as appear in the V-pd curves for air, Fig. 47.

The electrode separation could be measured with altogether greater accuracy than the voltage or the gas pressure, and no sensible error arose in this connection.

Also no appreciable error occurred in connection with
frequency measurements; the wavemeter readings agreed,
within the precision of reading, with the indicated
frequency of the oscillator.

---ooo000ooo---

Fig. 52.   The Oscillator.
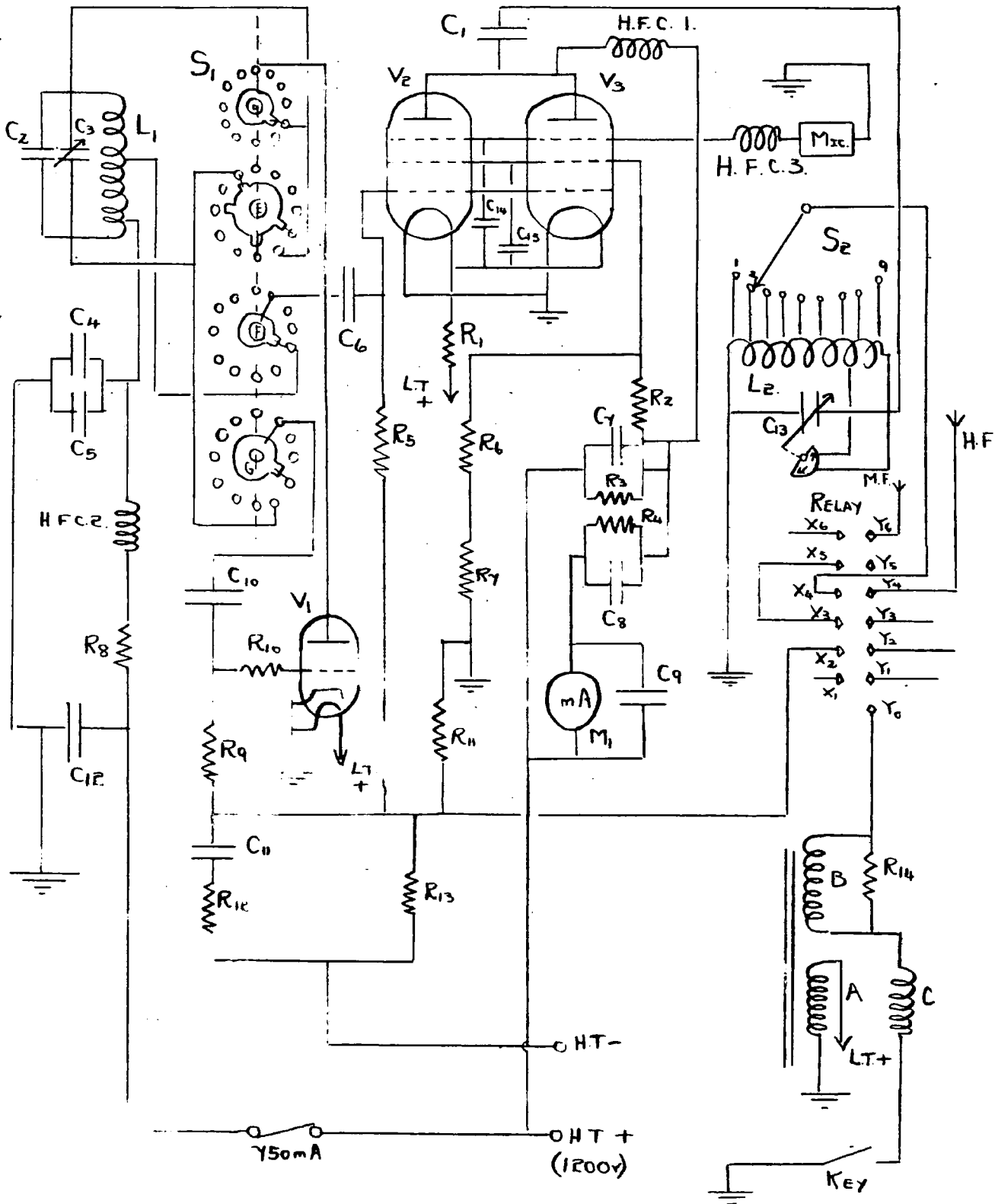
APPENDIX 1

THE OSCILLATOR

The oscillator circuit is shown in Fig. 52. Three frequency ranges were available, 5.5 Mc/s - 10.5 Mc/s; 3 Mc/s - 5.5 Mc/s; and 200 Kc/s - 500 Kc/s. The circuit of Fig. 52 only includes components relevant to the highest frequency range.

Oscillations were generated by a series-fed Hartley oscillator, based on value V_1 and the tuned elements $L_1 C_2 C_3$. Condenser C_2 was variable, and with C_{13} was fitted with a UNI slick 7-stop mechanism, arranged so that pre-determined frequencies could be rigidly held or returned to. These stops could be released at will. The condenser was trimmed to allow fine adjustment of frequency. The oscillations were fed, via S_1, to the control grid of the power amplification valves V_2 and V_3, strapped in parallel. H.T. for these valves, 1/200 volts, was delivered through current-limiting resistors and H.F.C. 1. A milliameter in the anode circuit, M_1, provided a useful guide for determining resonance conditions.

The oscillations were delivered to the output tuned circuit $L_2 C_{13}$ through C_1

Circuit Components

Valves V_1 VT104 (ML6)

        V_2 and V_3 VT105 (PT15)

Chokes   H.F.C.1   8.8 mH

           H.F.C.2   2.5 mH

           H.F.C.3   15.5 mH

Condensers			
C_1	.004 μ F	C_8	.003 μ F
C_2	10 μ F	C_9	.004 μ F
C_3	11-135 $\mu\mu$ F	C_{10}	.0002 μ F
C_4	.005 μ F	C_{11}	.5 μ F
C_5	.005 μ F	C_{12}	.004 μ F
C_6	.0002 μ F	C_{13}	.01 μ F
C_7	.0003 μ F	C_{14}	.004 μ F

Resistors			
R_1	1.5 Ω	R_8	50K Ω
R_2	20K Ω	R_9	15K Ω
R_3	10 Ω	R_{10}	7.5K Ω
R_4	19.5 Ω	R_{11}	5K Ω
R_5	20K Ω	R_{12}	5.1K Ω
R_6	75K Ω	R_{13}	350 Ω
R_7	12K Ω	R_{14}	20 Ω

---ooo000ooo---

LIST OF REFERENCES

Page

Biondi, M.A. and Brown, S.C. Phys. Rev., $\underline{75}$, 1700, (1949, a) 62

Biondi, M.A. and Brown, S.C. Phys. Rev., $\underline{76}$, 1697, (1949, b) 62

Bright, A.W. E.R.A. Tech. Report L/T 229 (1950) 6

Bradbury, N.E. and Nielson, R.E. Phys. Rev., $\underline{49}$, 338 (1936) 32

Brode, R.B. Rev. Mod. Phys., $\underline{5}$, 257, (1933) 43

Brown, S.C. and McDonald, Phys. Rev., $\underline{76}$, 1629 (1949) 41,45, 46,59

Brown, S.C. Proc. Am. I.R.E., $\underline{39}$, 1493 (1951) (Fig43)

Brown, S.C. Appl. Sci. Res., B, $\underline{5}$, 97 (1955) 48,89,90

Davydov, B, Phys. Rev. $\underline{64}$, 156 (1943) 63

Druyvesteyn, M. J. and Penning, F.M. Rev. Mod. Phys. $\underline{12}$, 87 (1940) (Fig43)

Dutton, J, Haydon, S, and Llewellyn Jones, F. Proc. Roy. Soc., $\underline{213}$, 203 (1952 b) 3

Ekstrand, P.A. Proc. I.R.E., $\underline{28}$, 262, (1940) 6

Fucks, W. Graf, L., Mues, G. and Miller, H.G., Zeits für Physik, $\underline{145}$, 1 (1956) 4,10, 34

Gill, E. W. B., and Donaldson, R. H. Phil. Mag., $\underline{12}$, 719, (1931) 7,36(a)

Gill, E. W. B. and Van Engel, Proc. Roy. Soc. A, $\underline{192}$, 446 (1948) 6,23

Gill, E. W. B. and Van Engel, A. Proc. Roy. Soc. A, $\underline{197}$, 107 (1949) 32

Githens, S. Phys. Rev., $\underline{57}$, 822 (1940) 9,59

Herlin, M.A. and Brown, S.C. Phys. Rev., $\underline{74}$, 291 (1948) 7,9, 35,37,38,39

Hartman, L. M. Phys. Rev., $\underline{73}$, 316, (1948) 38

	Page
Harrison, M.A and Geballe, R. Phys. Rev., **91**, 1, (1953)	91
Johnson, R.A. Elect. Eng., 136 (April 1954)	13
Jones, C. V. Brit. E. R. A. Report, Sect. L. Sub-Committee G (1953)	17
Kennard, E. H. Kinetic Theory of Gases, McGraw-Hill (1938)	39
Labrum. C.S.I.R. Report, Australia R.P.R., **85** (1947)	10,83
Llewellyn-Jones, F. and Morgan, G.D. Proc. Roy. Soc. B, **64**, 574 (1951)	60
Llewellyn-Jones, F. and Parker, A. B., Proc. Roy. Soc. A, **213**, 185 (1952 a)	3
Llewellyn-Jones, F. Extract from British Association Meeting (1952 c)	3
Loeb, L and Meek, J. M. "The Mechanism of the Electric Spark" (1940)	2
Morgan, G. D. Sci. Prog. **41**, 22 (1953)	4
McDonald, A. D. and Matthews, J. H. Phys. Rev., **98**, 1070 (1955)	(Fig43)
McDonald, A. D. and Brown, S. C., **76**, 1634, (1949)	9
Margeneau, H. Phys. Rev., **60**, 508 (1946)	36(a)
Nielson, R. A. Phys. Rev., **50**, 950 (1936)	66,78
Nielson, R. A. and Bradbury, N.E. Phys. Rev., **51**, 69 (1937)	85
Paska, R. A. Ballistic Labs. Report No. 1944 (1955) (Restricted Circulation)	92,93
Penning, F. M. Naturwiss, **15**, 818 (1927)	6,20
Pim, J. A. J.I.E.E., **96**, 117, (1949)	6,9, 88
Pim, J. A Nature, **161**, 683 (1948)	88
Prowse, W. A. J. Brit. I.R.E. **10**, 11 (1950)	93

                                                       Page

Prowse, W. A. and Jasinski, W. J.I.E.E., 98 (1951)   10

Prowse, W. A. and Jasinski, W. J.I.E.E., 99 (1952)   30,83

Prowse, W. A. and Lane, P. E. Appl. Sci. Rev., 5   10,26,
   127 (1955)   34,88

Reukema, L. E. Trans. Am. I. E. E., 47, 38 (1925)   5,31

Rogowski, W. Arch. für Elec. XII, 1, (1923)   16

Rowbotham, J. R. (to be published) (1956)   83

Seward, E. W. J.I.E.E., 84, 288 (1939)   6

Thomson, J. Phil. Mag., 23, 1 (1937)   9,15,
                                                       20,59

Townsend, J. S. Acad. Sci., Paris, 186, 55 (1928)   62

Townsend, J. S. "Electrons in Gases", Hutchinson (1947)   2,44

Varnerin, L. J. and Brown, S. C. Phys. Rev., 79,   (Fig43)
   946 (1950

Von Engel, A, and Steenbeck, M. Elec. Gasent, Vol. 1,   (Fig43)
   Springer (1932)

Williams, E. "Thermionic Valve Circuits". Pitmans   23
   (1952)

Zeleny, J. J. Appl. Phys., 13, 103 (1942)   2

---ooo000ooo---

$$\alpha/\rho = \ldots \times \ldots / A \ldots (E/\rho) \, \eta$$

$\frac{293}{273}$

4.6×10^{-3}

0.00

At $E/\rho = 20$ $\alpha/\rho = 2.678 \times \eta$

$\eta = 4.6 \times 10^{-4}$ $\alpha/\rho = 0.0184$. $\alpha/\rho_0 = 0.0197$

$\eta = 3.1 \times 10^{-4}$ $\alpha/\rho = 0.0083$. $\alpha/\rho_0 = 0.0089$.

At $E/\rho = 20$. α/ρ_0 (Rose) $= 0.0046$.

Value of $3 eV$ is too high, we Brown's curve

Clark's values for α/ρ.	(α/ρ_{20})	(α/ρ_0)	
$\eta = 4.6 \times 10^{-4}$	0.0147	0.0157 .	cf Rose (0.0046) .
$\eta = 3.1 \times 10^{-4}$	0.0099	0.0106	

$$\left(\frac{\alpha}{\rho}\right) = \left(\frac{D}{N}\right)\left(\frac{E}{\rho}\right) \eta .$$

$$= 1.6 \times 20 \times 3.1 \times 10^{-4}$$

$$= 99.2 \times 10^{-4} = 0.0099 .$$

$$D/\mu = \frac{2}{3} \frac{\overline{N}_{av}}{\epsilon} \qquad N \text{ in } eV .$$